이학박사 학위논문

중심체 단백질인 CROCC 및 pericentrin 의 결핍이 발생에 미치는 영향에 관한 연구

Developmental implications of CROCC and pericentrin deficiency: Insight into roles of centrosome proteins

2025 년 2 월

서울대학교 대학원

생명과학부

류 성 진

중심체 단백질인 CROCC 및 pericentrin 의 결핍이 발생에 미치는 영향에 관한 연구

Developmental implications of CROCC and pericentrin deficiency: Insight into roles of centrosome proteins

지도교수 이 건 수

이 논문을 이학박사 학위논문으로 제출함
2025 년 2 월

서울대학교 대학원
생명과학부
류 성 진

류성진의 이학박사 학위논문을 인준함
2025 년 2 월

위 원 장 _____(인)

부위원장 _____(인)

위 원 _____(인)

위 원 _____(인)

위 원 _____(인)

Developmental implications of CROCC and pericentrin deficiency: Insight into roles of centrosome proteins

A dissertation submitted in partial
fulfillment of the requirement
for the degree of

DOCTOR OF PHILOSOPHY

to the Faculty of
School of Biological Sciences
at
Seoul National University
by

Sung Jin Ryu

Date Approved:
February, 2025

_____
_____
_____
_____
_____

ABSTRACT

Developmental implications of CROCC and pericentrin deficiency: Insight into roles of centrosome proteins

Sung Jin Ryu

Department of Biological Sciences

The Graduate School

Seoul National University

The centrosome plays an essential role in microtubule organization, cell division, and cilia formation. Dysfunction in centrosome-associated proteins has been linked to developmental disorders, ciliopathies, and cancer. The centrosome consists of a pair of centrioles connected by inter-centriolar fibers and surrounded by a protein matrix called pericentriolar material (PCM). While CROCC is main component of inter-centriolar fiber and known to contribute to centriole cohesion and PCNT is known to PCM integrity during mitosis, the specific functions of these proteins at the cellular and tissue development levels remain unclear. Therefore, this study aims to investigate the roles of CROCC and PCNT in centrosome function and their impact on cellular integrity and tissue development.

In chapter I, I focused on understanding the role of inter-centriolar fibers in cilia assembly. CROCC is the main building block of inter-centriolar fibers, helping to

maintain centrosome cohesion, and forms a parallel homodimer as a basic unit. The inter-centriolar fiber is well known for its role in maintaining cilia stability. However, its specific role in the process of cilia formation has not been clearly elucidated. Therefore, I investigated the role of inter-centriolar fibers in ciliogenesis. I generated *CROCC* and *CEP250* KO cell lines to analyze their effects on cilia formation and the localization of PCM1, a representative centriolar satellite protein responsible for transporting essential proteins to the centrosome during cilia assembly. I found that the loss of CROCC and CEP250 disrupted PCM1 localization at the centrosome without affecting its expression levels. Additionally, PCM1 was found to bind directly to CROCC, a critical interaction for centriolar satellite accumulation near the centrosomes, essential for efficient cilia formation. This study revealed that inter-centriolar fibers play a critical role in organizing cilia assembly through interaction with centriolar satellites.

In chapter II, I focused on understanding the role of Pericentrin (PCNT) in deleopment. PCNT, a critical scaffolding protein within PCM, plays a central role in stabilizing the PCM. PCNT recruits γ-tubulin and CEP215 to the centrosome, facilitating the organization of microtubules and supporting PCM structure. PCNT deficiency impairs PCM structure and mitotic spindle pole. However, PCNT specific role in the development has not been clearly elucidated. Thus, I investigated the mechanistic role of PCNT in centrosome integrity, this study contributes to understanding of how PCNT mutation impacts the development of disorders like Microcephalic osteodysplastic primordial dwarfism II (MOPDII). I examined the effects of PCNT loss of function using *Pcnt* KO and MOPD II-mimicking knock-in (KI) mouse models and mouse embryonic fibroblasts (MEF) cells. KO and KI mice exhibited neonatal lethality, with embryos displaying similar phenotypes such as growth retardation, polydactyly, reduced brain, and cleft palate, further emphasizing the role of PCNT in development. In addition, both KO and KI MEF cells showed abnormal centriole separation, overduplication, and an increased aneuploidy. These findings not only emphasize PCNT role in centrosome integrity but

also link its dysfunction to the pathogenesis of MOPDII, offering potential targets for therapeutic interventions.

This research emphasizes the essential roles of centrosomal proteins CROCC and PCNT using CRISPR/Cas9-mediated KO cell lines and disease-mimicking mouse models in cellular organization and normal development. CROCC contributes to the precise assembly of cilia by organizing centriolar satellites, while PCNT stabilizes the PCM, supporting accurate chromosome segregation and preventing developmental defects. By demonstrating how disruptions in these proteins impact cellular and developmental processes, this study emphasizes the roles of CROCC and PCNT in centrosome integrity and development, offering novel insights into the molecular basis of centrosome-related disorders.

Keywords : Centrosome, Cilia formation, Inter-centriolar fiber, Pericentrin, Chromosomal instability

Student number : 2020-20188

CONTENTS

ABSTRACT.....i

CONTENTS.....iv

LIST OF FIGURES.....vii

BACKGROUND AND PURPOSE.....1

Background.....1

1. Centrosome.....1

1.1. Centrosome structure.....1

1.2. Centrosome function.....2

2. Inter-centriolar fiber, Centriolar satellites, and cilia.....4

2.1. Inter-centriolar fiber.....4

2.2. Centriolar satellite.....5

2.3. Primary cilia.....6

3. Pericentriolar material.....7

3.1. Pericentin.....7

Purpose.....16

Chapter I. Role of inter-centriolar fiber in cilia formation.....17

ABSTRACT.....18

INTRODUCTION.....19

MATERIALS AND METHODS.....22

Antibiodies.....22

Cell culture, transfection, and stable cell lines.....23

Generation of the knockout cell lines.....24

Immunoprecipitation.....24

Immunoblot analysies.....25
Immunocytochemistry and image processing.....25
Measurements and statistical analysis.....26
RESULTS.....27
Effects of *CROCC* and *CEP250* knockout on cilia formation.....27
Effect of CROCC depletion on cilia formation in *CEP250* KO cells.....28
The role of inter-centriolar fibers in the accumulation of centriolar satellites at the centrosome.....29
Identification of interaction regions between PCM1 and CROCC.....30
The interaction between CROCC and PCM1 is important for cilia assembly.....31
Identification of the PCM1 region that interacts with CROCC.....33
DISCUSSION.....49

Chapter II. Role of PCNT in centrosome integrity and development.....52
ABSTRACT.....53
INTRODUCTION.....54
MATERIALS AND METHODS.....56
Animals.....56
Immunoblot analyses.....56
Antibodies.....57
Cell culture, transfection, and stable cell lines.....57
Fluorescence in situ hybridization.....58
Immunocytochemistry and image processing.....58
Measurements and statistical analysis.....59
RESULTS.....60

Development abnormalities in *Pcnt* KO and KI mice.....60

Confirmation of *Pcnt* KO and KI MEF cells.....60

Effect of PCNT depletion on PCM localization at the centrosome.....61

Abnormal centriole separation and overduplication in *Pcnt* KO and KI MEF cells.....61

Chromosomal instability in *Pcnt* KO and KI MEF cells.....62

DISCUSSION.....71

CONCLUSION AND PERSPECTIVE.....76

REFERENCES.....78

ABSTRACT IN KOREAN (국문 초록) 86

감사의 글.....89

LIST OF FIGURES

Figure 1. Centrosome structure and Function.....8

Figure 2. Centrosome cycle depending on cell cycle.....9

Figure 3. Inter-centriolar fiber.....10

Figure 4. Centriolar satellite proteins.....11

Figure 5. Cilia structure and ciliogenesis.....12

Figure 6. Ciliopathies.....13

Figure 7. Pericentriolar material.....14

Figure 8. Pericentriolar material lattice structure at mitosis.....15

Figure 9. Generation of the *CROCC* and *CEP250* KO RPE1 cells.....35

Figure 10. Reduction of cilia assembly in the *CEP250* and *CROCC* KO cells.....36

Figure 11. Inter-centriolar fibers are essential for cilia assembly.....37

Figure 12. Inter-centriolar/rootlet fibers are important for proper formation of cilia in the *CEP250* KO cells.....38

Figure 13. Reduction of the centrosome/basal body levels of PCM1 in the *CEP250* and *CROCC* KO cells.....39

Figure 14. Augmentation of the proportion of cells with cilia by CEP72 depletion.....40

Figure 15. Definition of PCM1-interacting regions in the CROCC protein.....41

Figure 16. Expression of FLAG-CROCC^{FL} and FLAG-CROCC$^{303-1741}$ in *CROCC* KO RPE1 cells.....42

Figure 17. Specific interaction of CROCC with PCM1 is essential for cilia assembly.....43

Figure 18. Colocalization of PCM1 with subcellular CROCC.....44

Figure 19. Generation and feature of *PCM1* KO RPE1 cells.....45

Figure 20. Definition of the PCM1 regions for centrosome accumulation and cilia formation.....46

Figure 21. Definition of the CROCC-interacting region in the PCM1 proteins.....47

Figure 22. Model.....48

Figure 23. Phenotypic analysis in *Pcnt* KO mice.....63

Figure 24. Phenotypic analysis in *Pcnt* KI mice.....64

Figure 25. Confirmation of the *Pcnt* KO and KI MEF cells.....65

Figure 26. PCNT is important for CEP215 localization, but not γ-Tub at interphase.....66

Figure 27. PCNT is important for CEP215 and γ-Tub localization at mitosis.....67

Figure 28. Abnormal centriole separation and centriole number *Pcnt* KO and KI MEF cells..... 68

Figure 29. Occurrence of aneuploidy in *Pcnt* KO and KI MEF cells.....69

Figure 30. Model.....70

BACKGROUNDS

1. Centrosome

The centrosome is a major microtubule-organizing center (MTOC) in animal cells, crucial for maintaining cellular structure, intracellular transport, cell movement, and ensuring accurate chromosome segregation during cell division (Fig. 1). Initially discovered by Boveri in 1888, the centrosome is a unique organelle that exists exclusively in animal cells (Sathananthan et al., 2006). The centrosome duplicates once per cell cycle under precise regulatory mechanisms (Fig. 2). During interphase, it polymerizes and anchors microtubules to structure the cell's microtubule network, thereby regulating processes such as intracellular transport, cell morphology, and motility.

When cells enter mitosis, the centrosomes separate to opposite poles and form the mitotic spindle poles, playing a crucial role in chromosome segregation and ensuring genomic stability (Bettencourt-Dias & Glover, 2007). In non-dividing cells, the centrosome functions as a basal body to form cilia, which are essential for detecting extracellular signals during development. Due to these multifunctional roles, the centrosome is closely associated with various human diseases, including cancer and ciliopathies (Werner et al., 2017).

1.1 Centrosome structure

The centrosome consists of a pair of centrioles surrounded by an amorphous matrix known as the pericentriolar material. Each centriole is a cylindrical structure made up of nine triplets of microtubules arranged in a circular pattern. The centriole pair includes a mother and daughter centriole, each differing in structure and function. The

mother centriole, for example, contains appendages at its proximal end, which anchor microtubules (Bornens, 2012; Azimzadeh & Marshall, 2010). The PCM, surrounding the centrioles, is enriched with proteins essential for microtubule nucleation, such as γ-tubulin, CEP215, and pericentrin (Luders & Stearns, 2007).

Advances in super-resolution microscopy have revealed that PCM proteins are organized into a high-order hierarchical structure (Lawo et al., 2012), playing a critical role in spindle formation and centrosome integrity. PCM dynamically reorganizes throughout the cell cycle to control centrosome function, providing essential structural components for spindle pole formation during cell division. Defects in centrosome components can severely impact cellular stability and chromosome segregation, potentially leading to genomic instability (Mennella et al., 2012; Fry et al., 1998). Structural abnormalities in centrioles, in particular, can lead to cell division errors and disrupted spindle formation, impeding normal cell growth and development (Azimzadeh & Marshall, 2010; Conduit et al., 2015).

1.2 Centrosome function

The centrosome performs diverse functions, including forming intracellular microtubules that facilitate material transport, cell motility, cell adhesion, and polarity (Bornens & Azimzadeh, 2007). At the onset of mitosis, PCM significantly increases in volume to form the mitotic spindle poles, ensuring accurate chromosome segregation and enabling cell division. Thus, the centrosome is critical for organizing the mitotic spindle and maintaining genomic stability (Bornens, 2012).

Furthermore, the centrosome acts as the basal body for the primary cilium or flagellum, playing a vital role in sensing extracellular signals and cellular signaling (Breslow & Holland, 2019). During interphase, the mother centriole prepares for primary cilia formation, contributing to cellular response regulation by facilitating ciliary structure formation, enabling the cell to recognize and react to external signals (Singla & Reiter,

2006). Consequently, the centrosome plays a central role in maintaining normal cellular functions and physiology, and dysfunction in the centrosome can be linked to numerous diseases (Nachury et al., 2007; Sánchez & Dynlacht, 2016). For instance, centrosome dysfunction is associated with various pathologies, including neurological and immune disorders and developmental abnormalities.

2. Inter-centriolar Fiber, centriolar satellites, and cilia

The ciliary rootlet, first identified by Engelmann in 1880, is an anatomical structure present in both motile and immotile cilia, with a diameter of 80-100 nm and a characteristic stripe structure of 55-70 nm (Yang et al., 2002). It is most highly developed in retinal photoreceptors, where its core component, rootletin, is also found in the highest concentration. Centriolar satellites, such as PCM-1, the first identified satellite, play a crucial role in centrosome functions, including microtubule organization, centriole duplication, and primary cilia formation. PCM-1 acts as a scaffold for other satellite proteins and supports cilia formation by preventing MIB-1 mediated degradation of the ciliary protein TALPID3 (Wang et al., 2016). The primary cilium is a microtubule-based organelle that extends from the basal body in most animal cells. Golgi-derived vesicles dock at the mother centriole's tip to form the axoneme (Keeling et al., 2016), while the ciliary rootlet extends downward from the centriole, providing structural stability to the cilium.

2.1 Inter-centriolar fiber

The inter-centriolar fiber is a structural element within the centrosome that links two centrioles, helping to maintain centrosome cohesion. CROCC/rootletin and CEP68 are known components of the intercentriolar fiber (Bahe et al., 2005; Graser et al., 2007). Additional proteins, such as LRRC45, centlein, and CCDC102B, are also present in the fiber (Fig. 3; He et al., 2013; Fang et al., 2014; Xia et al., 2018; Hossain et al., 2020). CROCC is the main building block of intercentriolar/rootlet fibers and forms a parallel homodimer as a basic unit (Ko et al., 2020). The intercentriolar/rootlet fibers have indented lines that are 75 nm apart, suggesting that CROCC dimers are ordered in a staggered manner (Yang et al., 2002; Vlijmet al., 2018; Ko et al., 2020). The fibers are

anchored to the proximal ends of the mother centrioles via CEP250/C-NAP1 (Fry et al., 1998). Based on microscopic analysis, the intercentriolar/rootlet fibers form flexible, dynamic, and interdigitating networks (Mahen, 2018; Vlijm et al., 2018). During interphase, the inter-centriolar fiber securely links the centrioles, and in mitosis, this linkage is dissolved to allow the centrosomes to separate and form spindle poles (Yang et al., 2002; Graser et al., 2007). Rootletin, a critical protein within the inter-centriolar fiber, maintains cellular structure while regulating material exchange between centrosomes (Ko et al., 2020). CEP250, another essential component, ensures proper centriole positioning and angle by maintaining their cohesion (Fry et al., 1998). Failure of the inter-centriolar fiber to disassemble during mitosis can disrupt centrosome function, leading to irregular chromosome segregation.

2.2 Centriolar satellite

Centriolar satellites are dynamic, nonmembranous granules measuring 70–100 nm in diameter, situated around the centrosome. They are primarily involved in protein trafficking and play an essential role in protein assembly within the centrosome (Fig. 4 A; Dammermann & Merdes, 2002). Centriolar satellites are characterized by key proteins such as PCM1, which binds and organizes various other proteins essential for centrosome function and ciliogenesis (Fig. 4. A and B; Kubo & Tsukita, 2003). PCM1 acts by gathering and positioning proteins at the centrosome, contributing to centrosome structure and function (Hori & Toda, 2017). Satellites are distributed around the centrosome and travel along microtubules to deliver proteins, a process crucial for proper cilia formation (Prosser & Pelletier, 2020). PCM1-associated proteins are fundamental in ciliogenesis; when satellite function is compromised, ciliogenesis and maintenance can be significantly disrupted, potentially leading to diverse cellular dysfunctions and diseases (Gheiratmand et al., 2019).

2.3 Primary cilia

Primary cilia are sensory organelles protruding from the cell surface, essential for signal transduction and environmental sensing. Cilia are formed by the transformation of the mother centriole into a basal body, with primary cilia playing a critical role in detecting extracellular signals that regulate cellular responses (Fig. 5 A; Singla & Reiter., 2006). Cilia formation begins in G1 when specific proteins are transported and assembled at the basal body, undergoing disassembly and reassembly through the cell cycle (Fig. 5 B; Sánchez & Dynlacht, 2016). The ciliary membrane is highly specialized, containing receptors for pathways like Hedgehog and Wnt, which influence cell proliferation and differentiation (Breslow & Holland, 2019). Centriolar satellite proteins are essential in ciliogenesis, with PCM1 responsible for transporting these proteins to the ciliary base, supporting cilia formation and maintenance (Nachury et al., 2010). Defects in cilia formation can result in various conditions, including developmental disorders, obesity, and polycystic kidney disease (Fig. 6; Kumar et al., 2021).

3. Pericentriolar material

PCM is a matrix surrounding the centrioles, containing essential proteins that facilitate microtubule nucleation and spindle formation. PCM functions as a nucleation site for microtubule formation and serves as a core for spindle organization, ensuring accurate chromosome segregation (Mittasch et al., 2020). Key components of PCM include γ-tubulin and CEP215, with γ-tubulin promoting microtubule nucleation and CEP215 positioning γ-tubulin within the PCM (Fig. 7, Luders & Stearns, 2007). PCM is dynamically reorganized during the cell cycle, helping to stabilize centrosomal structure (Fig. 8; Mennella et al., 2012). PCM is critical for both spindle formation, with defects in PCM leading to centrosome dysfunction (Hatch et al., 2010). PCM instability can result in compromised centrosome function, contributing to chromosome instability and division errors.

3.1 Pericentrin

Pericentrin is a structural scaffolding protein within PCM that anchors microtubules and organizes PCM proteins. PCNT secures γ-tubulin to the centrosome, thereby supporting microtubule nucleation and maintaining centrosome integrity (Delaval & Doxsey, 2010). PCNT deficiency disrupts microtubule anchoring during cell division, potentially causing chromosomal missegregation (Zimmerman et al., 2004), which is critical for cell division and genomic stability. PCNT deficiency is linked to severe developmental disorders, such as MOPDII, underscoring its essential role in cellular integrity and function (Rauch et al., 2008). By forming a structural matrix within PCM, PCNT stabilizes centrosomal activity, securing γ-tubulin complexes to facilitate spindle formation and cell division (Jurczyk et al., 2004; Kim et al., 2006).

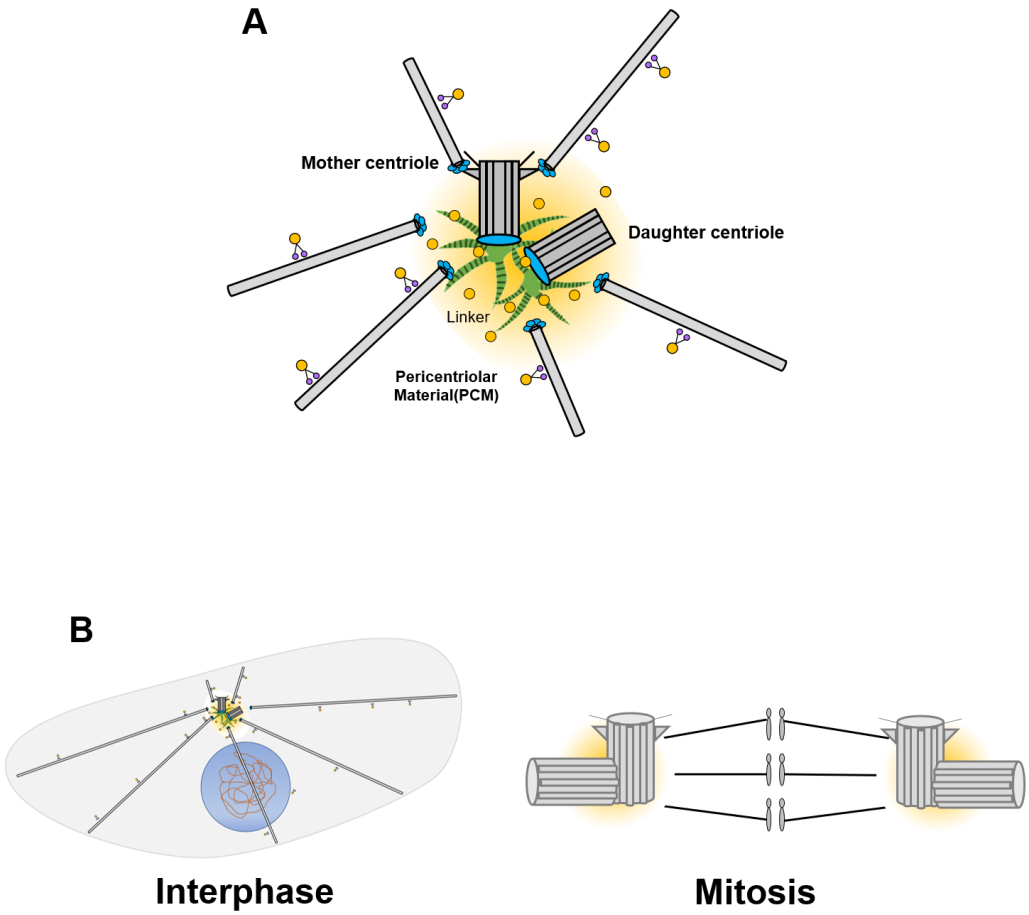

Figure 1. Centrosome structure and function

(A) Centrosome structure includes paired centrioles and pericentriolar material, facilitating microtubule nucleation and anchoring. (B) During interphase, the centrosome organizes the cytoplasmic microtubule network, and during mitosis, it forms a spindle pole to guide bipolar spindle assembly.

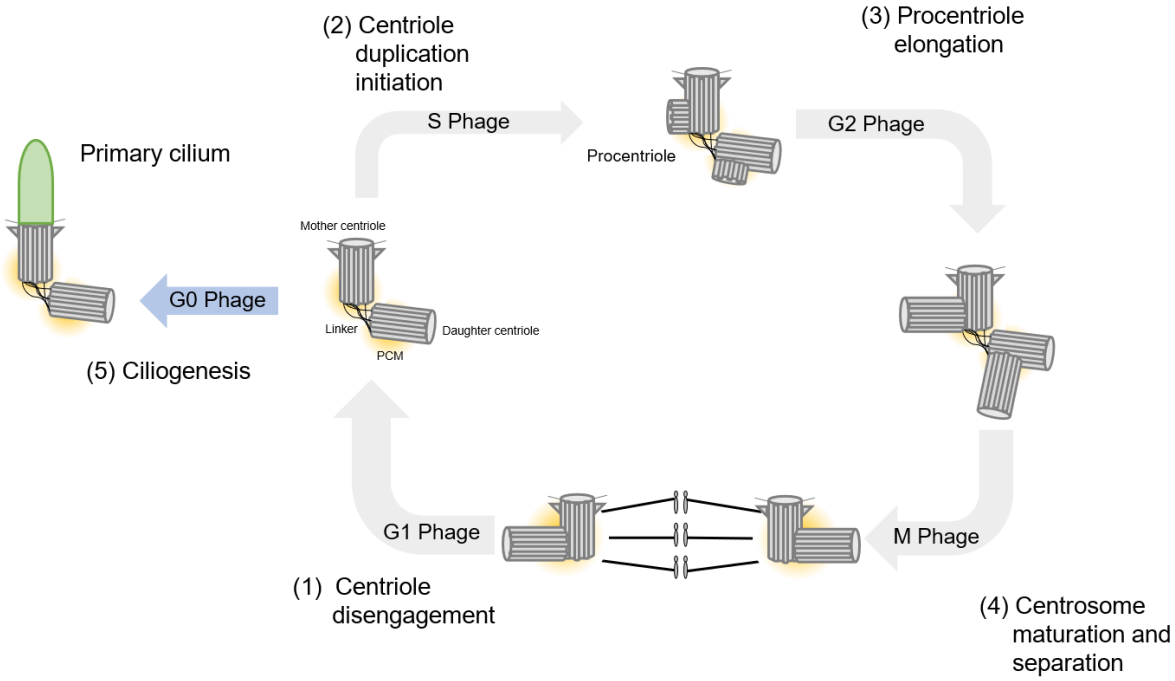

Figure 2. Centrosome cycle depending on cell cycle

The centrosome cycle aligns with the cell cycle, encompassing the following stages: (1) centriole disengagement, (2) initiation of centriole duplication, (3) procentriole elongation, (4) centrosome maturation and separation, and (5) ciliogenesis during G0 phase.

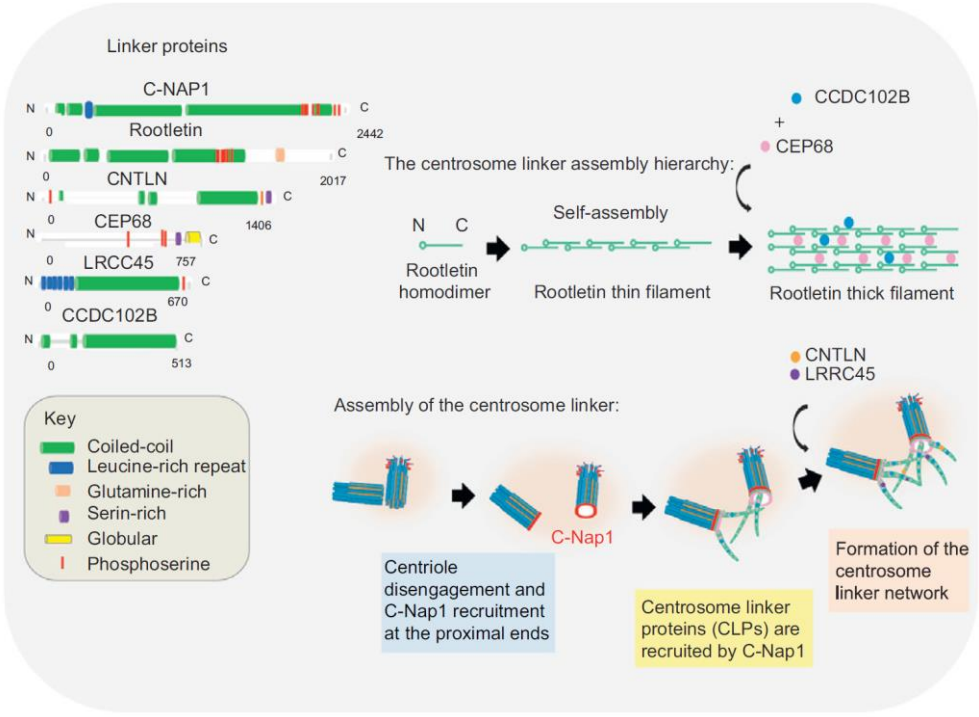

Figure 3. Inter-centriolar fiber

The assembly of the inter-centriolar linker involves key proteins such as C-NAP1, Rootletin, CNTLN, CEP68, LRRC45, and CCDC102B. Rootletin forms homodimers and assembles into thick filaments with CCDC102B and CEP68, creating the main structure. After centriole disengagement, C-NAP1 localizes to proximal ends, recruiting other linker proteins like CNTLN and LRRC45 to form the centrosome linker network, essential for maintaining centrosome cohesion. Taken from Remo et al., 2020

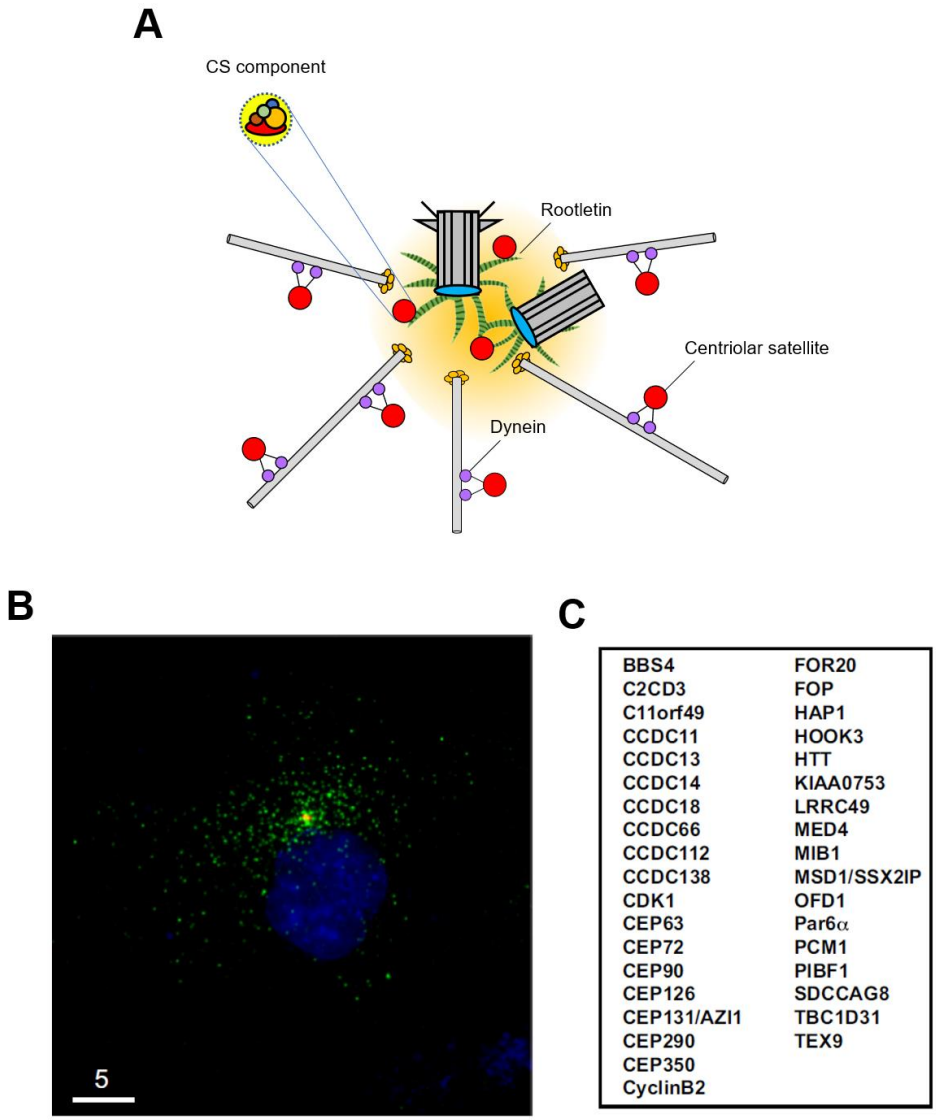

Figure 4. Centriolar satellite proteins

(A) Diagram of the centrosome highlighting centriolar satellites (CS components) surrounding the centriole pair. Dynein is shown as essential elements by transporting them along microtubules. (B) Anti-PCM1 (green) and γ-tubulin (red) antibodies were immunostained in RPE1 cells. Scale bar = 5 μm. (C) List of proteins of centriolar satellites. (B and C) Taken from Hori and Toda, 2017.

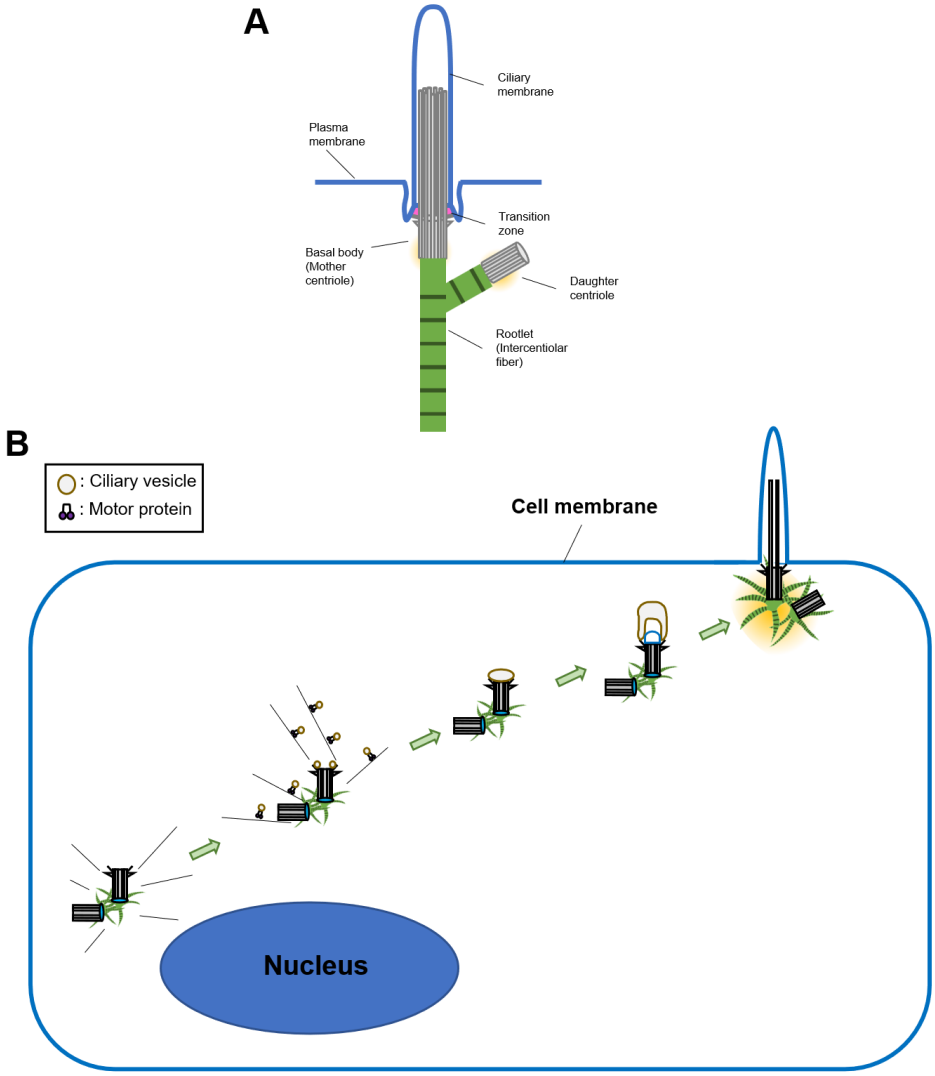

Figure 5. Cilia structure and ciliogenesis

(A) Structure of the primary cilium, illustrating the basal body (mother centriole) anchored at the plasma membrane, the transition zone, and the daughter centriole. The rootlet (intercentriolar fiber) supports the basal body, and the ciliary membrane extends from the cell surface. (B) Sequential steps of ciliogenesis, showing the progression from centriole positioning near the nucleus to the formation of the primary cilium at the cell membrane. Ciliary vesicles and motor proteins aid in transporting materials necessary for ciliogenesis.

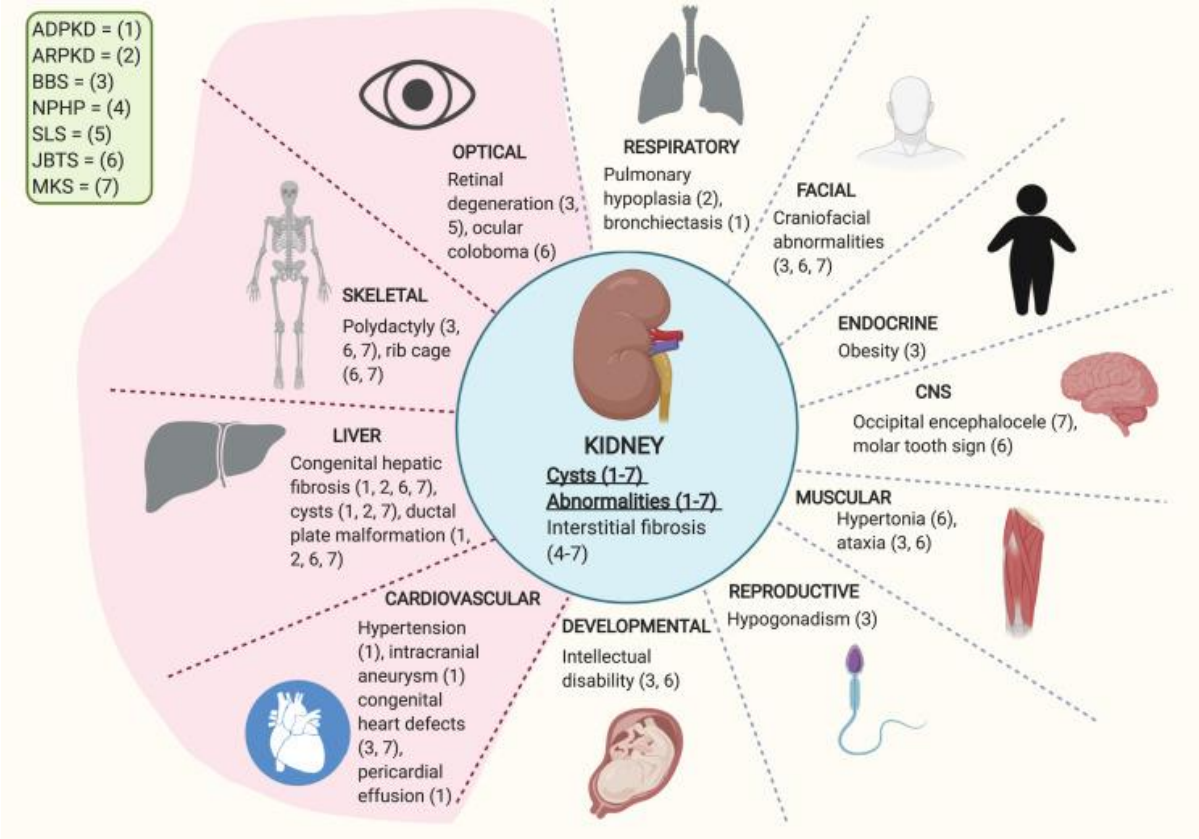

Figure 6. Ciliopathies

Overview of multisystemic symptoms associated with ciliopathies, as seen across various organ systems. Key abnormalities are indicated with corresponding ciliopathy types: ADPKD (1), ARPKD (2), BBS (3), NPHP (4), SLS (5), JBTS (6), and MKS (7). Central kidney symptoms include cysts and other structural abnormalities (1-7), with associated symptoms in optical, respiratory, skeletal, liver, cardiovascular, developmental, facial, endocrine, CNS, muscular, and reproductive systems. Taken from McConnachie et al., 2021

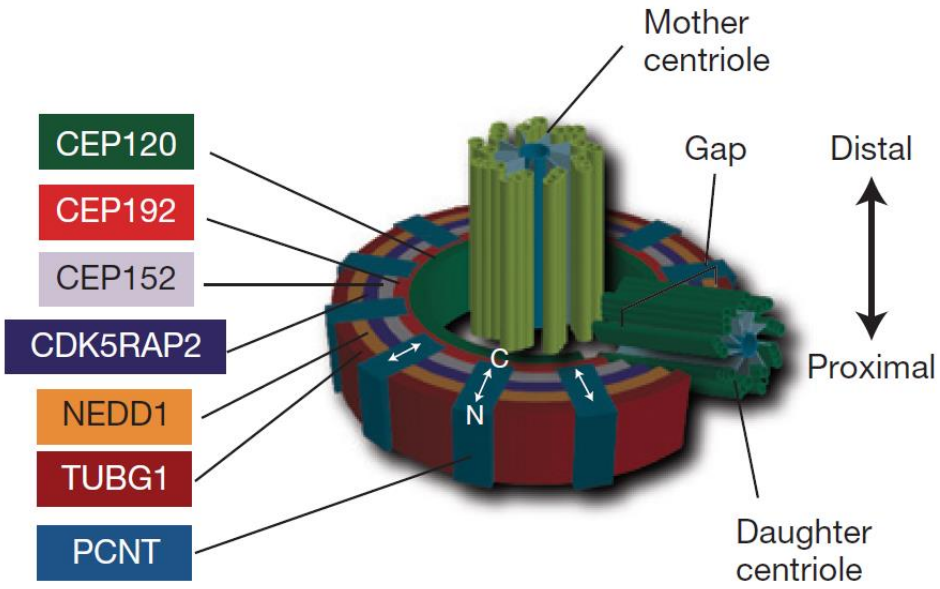

Figure 7. Pericentriolar material (PCM)

Key proteins involved in pericentriolar materials include CEP120, CEP192, CEP152, CDK5RAP2, NEDD1, TUBG1, and PCNT. The mother centriole is positioned proximal to the daughter centriole. Protein localization indicates specific roles within the proximal-distal axis of the centrosome. Taken from Lawo et al., 2012

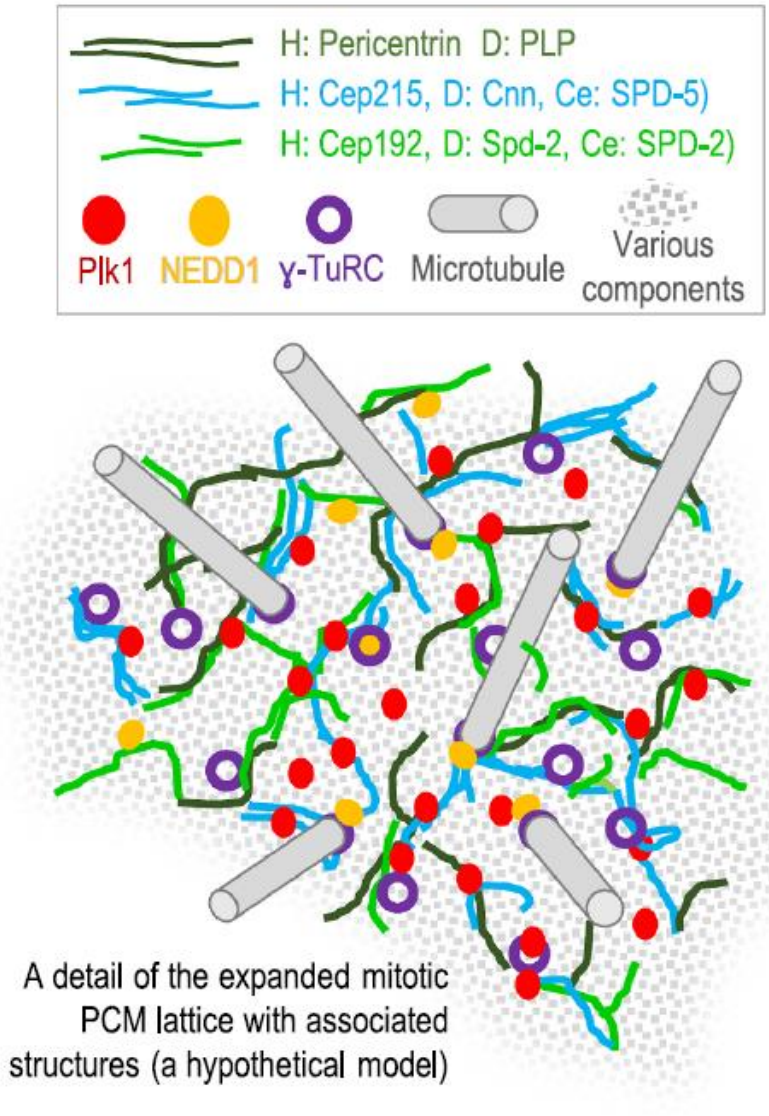

Figure 8. Pericentriolar material lattice structure at mitosis

The expanded mitotic PCM lattice, showing associated structures. Key proteins, including Pericentrin, Cep215, Cep192, Plk1, and γ-TuRC, are organized within the PCM lattice to facilitate microtubule nucleation and spindle assembly. Microtubules are embedded in the matrix, demonstrating the complex network of interactions crucial for centrosome function during mitosis. Taken from Limeta and Loncarek, 2021

Purpose

In animal cells, the centrosome regulates critical functions such as microtubule organization, cell division, and genomic stability. While extensive research has revealed the importance of centrosomal components, key proteins like PCNT and CROCC remain understudied in their specific roles in centrosome integrity and cellular processes. Dysfunction in these proteins has been implicated in developmental disorders, emphasizing the need for understanding of their mechanistic contributions.

This study addresses two central questions: (1) How does inter-centriolar fiber regulate cilia assembly? (2) What are the cellular and developmental consequences of PCNT mutation in centrosome integrity, chromosome stability, and tissue development?

To investigate these questions, CRISPR/Cas9 gene-editing technology was employed to generate *CROCC* and *CEP250* KO cell lines, providing insights into their roles in cilia assembly and centriolar satellite organization. Additionally, *Pcnt* KO and MOPDII-mimicking *Pcnt* mutant KI mouse models were used to study the effects of PCNT deficiency on centrosome stability, aneuploidy, and development.

The results demonstrated that CROCC is essential for cilia assembly by regulating the localization of centriolar satellites near centrosomes. Mutation of PCNT led to centrosome abnormalities, increased aneuploidy, and developmental defects, including growth retardation and development abnormalities in mice, emphasizing its critical role in genomic stability and tissue development.

By uncovering the distinct yet interconnected roles of CROCC and PCNT in centrosome biology, this study provides a comprehensive understanding of their contributions to cellular organization and development. These findings offer valuable insights into the molecular basis of centrosome-related disorders and provide the foundation for potential therapeutic strategies.

Chapter I.

Role of inter-centriolar fibers in cilia formation

ABSTRACT

Primary cilia are sensory organelles involved in signaling pathways, and their dysfunction can lead to ciliopathies affecting multiple organs. In animal cells, two mother centrioles are linked by inter-centriolar fibers, primarily composed of CROCC/rootletin. While these fibers are known to maintain centrosome cohesion, their role in cilia assembly is unclear. my preliminary experiments showed a decrease in cilia formation in *CROCC* knockdown (KD) cells, suggesting their involvement in ciliogenesis. To investigate the regulatory role of inter-centriolar/rootlet fibers in cilia assembly, I generated *CROCC* and *CEP250* KO cell lines to analyze their effects on cilia formation and the localization of PCM1, a representative centriolar satellite protein responsible for transporting essential proteins to the centrosome during cilia assembly. I found that the loss of CROCC and CEP250 disrupted PCM1 localization at the centrosome without affecting its expression levels. Additionally, PCM1 was found to bind directly to CROCC, a critical interaction for centriolar satellite accumulation near the centrosomes, essential for efficient cilia formation. my study provides evidence that inter-centriolar fibers act as docking sites for centriolar satellites, facilitating cilia assembly and enhancing my understanding of the molecular mechanisms underlying ciliogenesis.

INTRODUCTION

The centrosome, as the major microtubule-organizing center in animal cells, consists of a pair of centrioles and a surrounding protein matrix called the pericentriolar material. Centriole assembly and segregation are tightly linked to the cell cycle. During the S phase, a daughter centriole assembles next to a mother centriole and remains attached until the cell exits mitosis. During mitosis, a centrosome with a pair of centrioles functions as a spindle pole, pulling a set of chromosomes into daughter cells. At the end of mitosis, the daughter centriole separates from the mother centriole and becomes a young mother centriole. As a result, both young and old mother centrioles are always present in a single cell. During interphase, these two mother centrioles are linked by inter-centriolar fibers, which dissolve as the cell approaches mitosis, allowing the centrosomes to become spindle poles (Bahe et al., 2005; Graser et al., 2007).

CROCC/rootletin and CEP68 are known components of these inter-centriolar fibers, along with additional proteins such as LRRC45, centlein, CCDC102B, and CEP44, which are also part of the fiber network (He et al., 2013; Fang et al., 2014; Xia et al., 2018; Hossain et al., 2020). CROCC serves as the main structural component of the intercentriolar/rootlet fibers, forming parallel homodimers as the basic unit (Ko et al., 2020). These fibers are anchored to the proximal ends of the mother centrioles via CEP250/C-NAP1 (Fry et al., 1998), forming a flexible, dynamic network that interconnects the centrioles (Mahen, 2018; Vlijm et al., 2018). This network is crucial for maintaining centriole cohesion.

Centriolar satellites, which are 70–100-nm nonmembranous granules, assemble and disassemble in a cell cycle-dependent manner (Hori and Toda, 2017). They move along microtubules toward the centrosome in a dynein-dependent fashion (Dammermann and Merdes, 2002; Kubo and Tsukita, 2003). PCM1, a key scaffold protein of the

centriolar satellites, anchors over 65 different proteins at these sites, with recent proteomic analyses expanding the number of satellite-associated proteins to hundreds (Prosser and Pelletier, 2020; Gheiratmand et al., 2019; Quarantotti et al., 2019). These proteins play a critical role in protein trafficking to the centrosome, essential for cilia assembly and maintenance (Nachury et al., 2007; Kim et al., 2008a). Mutations in several centriolar satellite proteins are linked to ciliopathies, underscoring their importance in cilia-related functions. While the loss of PCM1 does not disrupt centriole duplication or cell cycle progression, it severely affects cilia formation in certain cell types (Wang et al., 2016; Odabasi et al., 2019).

Primary cilia, which protrude from the cell surface, act as signaling antennae in many mammalian cells. They originate from the old mother centriole, which possesses distal and subdistal appendages (Breslow and Holland, 2019). The formation of primary cilia is a tightly regulated, multistep process involving the elongation of the ciliary axoneme's nine doublet microtubules. These structures are anchored to the cell surface through distal appendages that form an interface between the centriole and the nascent ciliary membrane (Reiter et al., 2012). While the ciliary membrane is continuous with the plasma membrane, the cilia maintain a distinct composition of biomolecules through dedicated trafficking machinery and diffusional barriers at the cilium base (Nachury et al., 2010). Active transport of ciliary components is required for the assembly and maintenance of cilia (Kumar and Reiter, 2021).

Beyond the structural role of intercentriolar/rootlet fibers in cilia stability, there are regulatory implications as well. For example, in Drosophila, mutations in rootletin led to behavioral defects related to mechano- and chemosensation (Styczynska-Soczka and Jarman, 2015; Chen et al., 2015). These findings suggest that rootletin and its associated structures may have roles beyond simple mechanical stability. In this study, I investigate a further role of the intercentriolar/rootlet fibers in the regulation of cilia assembly. I propose that the intercentriolar/rootlet fibers act as docking sites for centriolar satellites,

facilitating cilia assembly by regulating the positioning and function of these key components.

MATERIALS & METHODS

Antibodies

Rabbit anti-CROCC (HPA021191; IS, 1:200; IB, 1:300; Sigma-Aldrich), ouse anti-acetylated tubulin (T6793; IS, 1:200; Sigma-Aldrich), mouse anti-α-tubulin (T6199; IS, 1:1,000; IB, 1:10,000; Sigma-Aldrich), goat anti-FLAG (ab1257; IS, 1:500; IB, 1:2,000; Abcam), rabbit anti-CEP290 (ab84870; IS, 1:100; IB, 1:200; Abcam), rabbit anti-OFD1 (ab97861; IS, 1:100; IB, 1:100; Abcam), mouse anti-FLAG (F3165; IS, 1:2,000; IB, 1:20,000; Sigma-Aldrich), rabbit anti-γ-tubulin (ab11317; IS, 1:300; Abcam), rabbit anti-centrin-2 (04-1624; IS, 1:500; Millipore), mouse anti-γ-tubulin (ab11316; IS, 1:300; Abcam), rabbit anti-CEP68 (15147-1-AP; IS, 1:100; IB, 1:500; Proteintech), rabbit anti-CEP72 (A301-297A; IS, 1:500; IB, 1:500; Bethyl), and mouse anti-GAPDH (AM4300; IB, 1:10,000; Invitrogen) antibodies were purchased from commercial suppliers. Rabbit anti-PCM1 (Kim et al., 2012), rabbit anti-CEP250/C-NAP1 (Jeong et al., 2007), and rabbit anti-CEP90 (Kim and Rhee, 2011) polyclonal antibodies were prepared as described previously. The human CEP131 cDNA clone (Gene Bank accession number: AB029041) was purchased from the German Resource Center for Genome Research.We PCR-amplified the 341–1,008 fragment of the CEP131 cDNA and subcloned it at the EcoRI site of the pGEX-4T-1 vector (28-9545-49; Cytiva). The pGST-CEP131341–1008 plasmid was transformed into the E. coli BL21(DE3)pLysS strain. The bacteria were cultured to OD 0.8, treated with IPTG (isopropyl β-D-1-thiogalactopyranoside) to a final concentration of 0.5 mM for 4 h, and harvested. The GST-CEP131$^{341–1008}$ fusion protein was purified using the GST beads (EBE-1041; Elpis Biotech). A pair of rabbits were immunized with a complete adjuvant (F5881-10ML; Sigma-Aldrich), which was combined with 150 μg of the GST-CEP131$^{341–1008}$ fusion protein and boosted with the same adjuvant containing the fusion protein in a 2-wk interval. 8 wk later, the rabbits

were sacrificed, and the blood was drawn for collection of the CEP131 anti-sera. For the CEP131 antibody purification, 0.2 ml of the anti-serum was incubated for 2 h at room temperature with a PVDF (polyvinylidene fluoride) membrane on which 50 μg of the GST-CEP131$^{341–1008}$ fusion protein was blotted. The PVDF membrane was washed with TBST (Tris-buffered saline with 0.1% Tween 20) three times and incubated with 0.2 ml of an elution buffer (50 mM Tris pH 8.0, 100 mM NaCl, 4 mg/ml L-glutathione reduced) for 0.5 h. For neutralization, 20 μl of 1.5 M Tris (pH 8.8) was added to the CEP131 antibody eluent. Alexa Fluor 488- and 594-conjugated secondary antibodies (Z25302; Invitrogen, Z25307; IS, 1:1,000; Invitrogen) were used for immunostaining. Anti-mouse IgG-HRP (A9044; IB, 1:1,000; Sigma-Aldrich), anti-rabbit IgG-HRP (AP132P; IB, 1:1,000; Millipore), and anti-goat IgG-HRP (SC-2056; IB, 1:500; Santa Cruz) were used as secondary antibodies for the immunoblot analyses. The CROCC/rootletin mutant subclones were previously described (Ko et al., 2020).

Cell culture, transfection, and stable cell lines

The hTERT-RPE1 cells in my experiments were obtained from Dr. Kyung S. Lee (National Institutes of Health, Bethesda, MD, USA) (Soung et al., 2009). RPE1, and HEK293T cells were cultured in Dulbecco's modified eagle medium/Nutrient mixture F-12 (F12/DMEM) or DMEM supplemented with 10% FBS at 37°C under 5% CO2. To induce cilia formation, the cells were transferred to a medium supplemented with 0.1% FBS and cultured for 48 h. I usually seed 2.5 × 10^4 cells per well in fourwell dishes (1.96 cm^2/well) to become 1.3 × 10^4 cells/cm^2. The RPE1 cells were transfected with siRNAs using RNAiMAX (Invitrogen) and with the plasmids using Lipofectamine3000 (Invitrogen) according to the manufacturer's instructions. The siRNAs used in this study were siCTL (5'-GCAAUCGAAGCUCGGCUACTT-3'), siCROCC (5'-AAGCCAGUC UAGACAAGGATT-3'), siCEP250 (5'-CUGGAAGAGCGUCUAACUGAUTT-3'), siPCM1 (5'-UCAGCUUCGUGAUUCUCAGTT-3'), siCEP68 (5'-CACCCUCAAAUC

ACCUACUAATT-3'), siCEP72 (5'-UUGCAGAUCGCUGGACUUCAATT-3'), and siCEP131 (5'-GCUAACAACAGGAGCAACATT-3'). To establish stable cell lines, CROCC, PCM1, and their mutants were subcloned into a pcDNA5 FRT/TO vector from Dr. Hyun S. Lee (Seoul National university, Seoul, Korea). For inducible expression, the RPE1 cells were transfected with the plasmids using Lipofectamine3000 (Invitrogen) and selected with G418 (5.09290; 400 μg/ml; Millipore) for 2 wk. For the immunoprecipitation assays, the plasmids were transiently transfected into HEK293T cells using the polyethyleneimine method.

Generation of the knockout cell lines

gRNAs with high efficiency were designed using the CRISPR guide tool on the Benchling website (https://www.benchling. com/): CROCC gRNA1 (5'-AAACTGTCATGTGCTG GGTATGCAC-3' and 5'-CACCGTGCATACCCAGCACATGACA-3') and gRNA2 (5'-CACCGATACTGTTTCATCCCCGGA-3' and 5'-AAACTCCGGGGATGAAACAGTA TC-3') (Doench et al., 2016). CEP250 gRNA1 (5'-CACCGAAGCTGAAGAACTCCCA GG-3' and 59-AAACCCTGGGAGTTCTTCAGCTTC-3'). PCM1 gRNA1 (5'-CACCG AGCATTGGAAGTGATTCCCA-3' and 5'-AAACTGGGAATCACTTCCAATGCTC-3'). For CRISPR/Cas9 cloning, I used the plasmid pSpCas9(BB)-2A-Puro (PX459) V2.0 (Plasmid #62988) as a gRNA vector backbone. The donor vector was digested with BbsI and ligated with annealing gRNA using T4 DNA ligase (10481220001; Roche). RPE1 cells were transfected using Lipofectamine3000 (Invitrogen). After transfection, the cells were selected with 4 μg/ml puromycin (P8833; Sigma-Aldrich) for 48 h.

Immunoprecipitation

The cells were lysed on ice for 15 min with lysis buffer (50 mM Tris-HCl pH 8.0, 5 mMEDTA, 150 mMNaCl, 0.5% Triton X-100, 1× protease inhibitor [P8340; Sigma-Aldrich], 0.5 mM phenylmethylsulfonyl fluoride, and 1 mM dithiothreitol). After

centrifugation at 12,000 rpm for 15 min, the supernatants were incubatedwith FLAG-M2 Affinity Gel (A2220; Sigma-Aldrich) or Protein A Sepharose CL-4B (17-0780-01; Cytiva) for 90 min at 4°C. The beads were washed three times with lysis buffer and subjected to immunoblot analyses. All procedures were performed at 4°C.

Immunoblot analyses

The cells were lysed on ice for 10min with RIPA buffer (150mM NaCl, 1% Triton X-100, 0.5% sodium deoxycolate, 0.1% SDS, 50 mM Tris-HCl at pH 8.0, 10 mM NaF, 1 mM Na3VO4, 1 mM EDTA, and 1 mM EGTA) containing a protease inhibitor cocktail (P8340; Sigma-Aldrich) and centrifuged with 12,000 rpm for 10 min at 4°C. The supernatants were mixed with 4×SDS sample buffer (250 mM Tris-HCl at pH 6.8, 8% SDS, 40% glycerol, and 0.04% bromophenol blue) and 10mMDTT (0281-25G; Amresco). Mixtures were boiled for 5 min. The protein samples were loaded in SDS polyacrylamide gels (3% stacking gel and 4–10% separating gel), electrophoresed, and transferred to Protran BA85 nitrocellulose membranes (10401196; GE Healthcare Life Sciences). The membranes were blocked with blocking solution (5% nonfat milk in 0.1% Tween 20 in TBS or 5% bovine serum albumin in 0.1% Tween 20 in TBS) for 2 h, incubated with primary antibodies diluted in blocking solution for 16 h at 4°C, washed four times with TBST (0.1% Tween 20 in TBS), incubated with secondary antibodies in blocking solution for 30 min, and washed again. To detect the signals of secondary antibodies, the ECL reagent (ABfrontier, LF-QC0101) and x-ray films (Agfa, CPBU NEW) were used.

Immunocytochemistry and image processing

The cells were cultured on 12-mm coverslips and fixed with cold methanol for 10 min or the PEM buffer (80 mM PIPES pH 6.9, 1 mM MgCl2, 5 mM EGTA, and 0.5% Triton X-100). To detect primary cilia, microtubules were depolymerized via cold treatment for 60 min before fixation. The samples were blocked in PBST (PBS with 0.3% Triton X-100)

with 3% BSA for 20 min, incubated with the primary antibodies for 1 h, and incubated with Alexa Fluor 488- and Alexa Fluor 594-conjugated secondary antibodies for 30 min (Life Technologies). 49,6-Diamidino-2-phenylindole (DAPI) solution was used for DNA staining. The samples were mounted in ProLong Gold antifade reagent (P36930; Invitrogen) and observed using a fluorescence microscope (IX51; Olympus) equipped with a CCD (Qicam Fast 1394; Qimaging) camera using PVCAM (version 3.9.0; Teledyne Photometrics). I also used a super-resolution microscope (ELYRA PS.1; Carl Zeiss) for imaging CROCC at the centrosomes. The images were analyzed using ImagePro 5.0 software (Media Cybernetics, Inc.). Images were saved as Adobe Photoshop 2021 (version 22.4.2). For super-resolution images, the samples were observed using a super-resolution microscope (ELYRA PS.1; Carl Zeiss). SIM processing was performed with ZEN software 2012, black edition (Carl Zeiss), and the images were analyzed using ZEN lite software (Carl Zeiss).

Measurements and statistical analysis

Imaging was performed with an Olympus IX51 microscope equipped with a CCD (Qicam Fast 1394; Qimaging) camera using PVCAM (version 3.9.0; Teledyne Photometrics). The fluorescence intensity and ciliary length were measured using ImageJ 1.53e software (National Institutes of Health). The fluorescence intensity was quantified by assessing the cumulative intensity within a circular region (20 μm^2) centered between the centrioles. Statistical significance was determined using an unpaired two-tailed t-test and one-way analysis of variance (ANOVA) on Prism 6 (GraphPad software). Box and whisker plots display the median as a black center line, the interquartile range within the black box, and whiskers extending to the 10th and 90th percentiles. Bar graphs represent values as mean and SEM. In one-way ANOVA, groups sharing the same letter were not significantly different according to Tukey's post hoc test. *$P < 0.05$; P value of unpaired two-tailed t test.

RESULTS

Effects of *CROCC* and *CEP250* knockout on cilia formation

The structural importance of the inter-centriolar fiber is well known for maintaining cilia stability (Yang et al., 2002). However, its specific role in the process of cilia formation has not been clearly elucidated. To investigate this, I generated RPE1 cell lines with *CROCC* and *CEP250* KO cells using the CRISPR/Cas9 system, targeting the major components of the inter-centriolar fiber. I confirmed the absence of the CROCC and CEP250 proteins with immunoblot and immunostaining analyses (Fig. 9). Interestingly, the KO of *CROCC* or *CEP250* did not affect the expression of the other protein, indicating that the loss of one did not impact the expression of the other (Fig. 9, B and D).

First, I examined the conditions for optimal cilia formation in RPE1 cells. Analysis of cilia formation rates under different serum concentrations and cell densities revealed that cilia formation was approximately 60% under 0.1% serum and a density of 1.3×10^4 cells/cm² (Fig. 10, A and B). The cilia formation in *CROCC* and *CEP250* KO cells reduced about 30% compared to WT cells (Fig. 10, C and D). I suggest that both CROCC and CEP250 may be essential for efficient cilia formation.

The old mother centrioles/basal bodies and young mother centrioles are expected to separate once the inter-centriolar linkers are removed (Flanagan et al., 2017; Panic et al., 2015). Additionally, I treated the cells with Nocodazole to disrupt microtubule and observe centriole separation. In *CROCC* KO cells, no significant changes in centriole separation were observed in the absence of Nocodazole treatment. However, in *CEP250* KO cells, centriole separation increased significantly in the presence of intact microtubules (Fig. 11 A). After Nocodazole treatment, both *CROCC* and *CEP250* KO cells showed an increase in centriole separation (Fig. 11 A). Furthermore, in *CEP250* KO

cells, cilia formation rates were similarly reduced regardless of centriole separation, indicating that centriole disjunction does not directly impact cilia formation in these cells (Fig. 11, B and C). These findings suggest that defects in the inter-centriolar fiber result in impaired cilia formation, independent of the presence of a young mother centriole near the basal body. These results indicate that the inter-centriolar fiber may be crucial for cilia formation.

Effect of CROCC depletion on cilia formation in *CEP250* KO cells

There is ongoing debate about whether the rate of cilia formation is reduced in *CEP250* KO cells (Panic et al., 2015; Mazo et al., 2016; Flanagan et al., 2017). To investigate the cilia formation in *CEP250* KO cells, I measured the cilia formation rates under various cell density conditions. In *CROCC* KO cells, increasing cell density had no significant effect on the cilia formation rate. However, in *CEP250* KO cells, the cilia formation rate remained consistent even with increased cell density (Fig. 12 A). This result supports the idea that CROCC plays a critical role in cilia formation, while also raising the question of why cilia formation remains unchanged in *CEP250* KO cells despite increasing cell density.

I hypothesized that in *CEP250* KO cells, the remaining CROCC may still contribute to cilia formation. To test this, I examined the expression of CROCC in *CEP250* KO cells. Immunostaining revealed that CROCC was still present at the centrosome and basal body in *CEP250* KO cells (Fig. 12 B), suggesting that even in the absence of CEP250, CROCC can influence cilia formation.

To investigate why the cilia formation rate remained unchanged in *CEP250* KO cells, I analyzed the function of CROCC under different cell density conditions. The results revealed that CROCC plays a crucial role in regulating cilia formation, with its impact becoming more significant at higher cell densities (Fig. 12 C). This indicates that CROCC maintains cilia formation independently in *CEP250* KO cells. Furthermore, I

compared changes in cilia formation rates under varying cell density conditions, observing that CROCC was localized at the centrosomes in approximately 30% of *CEP250* KO cells, a number that increased to nearly 50% in serum-deprived conditions (Fig. 12, B and C). At high cell density, this proportion rose to 65% (Fig. 12 C). Additionally, in serum-deprived conditions, most *CEP250* KO cells with cilia had CROCC at the centrosomes, whereas only about half of the cells without cilia displayed centrosomal CROCC (Fig. 12 D).

These findings indicate that CROCC is essential for cilia formation and acts as a key regulator, even in absence of CEP250 conditions, to support cilia formation to some extent.

The role of inter-centriolar fibers in the accumulation of centriolar satellites at the centrosome

I analyzed the intracellular distribution of major centriolar satellite proteins in *CEP250* and *CROCC* KO RPE1 cells. Immunostaining revealed that key centriolar satellite proteins, such as PCM1, CEP290, OFD1, CEP131, and CEP90, were dispersed throughout the cytoplasm of *CEP250* and *CROCC* KO cells (Fig. 13, A and B). As a result, the concentrations of these proteins around the centrosome and basal body were significantly reduced, although the total levels of these proteins remained unchanged regardless of *CEP250* or *CROCC* KO (Fig. 13 C). This supports the hypothesis that inter-centriolar fibers are essential for the proper accumulation of centriolar satellites near the centrosome.

Next, I examined the impact of CEP72 depletion, a protein known to interact with PCM1 and to play a critical role in the transport of satellite proteins to cilia, on centriolar satellite accumulation. Previous studies have shown that CEP72 depletion leads to increased accumulation of satellite proteins at the centrosome (Stowe et al., 2012; Conkar et al., 2019), likely due to impaired delivery of key components required for cilia

formation. Similarly, I observed that PCM1 levels were excessively loaded at the centrosomes in CEP72-depleted *CEP250* and *CROCC* KO cells (Fig. 14, A and B). Furthermore, CEP72 depletion resulted in a slight reduction in cilia formation rates (Fig. 14 C). However, in *CEP250* and *CROCC* KO cells with CEP72 depletion, both cilia formation rates and PCM1 loading at the centrosome were partially rescued (Fig. 14, A-C). The increased accumulation of centriolar satellites in the absence of CEP72 appeared to compensate for the defects in cilia formation. These results support the hypothesis that inter-centriolar fibers play a crucial role in centriolar satellite accumulation and cilia formation, and that CEP72 depletion can partially compensate for the absence of these fibers.

In conclusion, inter-centriolar fibers are essential structural elements that facilitate cilia formation by supporting the proper positioning and function of centriolar satellites near the centrosome.

Identification of interaction regions between PCM1 and CROCC

This data is cited from Dr. Ko's work.

The specific interaction between CROCC and PCM1 is crucial for cilia assembly. To investigate the physical associations between CROCC and centriolar satellite proteins, he conducted coimmunoprecipitation assays. Due to the high insolubility of endogenous CROCC, he utilized ectopic FLAG-tagged CROCC for these experiments (Yang et al., 2002). The results showed that both PCM1 and CEP131 were coimmunoprecipitated with FLAG-CROCC, while CEP290 and OFD1 were not (Fig. 15 A). Reciprocal coimmunoprecipitation using the PCM1 antibody further confirmed the physical interaction between PCM1 and FLAG-CROCC (Fig. 15 B). Interestingly, in CEP131-depleted cells, PCM1 was still coimmunoprecipitated with FLAG-CROCC, but in PCM1-depleted cells, CEP131 was not effectively coimmunoprecipitated with FLAG-CROCC

(Fig. 15 C). This suggests that CEP131 may associate indirectly with FLAG-CROCC via PCM1.

To pinpoint the specific domain of CROCC that binds PCM1, he performed coimmunoprecipitation assays using truncated FLAG-CROCC mutants. The analysis identified two binding sites for PCM1, located at the N-terminal and C-terminal regions of CROCC (Fig. 15 D). When both binding sites were truncated in the FLAG-CROCC$^{303–1741}$ mutant, PCM1 was no longer coimmunoprecipitated, confirming the importance of these regions for the CROCC-PCM1 interaction (Fig. 15 E).

The interaction between CROCC and PCM1 is important for cilia assembly

To investigate the role of the interaction between CROCC and PCM1 in PCM1 centrosomal localization and cilia formation, I generated inducible stable lines expressing FLAG-CROCC^{FL} and FLAG-CROCC$^{303-1741}$ in *CROCC* KO RPE1 cells. The expression of FLAG-CROCC proteins was confirmed by analyzing doxycycline-dependent expression using immunostaining and Western blot (Fig. 16, A and B). The results showed that FLAG-CROCCs were adequately expressed, and even with leaky expression, inter-centriolar fibers were properly formed, as confirmed by super-resolution microscopic analysis (Fig. 16 C).

First, I observed that PCM1 was not concentrated at the centrosomes in cells expressing FLAG-CROCC$^{303-1741}$ (Fig. 17, A and B). Although FLAG-CROCC$^{303-1741}$ was able to form normal inter-centriolar fibers, PCM1 failed to properly accumulate at the centrosomes, indicating that the physical interaction between CROCC and PCM1 is crucial for centrosomal localization of PCM1. Additionally, cells expressing FLAG-CROCC$^{303-1741}$ did not recover their cilia formation rate (Fig. 17, C and D). These results suggest that the interaction between CROCC and PCM1 is essential not only for centrosomal localization of PCM1 but also for cilia formation.

Centriolar satellites are transported through microtubule networks (Dammermann and Merdes, 2002; Kubo and Tsukita, 2003). I further treated *CROCC* and *CEP250* KO cells with nocodazole to determine whether the interaction between inter-centriolar fibers and centriolar satellites is dependent on the microtubule network. I found that the centrosomal intensity of PCM1 was reduced in *CROCC* KO cells after nocodazole treatment (Fig. 18, A and B), but the physical interaction between FLAG-CROCC and PCM1 was not affected (Fig. 18 C), suggesting that the interaction between inter-centriolar fibers and centriolar satellites is independent of the microtubule network.

I also analyzed the subcellular distribution of FLAG-CROCC proteins in *CROCC* KO cells. FLAG-CROCC was detected at the centrosomes, while excess proteins were also found at the nuclear membrane (Fig. 18 D). PCM1 followed the distribution of FLAG-CROCC, being present both at the centrosomes and the nuclear membrane. Even after nocodazole treatment, the distribution of PCM1 at the nuclear membrane remained unchanged, suggesting that the interaction between PCM1 and CROCC remains stable in the cell (Fig. 18 D). On the other hand, FLAG-CROCC$^{\Delta R3}$, lacking the third coiled-coil domain of CROCC, failed to form inter-centriolar fibers but localized to the nuclear membrane (Fig. 18 D; Ko et al., 2020). PCM1 followed the subcellular distribution of FLAG-CROCC$^{\Delta R3}$ in the cytoplasm. Although nocodazole affected the cellular distribution of FLAG-CROCC$^{\Delta R3}$, it still co-localized with PCM1 (Fig. 18 D). In contrast, FLAG-CROCC$^{303–1741}$ was detected at the centrosomes but not at the nuclear membrane, likely due to the absence of a nesprin1 binding domain in the N-terminal region of CROCC (Fig. 18 D; Potter et al., 2017). In FLAG-CROCC$^{303–1741}$-expressing cells, PCM1 was dispersed in the cytoplasm.

In conclusion, the physical interaction between CROCC and PCM1 plays a crucial role in determining the cellular distribution of centriolar satellites, and specific regions of CROCC are essential for this interaction. Such findings strongly suggest that

the physical association between CROCC and PCM1 is critical for the cellular distribution of centriolar satellites in cells.

Identification of the PCM1 region that interacts with CROCC

Using the CRISPR/Cas9 method, I generated *PCM1* KO cell lines and confirmed the absence of the PCM1 protein through immunoblot and immunostaining analyses (Fig. 19, A and B). Major centriolar satellite proteins such as CEP290, OFD1, CEP131, and CEP90 were dispersed from the centrosomes in the *PCM1* KO cells, and although their expression levels were not significantly affected, their localizations at the centrosome were notably reduced (Fig. 19, D and E). Furthermore, I confirmed that the position and protein expression of the inter-centriolar fibers were unaffected in the *PCM1* KO cells (Fig. 19, F-H).

Analysis of the cilia formation rate revealed that the *PCM1* KO cells exhibited more than a fourfold decrease in cilia formation (Fig. 20, A and B). Next, I generated truncated FLAG-PCM1 mutants and stably expressed them in *PCM1* KO cells to assess their localization at the centrosome (Fig. 20, C-E). The experimental results showed that most FLAG-PCM1 proteins were localized at the centrosome, but the FLAG-PCM1$^{1201–2016}$ and FLAG-PCM1$^{\Delta 551–1200}$ mutants were not. This suggests that the 551–1,200 region of PCM1 plays a critical role in its centrosomal localization (Fig. 20, C and E). The cilia formation rate was fully restored in cells expressing full-length FLAG-PCM1, while the truncated mutants containing the 551–1,200 region only partially restored cilia formation. However, the FLAG-PCM1 proteins lacking the 551–1,200 region did not rescue cilia formation at all (Fig. 20 F). This indicates that the 551–1,200 region of PCM1 is essential not only for centrosome localization but also for cilia assembly.

To investigate the physical interaction between PCM1 and CROCC, I co-expressed the truncated FLAG-PCM1 mutants with GFP-CROCC and performed co-immunoprecipitation assays using the FLAG antibody. The FLAG-PCM1 proteins were

all successfully expressed and immunoprecipitated with the FLAG antibody (Fig. 21 A). Furthermore, GFP-CROCC was co-immunoprecipitated with FLAG-PCM1^{FL}, FLAG-PCM1$^{551–1200}$, and FLAG-PCM1$^{551–2016}$ (Fig. 21 A). However, there was no interaction between GFP-CROCC and FLAG-PCM1$^{\Delta 551–1200}$, indicating that the 551–1,200 region of PCM1 contains the CROCC-interacting domain. Reciprocal co-immunoprecipitation assays further confirmed that GFP-PCM1^{FL} and GFP-PCM1$^{551–1200}$ interacted with CROCC, while GFP-PCM1$^{\Delta 551–1200}$ did not (Fig. 21 B). This supports the conclusion that the 551–1,200 region of PCM1 is responsible for interacting with CROCC.

In conclusion, the 551–1,200 region of PCM1 plays a crucial role in its physical interaction with CROCC and centrosome localization. The absence of this region leads to impaired cilia formation, indicating that specific domains of PCM1 are essential for protein localization at the centrosome and for cilia assembly.

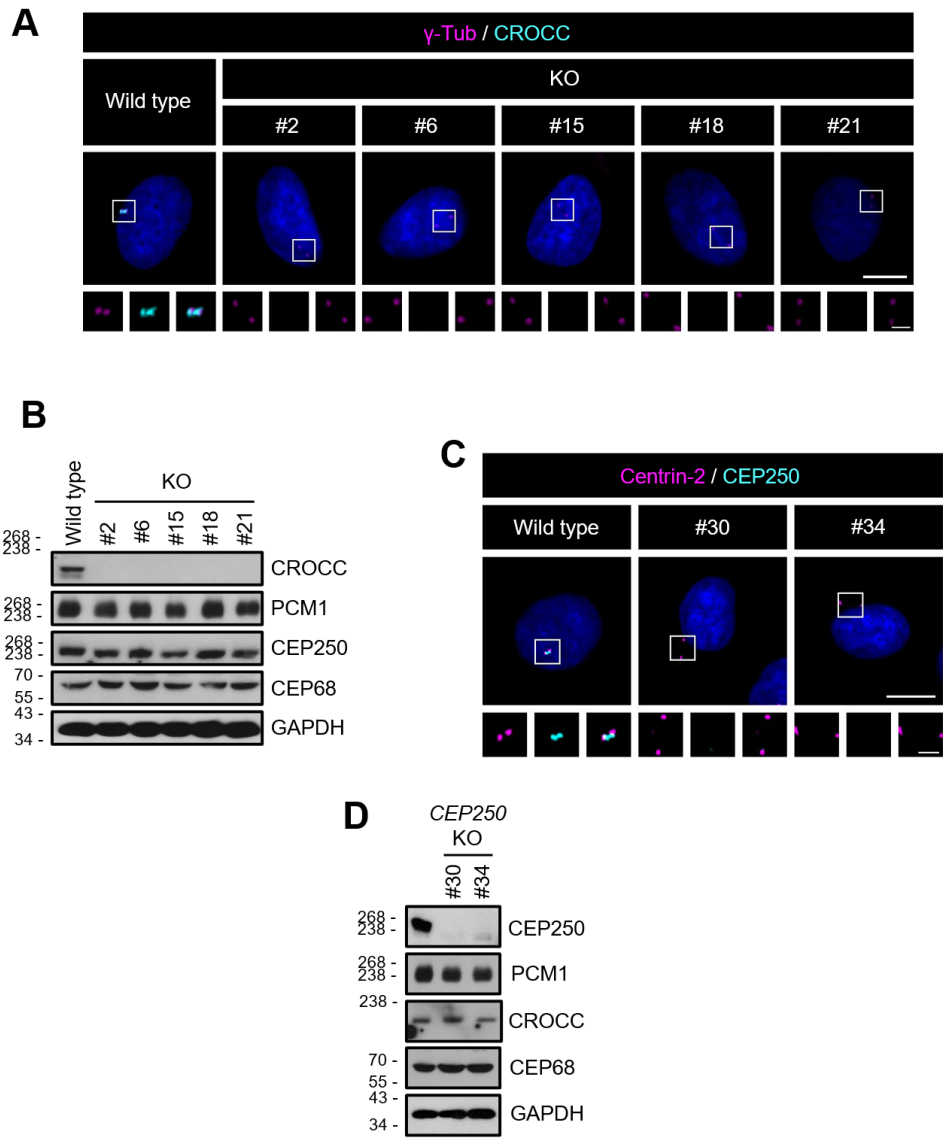

Figure 9. Generation of the *CROCC* and *CEP250* KO RPE1 cells
(A) The *CROCC* KO RPE1 cells were coimmunostained with antibodies specific to γ-tubulin (magenta) and CROCC (cyan). (B) The *CROCC* KO cells were subjected to immunoblot analyses with antibodies specific to CROCC, PCM1, CEP250, CEP68, and GAPDH. (C) The *CEP250* KO RPE1 cells were coimmunostained with antibodies specific to centrin-2 (magenta) and CEP250 (cyan). (D) The *CEP250* KO cells were subjected to immunoblot analyses with antibodies specific to CEP250, PCM1, CROCC, CEP68, and GAPDH. (A and C) Scale bar, 10 μm; Inlet scale bar, 2 μm.

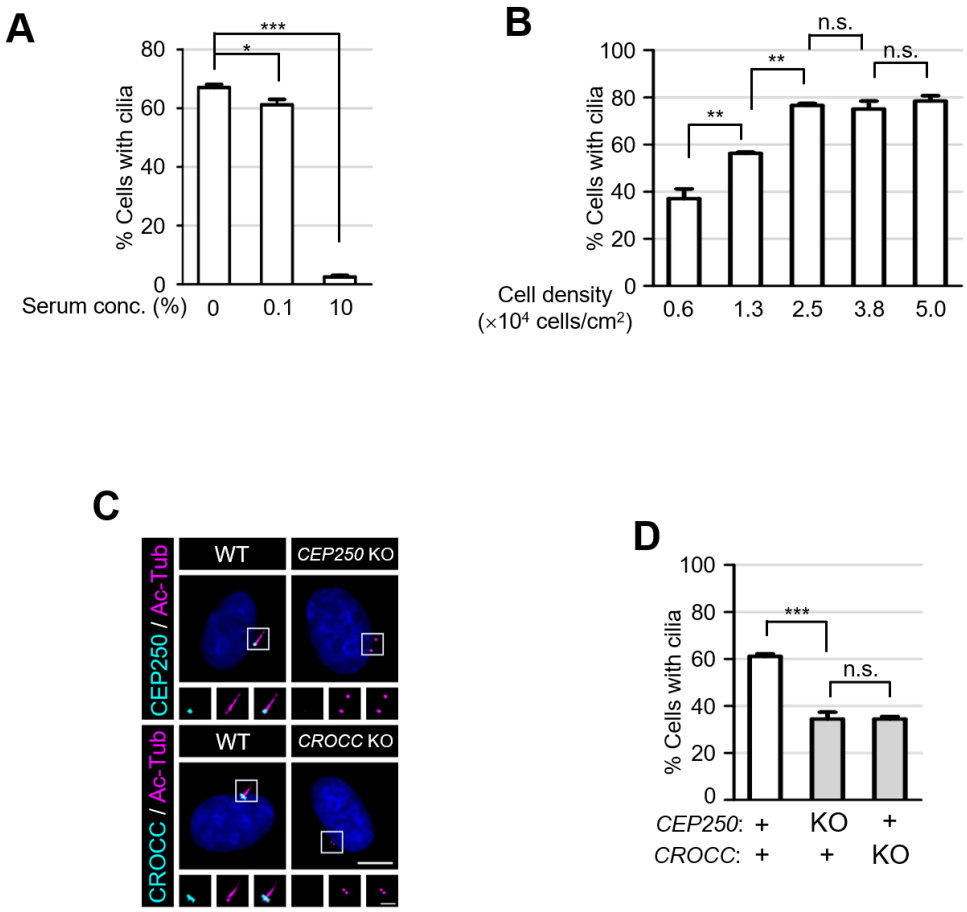

Figure 10. Reduction of cilia assembly in the *CEP250* and *CROCC* KO cells
(A) The number of cells with cilia was counted in RPE1 cells cultured in different serum concentrations. (B) The number of cells with cilia was counted in RPE1 cells cultured at different cell densities. (C) The *CEP250* and *CROCC* KO RPE1 cells were cultured in serum-deprived medium for 48 h, and subjected to coimmunostaining analyses with antibodies specific to CEP250 (cyan), CROCC (cyan) and acetylated tubulin (magenta). Scale bar, 10 μm; Inlet scale bar, 2 μm. (D) The number of cells with cilia was counted. More than 30 cells per group were counted in three independent experiments. Graph values are expressed as mean and SEM. Statistical significance was determined using one-way ANOVA with Tukey's post hoc test (*, $P < 0.05$; **, $P < 0.01$; ***, $P < 0.001$; n.s., not significant).

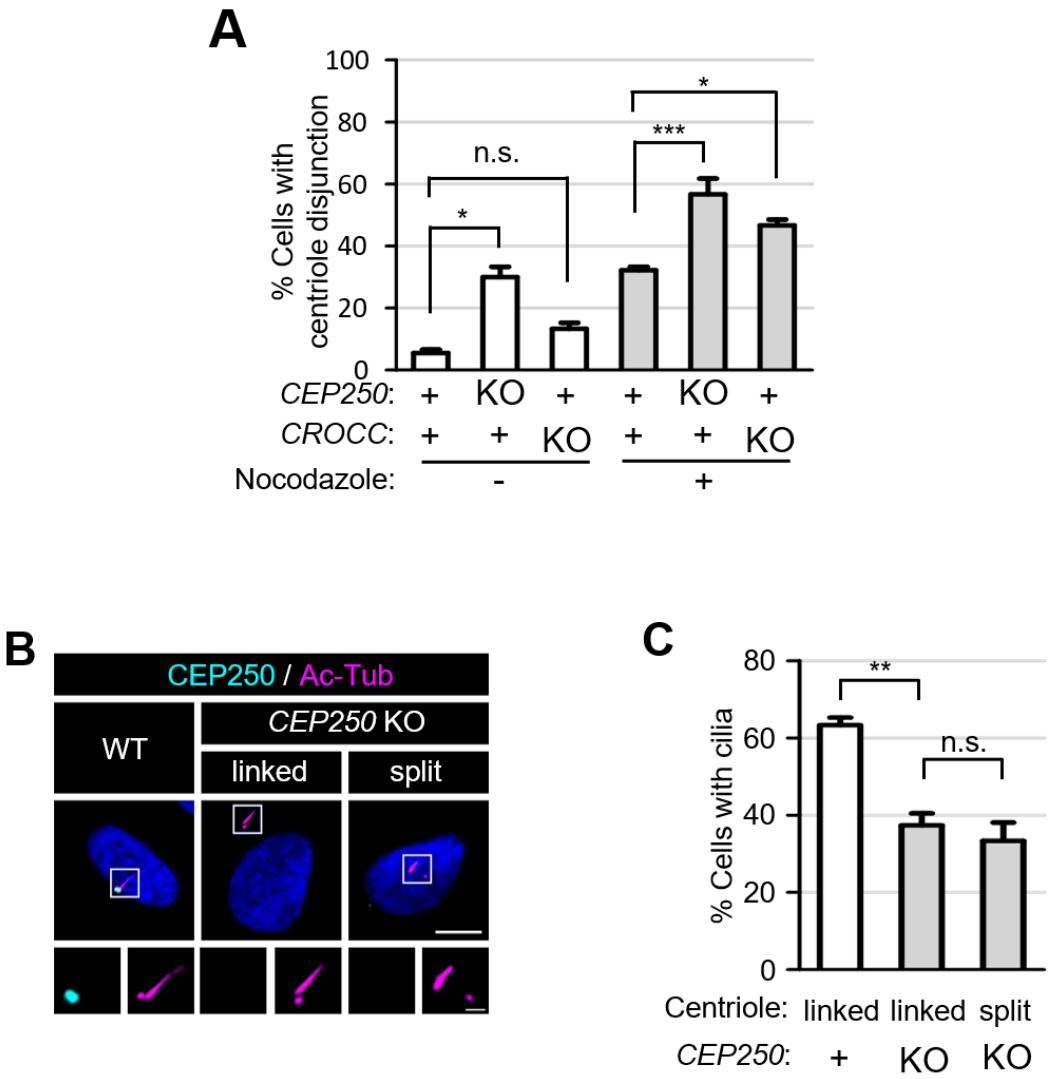

Figure 11. Inter-centriolar fibers are essential for cilia assembly
(A) The number of cells with centriole disjunction (>2 μm) was counted after treatment of 20 μM nocodazole for 2 h. (B) The *CEP250* KO cells were cultured in serum-deprived medium for 48 h to induce cilia assembly, and subjected to coimmunostaining analysis with antibodies specific to CEP250 (cyan) and acetylated tubulin (magenta) with and without daughter centriole association. Scale bar, 10 μm; Inlet scale bar, 2 μm. (C) The number of cells with cilia was counted in *CEP250* KO cells with and without daughter centriole association. More than 30 cells per group were counted in three independent experiments. Graph values are expressed as mean and SEM. Statistical significance was determined using one-way ANOVA with Tukey's post hoc test (*, $P < 0.05$; **, $P < 0.01$; ***, $P < 0.001$; n.s., not significant).

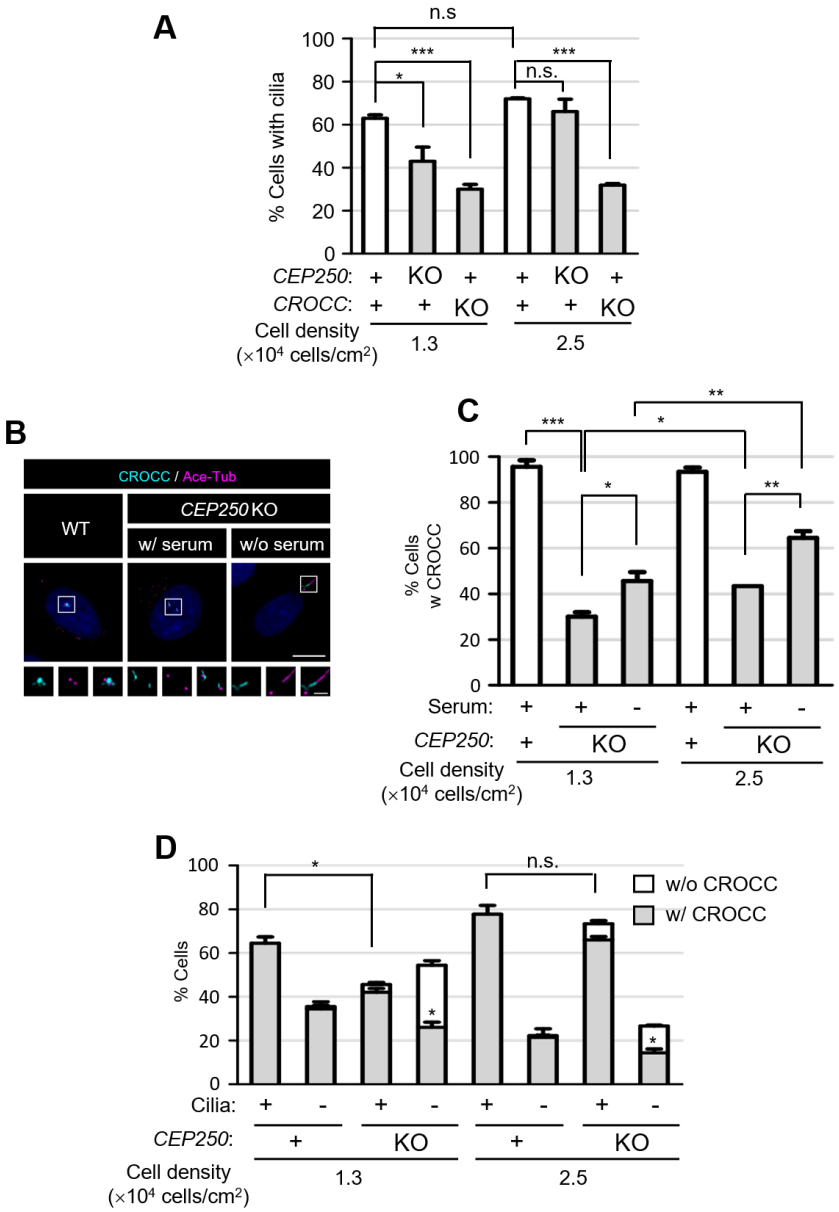

Figure 12. Inter-centriolar/rootlet fibers are important for proper formation of cilia in the *CEP250* KO cells

(A) The number of cells with cilia was counted in *CEP250* and *CROCC* KO cells cultured at different cell densities. (B) The *CEP250* KO cells were cultured in normal and serum-deprived media or 48 h, and subjected to coimmunostaining analysis with antibodies specific to CROCC (cyan) and acetylated tubulin (magenta). Scale bar, 10 μm; Inlet scale bar, 2 μm. (C) The number of cells with centrosome/basal body CROCC signals was counted in *CEP250* KO cells cultured in two different cell densities. (D) The number of cells with centrosome/basal body CROCC signals was counted in *CEP250* KO cells with and without cilia in two different cell densities. More than 30 cells per group were counted in three independent experiments. Graph values are expressed as mean and SEM. Statistical significance was determined using one-way ANOVA with Tukey's post hoc test (*, $P < 0.05$; **, $P < 0.01$; ***, $P < 0.001$; n.s., not significant).

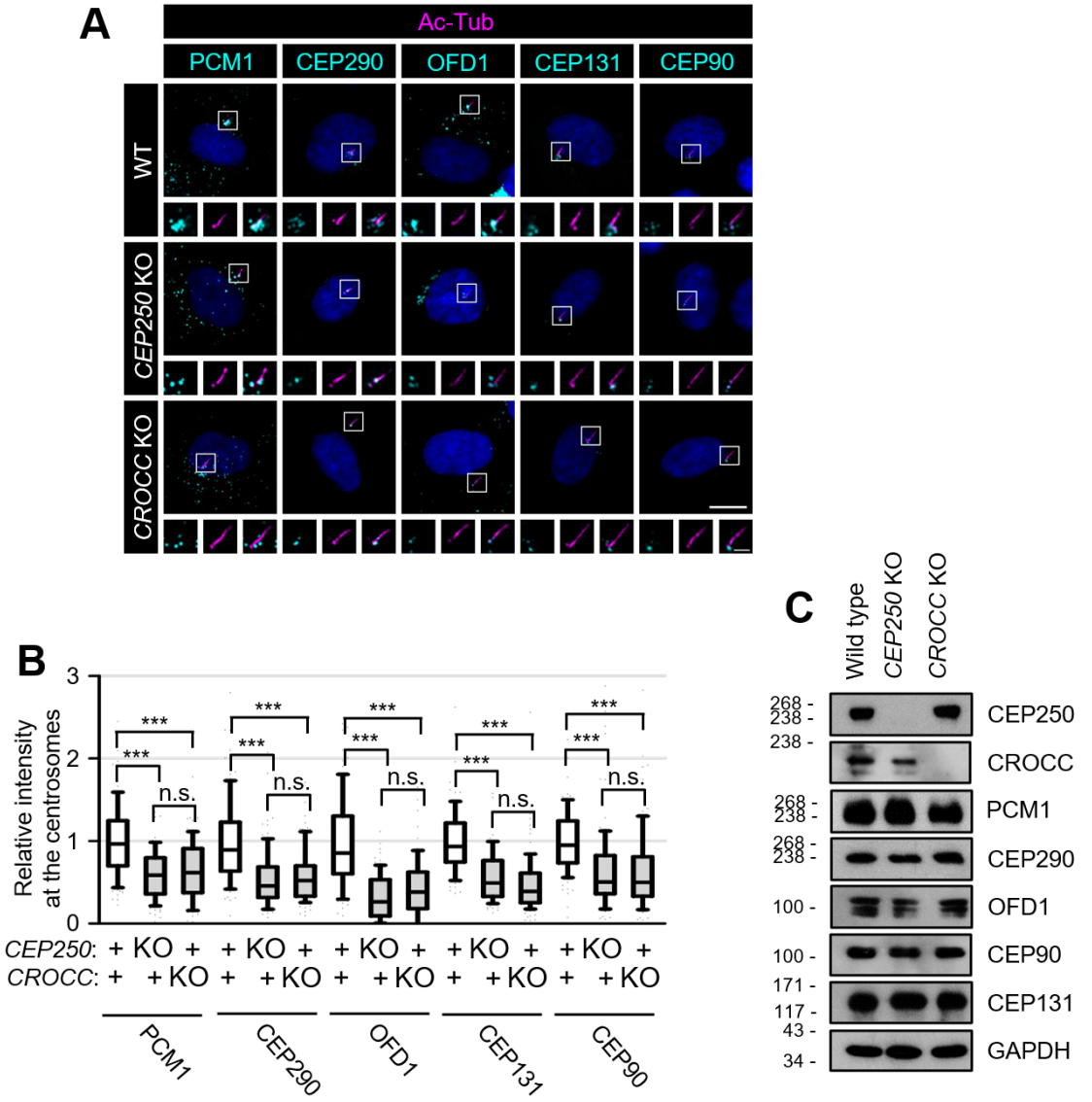

Figure 13. Reduction of the centrosome/basal body levels of PCM1 in the *CEP250* and *CROCC* KO cells

(A) The *CEP250* and *CROCC* KO RPE1 cells were cultured in serum-deprived medium for 48 h to induce cilia assembly, and coimmunostained with antibodies specific to acetylated tubulin (magenta), along with PCM1, CEP290, OFD1, CEP131, and CEP90 (cyan). Scale bar, 10 μm; Inlet scale bar, 2 μm. (B) Centrosome intensities of PCM1, CEP290, OFD1, CEP131 and CEP90 were determined. More than 30 cells per group were counted in three independent experiments. Within each box, the black center line represents the median value, the black box contains the interquartile range, and the black whiskers extend to the 10th and 90th percentiles. Statistical significance was determined using one-way ANOVA with Tukey's post hoc test (***, $P < 0.001$; n.s., not significant). (C) The *CEP250* and *CROCC* KO RPE1 cells were subjected to immunoblot analyses with antibodies specific to CEP250, CROCC, PCM1, CEP290, OFD1, CEP90, CEP131, and GAPDH.

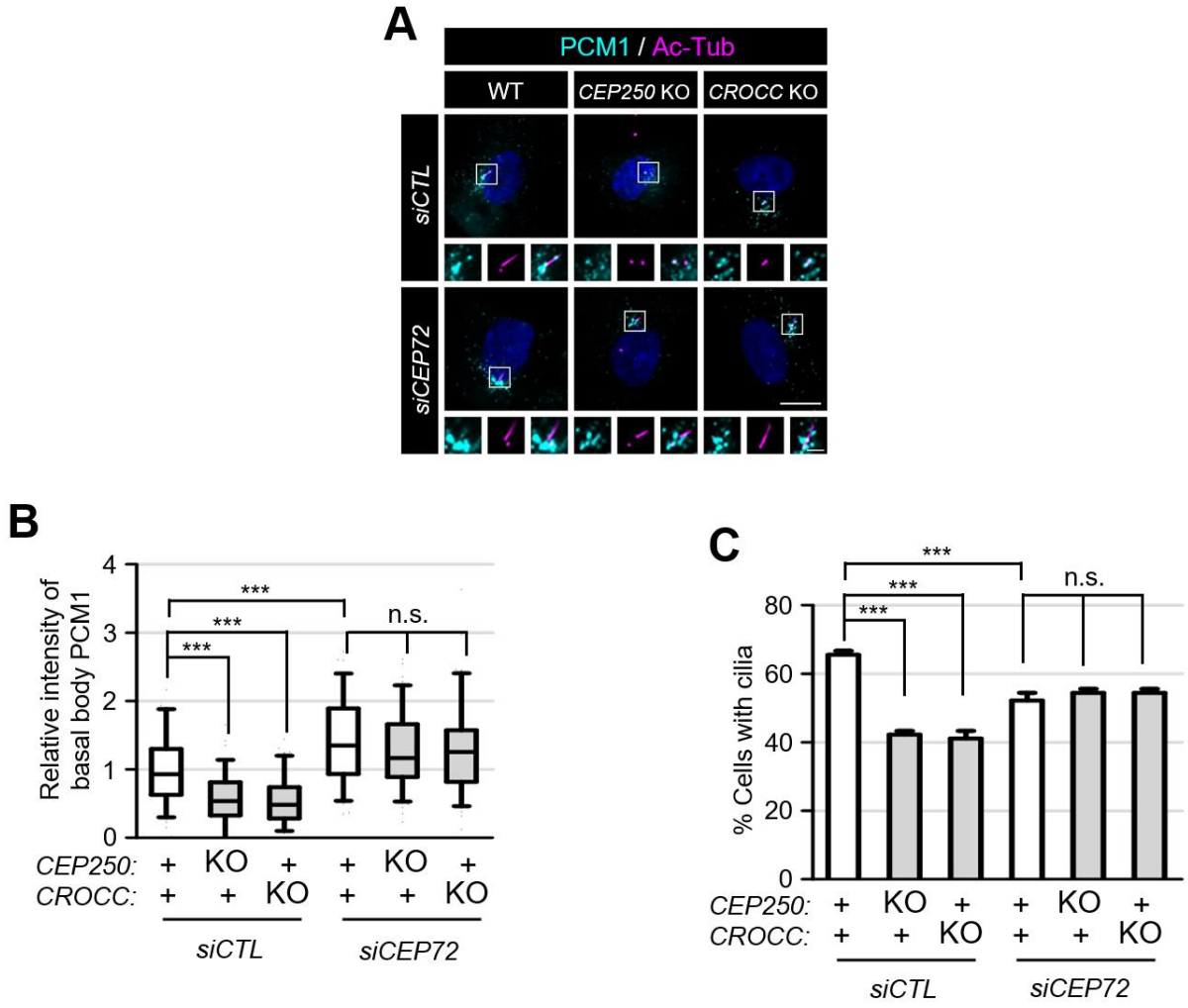

Figure 14. Augmentation of the proportion of cells with cilia by CEP72 depletion
(A) CEP72 was depleted in the *CEP250* and *CROCC* KO cells and subjected to coimmunostaining analysis with antibodies specific to PCM1 (cyan) and acetylated tubulin (magenta). Scale bar, 10 μm; Inlet scale bar, 2 μm. (B) Intensities of PCM1 at the basal bodies were determined. Within each box, the black center line represents the median value, the black box contains the interquartile range, and the black whiskers extend to the 10th and 90th percentiles. More than 30 cells per group were counted in three independent experiments. Within each box, the black center line represents the median value, the black box contains the interquartile range, and the black whiskers extend to the 10th and 90th percentiles. Statistical significance was determined using one-way ANOVA with Tukey's post hoc test (***, $P < 0.001$; n.s., not significant). (C) The number of cells with cilia was counted. Graph values are expressed as mean and SEM. Statistical significance was determined using one-way ANOVA with Tukey's post hoc test (*, $P < 0.05$; **, $P < 0.01$; ***, $P < 0.001$; n.s., not significant).

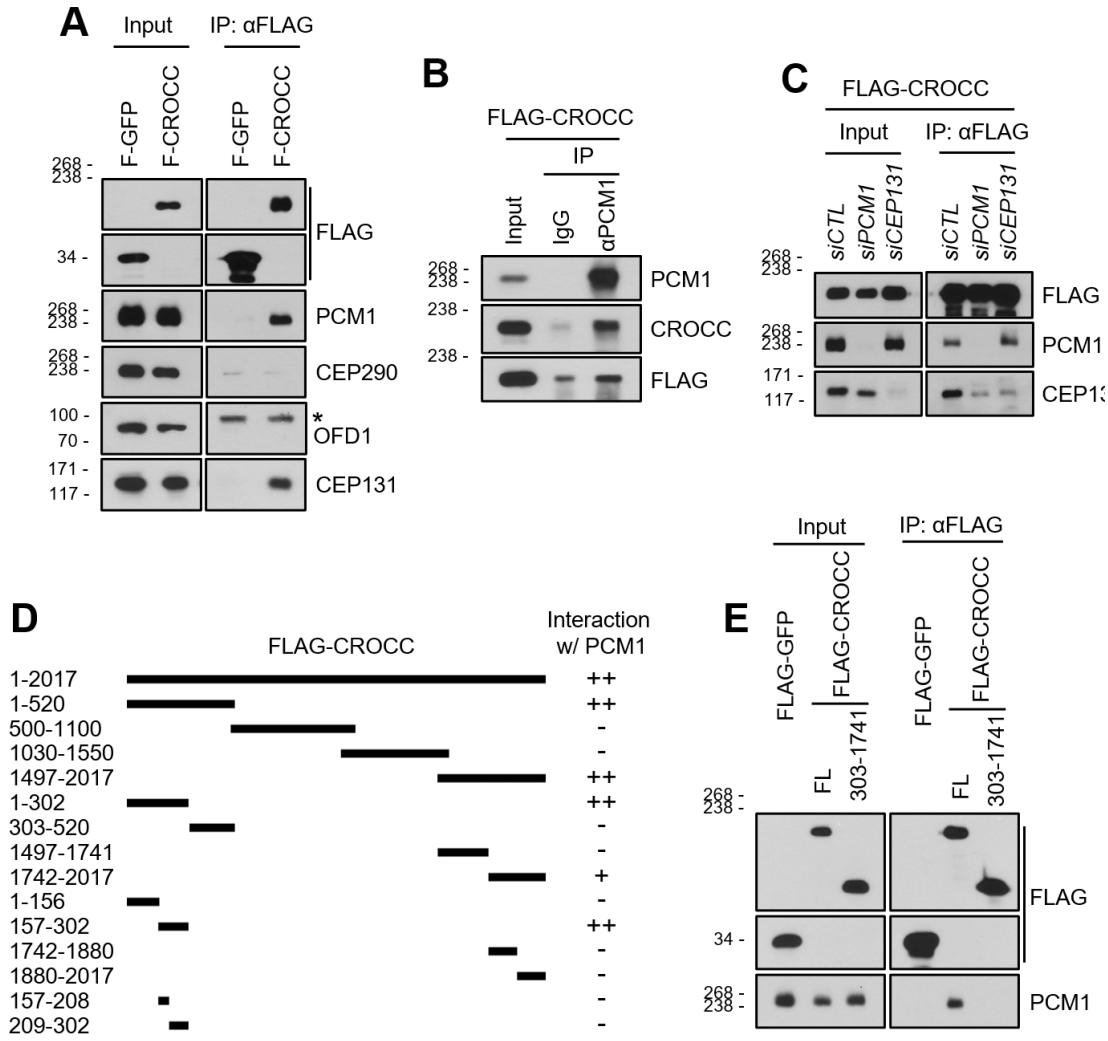

Figure 15. Definition of PCM1-interacting regions in the CROCC protein
(A) Lysates of the RPE1 cells expressing the ectopic FLAG-GFP and FLAG-CROCC proteins were immunoprecipitated with the FLAG antibody and subsequently immunoblotted with antibodies specific to FLAG, PCM1, CEP290, OFD1, and CEP131. The asterisk indicates non-specific band with the OFD1 antibody. (B) The same cell lysates were immunoprecipitated with the PCM1 antibody and subsequently immunoblotted with antibodies specific to PCM1, CROCC, and FLAG. Rabbit IgG was used as a negative control. (C) Endogenous CROCC and CEP131 were depleted in a stable RPE1 cells expressing FLAG-CROCC. The cell lysates were immunoprecipitated with the FLAG antibody and subsequently immunoblotted with antibodies specific to FLAG, PCM1, and CEP131. (D) Schematic of the truncated mutants of FLAG-CROCC. The interactions between the CROCC truncated mutants and endogenous PCM1 are summarized on the right. (E) Lysates of the stable cell lines expressing FLAG-CROCC^{FL} and FLAG-CROCC$^{303\text{-}1741}$ were immunoprecipitated with the FLAG antibody and subsequently immunoblotted with antibodies specific to FLAG and PCM1. This data is cited from Dr. Ko's work.

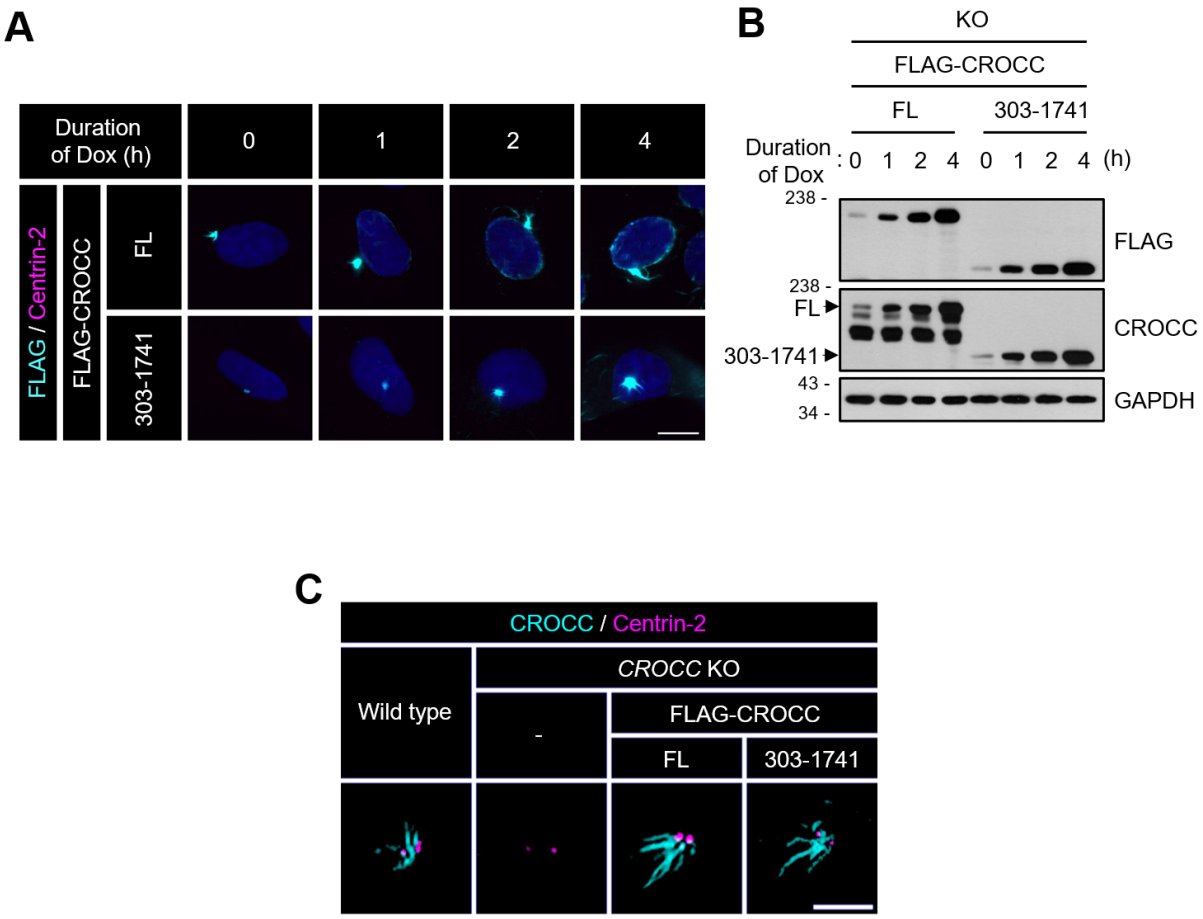

Figure 16. Expression of FLAG-CROCC^{FL} and FLAG-CROCC$^{303-1741}$ in *CROCC* KO RPE1 cells

(A) Ectopic expression of FLAG-CROCC^{FL} and FLAG-CROCC$^{303-1741}$ were induced with 1 μg/ml doxycycline for up to 4 h in the *CROCC* KO cells. The cells were coimmunostained with antibodies specific to FLAG (cyan) and Centrin-2 (magenta). Scale bar, 10 μm. (B) The cells were immunoblotted with antibodies specific to FLAG, CROCC, and GAPDH. (C) FLAG-CROCC^{FL} and FLAG-CROCC$^{303-1741}$ were stably expressed in the *CROCC* KO RPE1 cells. The cells were coimmunostained with antibodies specific to CROCC (cyan) and centrin-2 (magenta). The CROCC fibers were observed with a super-resolution microscope. Scale bar, 2 μm.

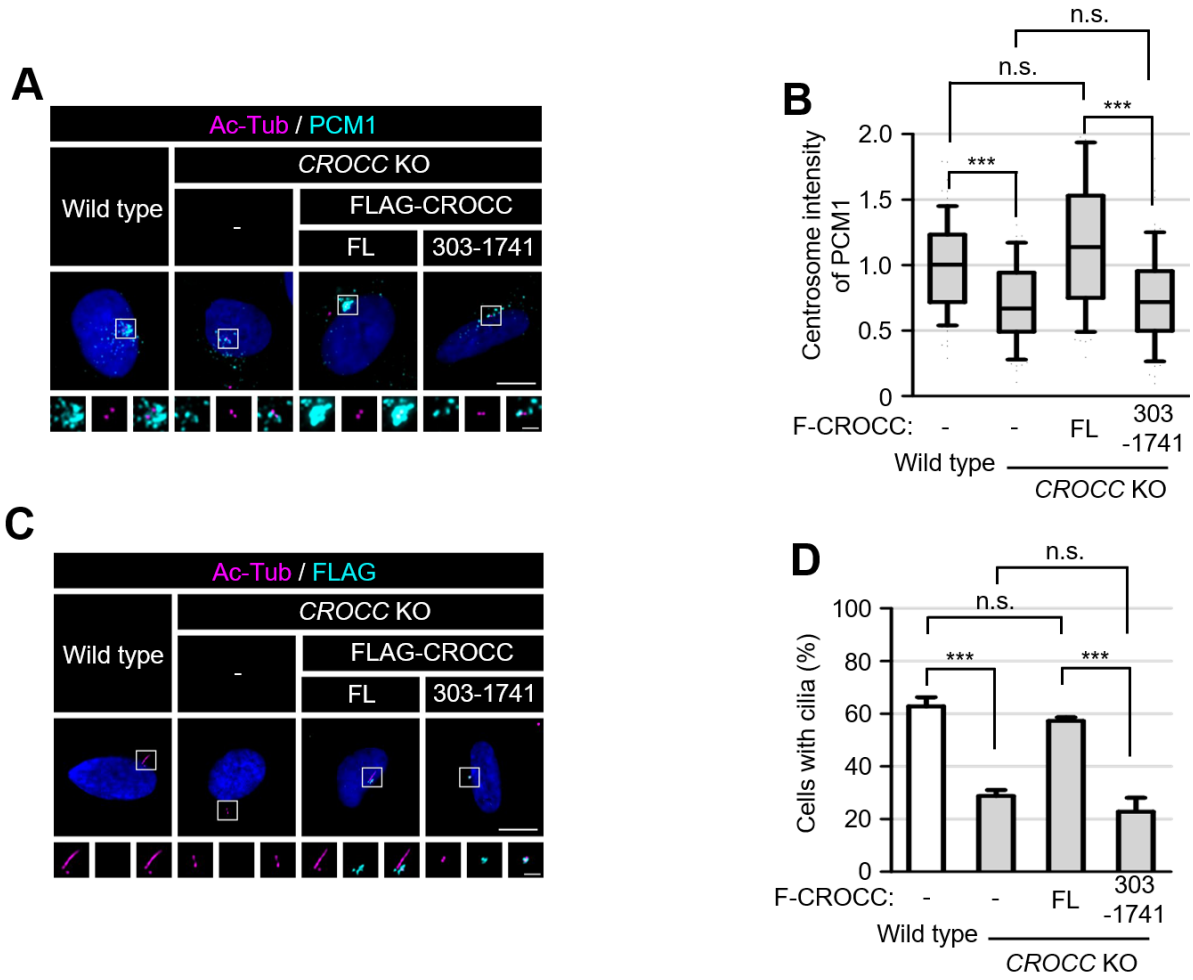

Figure 17. Specific interaction of CROCC with PCM1 is essential for cilia assembly
(A) The cells were coimmunostained with antibodies specific to PCM1 (cyan) and acetylated tubulin (magenta). (B) Intensities of PCM1 at the centrosomes were determined. Within each box, the black center line represents the median value, the black box contains the interquartile range, and the black whiskers extend to the 10th and 90th percentiles. (C) The cells were cultured in serum-deprived medium for 48 h, and coimmunostained with antibodies specific to FLAG (cyan) and acetylated tubulin (magenta). (D) The number of cells with cilia was counted. Graph values are expressed as mean and SEM. (A, C) Scale bars, 10 μm; Inlet scale bars, 2 μm. (B, D) More than 30 cells per group were counted in three independent experiments. Statistical significance was determined using one-way ANOVA with Tukey's post hoc test (***, $P < 0.001$; n.s., not significant).

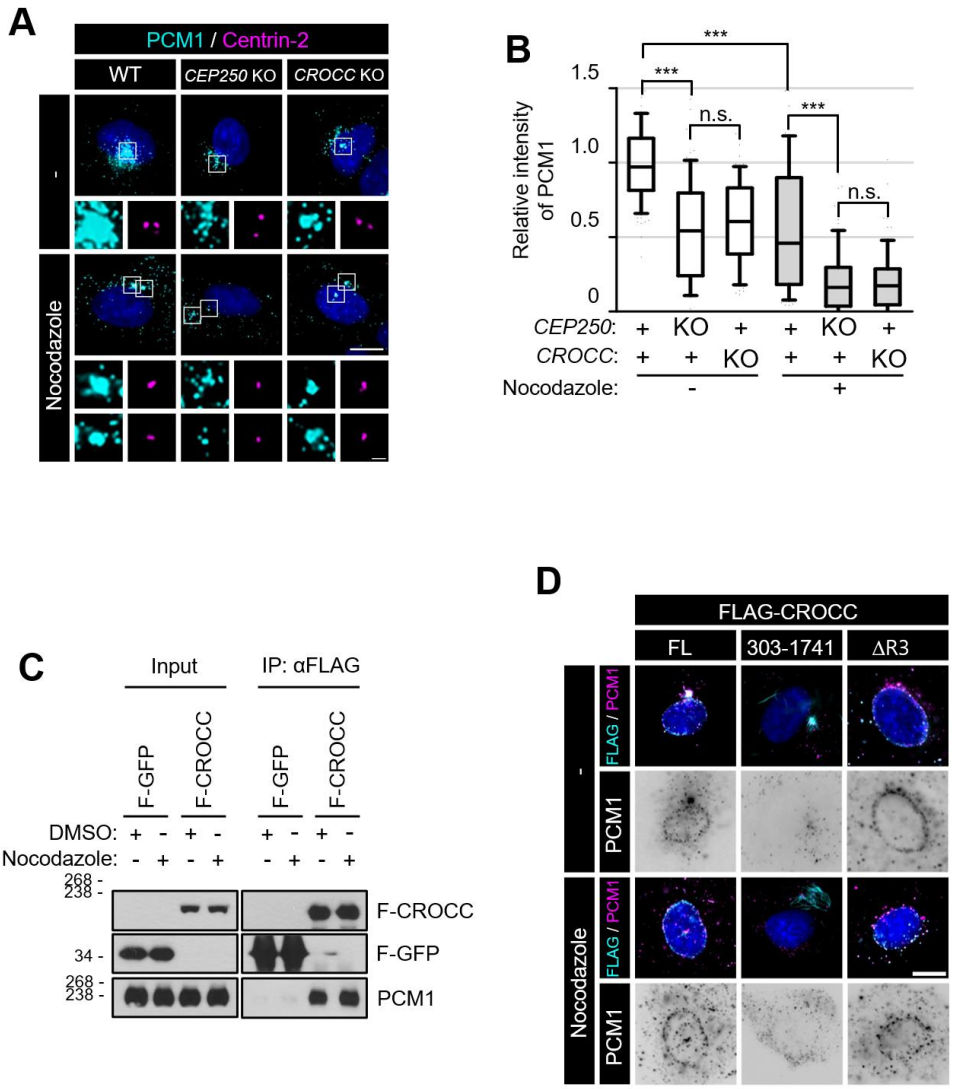

Figure 18. Colocalization of PCM1 with subcellular CROCC

(A) Intensities of PCM1 at the centrosome were determined. More than 30 cells per group were counted in three independent experiments. Within each box, the black center line represents the median value, the black box contains the interquartile range, and the black whiskers extend to the 10th and 90th percentiles. Statistical significance was determined using one-way ANOVA with Tukey's post hoc test (***, $P < 0.001$; n.s., not significant). (B) The cells expressing the ectopic FLAG-CROCC protein were treated with nocodazole for 2 h and subjected to immunoprecipitation analysis with the FLAG antibody, followed by immunoblot analyses with antibodies specific to FLAG and PCM1. (C) The cells expressing the ectopic FLAG-CROCC protein were treated with 20 μM nocodazole for 2 h and subjected to immunoprecipitation analysis with the FLAG antibody, followed by immunoblot analyses with antibodies specific to FLAG and PCM1. (D) FLAG-CROCC^{FL}, FLAG-CROCC$^{303\text{-}1741}$, and FLAG-CROCC$^{\Delta R3}$ were stably expressed in the *CROCC* KO RPE1 cells. The cells were treated with nocodazole for 2 h and coimmunostained with antibodies specific to FLAG (cyan) and PCM1 (magenta). (A and D) Scale bars, 10 μm; Inlet scale bar, 2 μm.

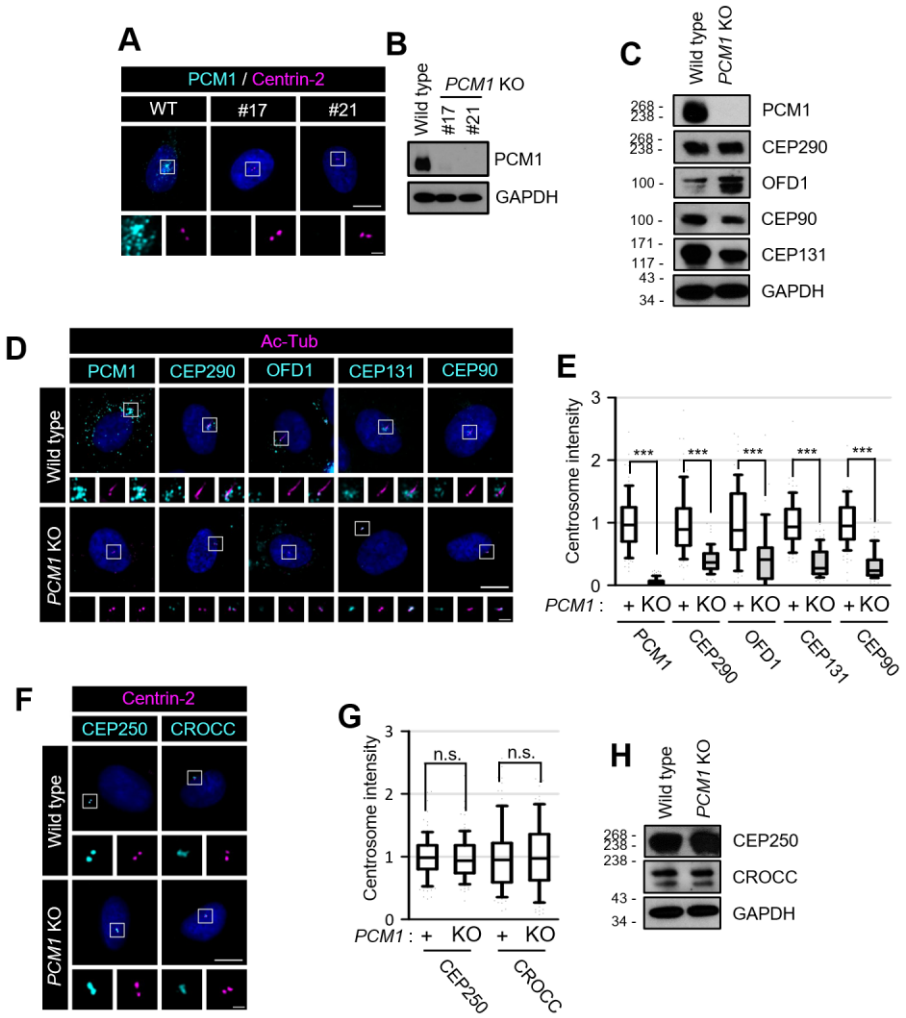

Figure 19. Generation and feature of *PCM1* KO RPE1 cells

(A) The *PCM1* KO RPE1 cells were coimmunostained with antibodies specific to PCM1 (cyan) and centrin-2 (magenta). (B) The *PCM1* KO cells were subjected to immunoblot analyses with antibodies specific to PCM1 and GAPDH. (C) The *PCM1* KO cells were subjected to immunoblot analyses with antibodies specific to PCM1, CEP290, OFD1, CEP90, CEP131 and GAPDH. (D) The *PCM1* KO cells were cultured in serum-deprived medium for 48 h and coimmunostained with antibodies specific to acetylated tubulin (magenta), along with PCM1, CEP290, OFD1, CEP131, and CEP90 (cyan). (E) Centrosome intensities of PCM1, CEP290, OFD1, CEP131, and CEP90 were determined. (F) The *PCM1* KO cells were coimmunostained with antibodies specific to centrin-2 (magenta), along with CEP250 and CROCC (cyan). (G) Centrosome intensities of CEP250 and CROCC were determined. (H) The *PCM1* KO cells were subjected to immunoblot analyses with antibodies specific to CEP250, CROCC, and GAPDH. (A, D, F) Scale bars, 10 μm, Small scale bars, 2 μm. (E, G) More than 30 cells per group were counted in three independent experiments. Within each box, the black center line represents median values, the black box contains the interquartile range, and the black whiskers extend to the 10th and 90th percentiles. Statistical significance was determined using one-way ANOVA with Tukey's post hoc test. (***, $P < 0.001$; n.s., not significant).

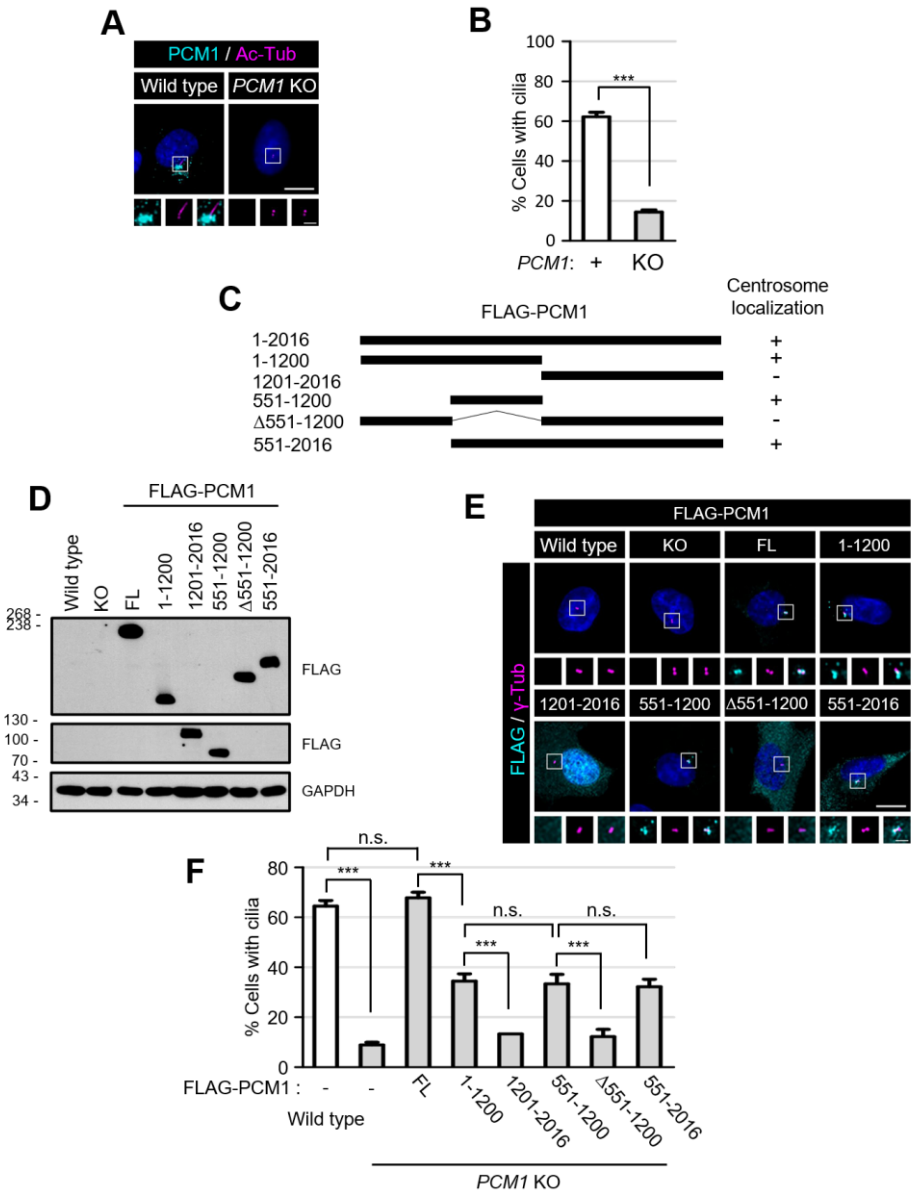

Figure 20. Definition of the PCM1 regions for centrosome accumulation and cilia formation

(A) The *PCM1* KO RPE1 cells were cultured in serum-deprived medium for 48 h and coimmunostained with antibodies specific to PCM1 (cyan) and acetylated tubulin (magenta). (B) The number of cells with cilia was counted. (C) Schematic of the truncated mutants of FLAG-PCM1. Centrosome localizations of the PCM1 truncated mutants are summarized on the right. (D) Truncated mutants of FLAG-PCM1 were expressed in the *PCM1* KO RPE1 cells and subjected to immunoblot analyses with antibodies specific to FLAG and GAPDH. (E) The cells were coimmunostained with antibodies specific to FLAG (cyan) and γ-tubulin (magenta). (F) The number of cells with cilia was counted. (A, E) Scale bars, 10 μm; Inlet scale bars, 2 μm. (B, F) More than 30 cells per group were counted in three independent experiments. Graph values are expressed as mean and SEM. Statistical significance was determined using one-way ANOVA with Tukey's post hoc test (***, $P < 0.001$; n.s., not significant).

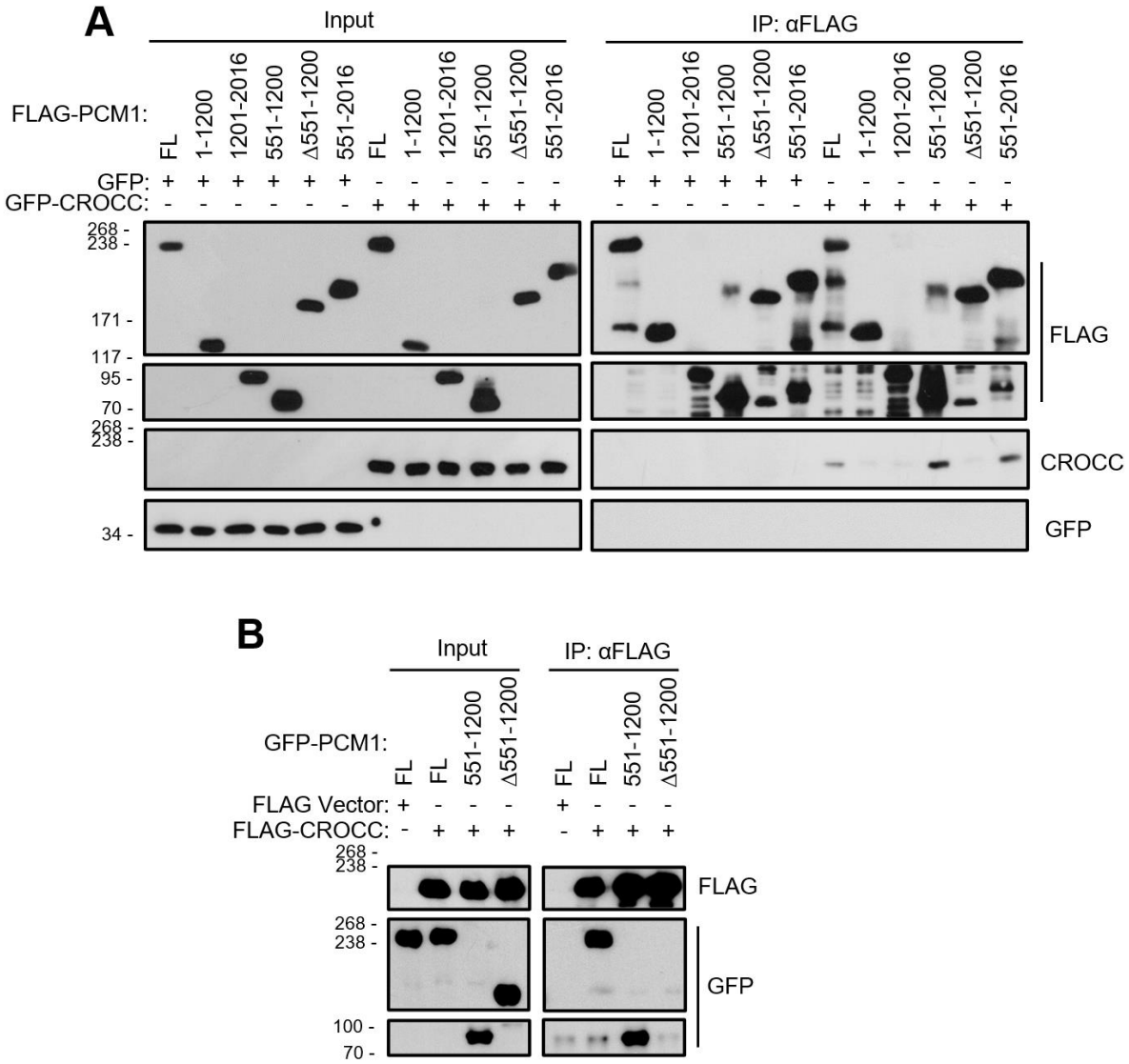

Figure 21. Definition of the CROCC-interacting region in the PCM1 protein
(A) Lysates of the 293T cells expressing the ectopic FLAG-PCM1 truncated proteins and GFP-CROCC were immunoprecipitated with the FLAG antibody and subsequently immunoblotted with antibodies specific to CROCC, GFP, and FLAG. (B) Lysates of the 293T cells expressing the ectopic FLAG-CROCC and GFP-PCM1 truncated proteins were immunoprecipitated with the FLAG antibody and subsequently immunoblotted with antibodies specific to FLAG and GFP.

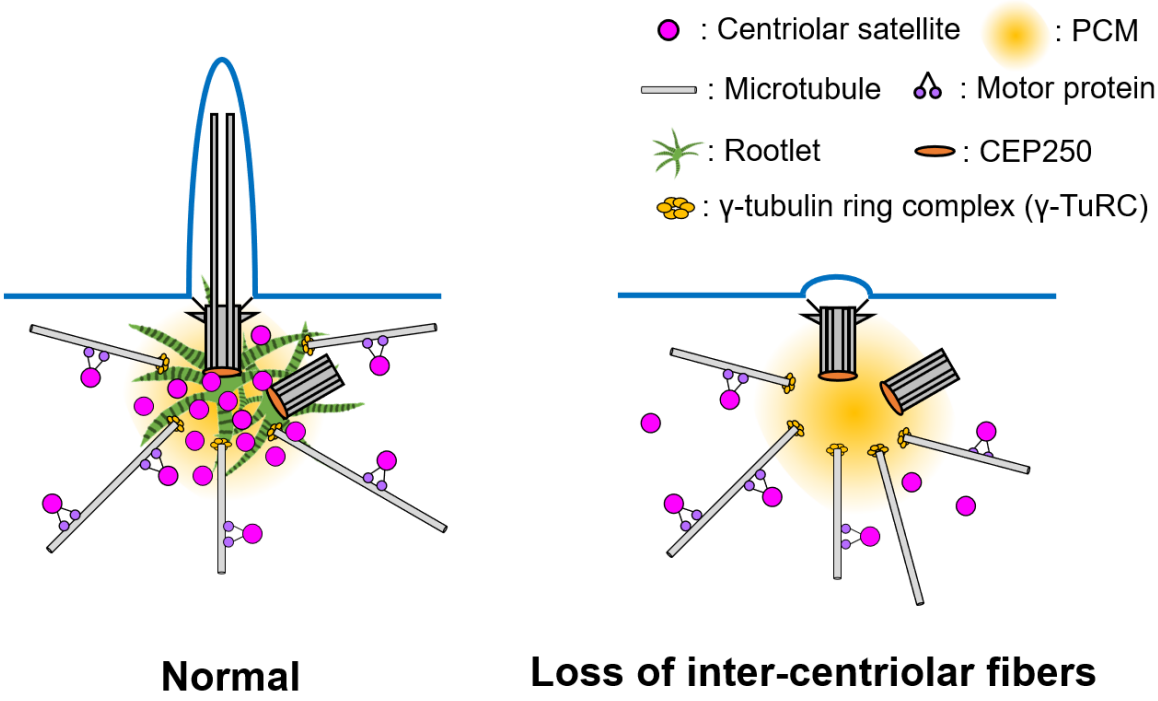

Figure 22. Model.
The centriolar satellites travel through the microtubule network to reach the inter-centriolar/rootlet fibers near the centrosomes and cilia. The specific interaction between CROCC and PCM1 is essential for recruiting centriolar satellites near the centrosomes and cilia. The inter-centriolar/rootlet fiber may serve as a docking site for centriolar satellites near the centrosomes/basal bodies. As a result, cargoes from the centriolar satellites are efficiently delivered to vicinity of the centrosomes/basal bodies and facilitate the cilia assembly process.

DISCUSSION

In this study, I investigated the role of inter-centriolar fibers in cilia assembly. I generated *CROCC* and *CEP250* KO cells to analyze their effects on cilia formation and PCM1 localization, a centriolar satellite protein responsible for transporting essential proteins to the centrosome. I found that the loss of CROCC and CEP250 disrupted PCM1 localization at the centrosome. Additionally, PCM1 binds directly to CROCC, critical for centriolar satellite accumulation near the centrosomes and efficient cilia formation. My study shows that inter-centriolar fibers act as docking sites for centriolar satellites, facilitating cilia assembly and enhancing my understanding of the mechanisms underlying ciliogenesis (Fig. 22).

In *CROCC* KO cells, the centrosome pair remained closely associated through the microtubule network, yet the centriolar satellites were observed to disperse from the centrosome (Fig. 13; Flanagan et al., 2017). This is similar to the dispersion of centriolar satellites and reduction in cilia formation observed with the loss of other inter-centriolar fiber components such as LRRC45 (He et al., 2013; Kurtulmus et al., 2018). These results suggest that inter-centriolar fibers play a critical role in regulating the distribution of centriolar satellites.

Centriolar satellites are transported via the microtubule network to deliver proteins near the centrosome and cilia (Prosser and Pelletier, 2020; Aydin et al., 2020). When the microtubule network is disrupted, the centriolar satellites disperse from the centrosome, limiting cilia formation (Dammermann and Merdes, 2002; Kubo and Tsukita, 2003). In *PCM1* KO cells, cilia formation rates were significantly lower than in *CROCC* and *CEP250* KO cells, suggesting that PCM1 plays a key role in transporting proteins necessary for cilia formation to the centrosome. However, even in *CROCC* and *CEP250* KO cells, some PCM1 remains, allowing partial delivery of proteins to the centrosome

(Fig. 13). Although cilia formation rates significantly decreased in *PCM1* KO cells, some cilia were found to be detached from the centrosome. This indicates that while PCM1 is important in cilia formation, it also plays a crucial role in positioning and maintaining cilia at the centrosome. The precise mechanism needs further research, but this could lead to new discoveries.

Contrary to previous studies that suggested *CEP250* KO does not affect cilia formation, my study observed reduced cilia formation rates in *CEP250* KO cells (Fig. 11 and 12; Panic et al., 2015; Mazo et al., 2016; Flanagan et al., 2017). This discrepancy could stem from differences in cell culture conditions, as I observed that high-density culture increased cilia formation rates (Fig. 12. C and D). This suggests that changes in cellular states, such as cell cycle exit, may be related to these observations.

Additionally, I found that CROCC can independently support cilia formation without CEP250. In *CEP250* KO cells, CROCC remained at the centrosome, and its role became more pronounced at higher cell densities (Fig. 12. B-D). This implies that CROCC acts as a key regulator of cilia formation, even in the absence of CEP250, emphasizing that CROCC not only works in cooperation with CEP250 but also performs essential functions on its own.

The interaction between CROCC and PCM1 plays a crucial role in the cilia formation process. Through immunoprecipitation experiments, I confirmed that CROCC and PCM1 directly bind, and this interaction is essential for the accumulation of centriolar satellites at the centrosome (Fig. 15 and 17). Specifically, in mutant cells where specific binding sites of CROCC were removed, PCM1 failed to localize to the centrosome, leading to a significant reduction in cilia formation (Fig. 17). This supports the idea that the physical interaction between CROCC and PCM1 is critical for the proper positioning of centriolar satellites and the formation of cilia.

In conclusion, this study reveals that CROCC and CEP250 play important roles in promoting centriolar satellite accumulation and cilia formation. Additionally, CROCC

can regulate cilia formation independently of CEP250, providing insights for research on ciliopathies. Future studies should explore how the interaction between CROCC and PCM1 changes in disease conditions, particularly in models with defects in cilia formation. Altogether, I believe that the CROCC–PCM1 interaction facilitates the unloading of ciliary materials near the cilia assembly area.

Chapter II.

Role of PCNT in centrosome integrity and development

ABSTRACT

The centrosome plays a pivotal role in microtubule organization, genomic stability, and proper cell division in animal cells. PCNT, a structural component of the PCM, is essential for maintaining centrosome integrity, with its deficiencies linked to developmental disorders such as MOPDII. This study investigates the role of PCNT in centrosome integrity, chromosomal stability, and normal development by utilizing both *Pcnt* KO and MOPDII-mimicking *Pcnt* KI mouse models. My results demonstrate that both KO and KI models exhibit similar phenotypes, including disrupted centriole cohesion, excessive centriole duplication, and chromosomal instability, ultimately leading to aneuploidy. Developmental abnormalities, such as growth retardation, polydactyly, reduced brain, and cleft palate, were observed in *Pcnt* KO and KI mice, emphasizing the critical role of PCNT in development. These findings highlight the indispensability of PCNT in centrosome integrity and accurate chromosome segregation, offering insights into the pathogenesis of PCNT-related diseases and potential therapeutic strategies for addressing centrosome-associated developmental disorders.

INTRODUCTION

The centrosome, a key organelle in animal cells, plays a critical role in cellular organization and division. Serving as the main MTOC, the centrosome consists of a pair of centrioles surrounded by a protein matrix called PCM. This structure coordinates key cellular processes such as intracellular transport, cell polarity, and mitotic spindle formation, making it essential for maintaining cell integrity. The centrosome undergoes duplication once per cell cycle, supporting accurate chromosome segregation and genomic stability during mitosis (Bettencourt-Dias & Glover, 2007; Luders & Stearns, 2007).

Each centrosome contains a mother and daughter centriole arranged perpendicularly, with the daughter centriole engaged with the mother until the completion of mitosis. At the end of mitosis, the daughter centriole disengages, matures, and recruits its own PCM to become the new mother centriole, forming a centrosome within each daughter cell (Wang et al., 2011). This sequential structural reorganization is essential for centrosome cohesion and proper spindle pole formation, thereby ensuring accurate chromosome segregation (Fukasawa, 2007). Disruption of this precise process can lead to chromosomal instability, underscoring the role of the centrosome in safeguarding genomic stability.

The PCM is a dynamic matrix that surrounds the centrioles, containing critical components such as γ-tubulin and CEP215, which facilitate microtubule nucleation and spindle organization (Mittasch et al., 2020). These components are strategically positioned within PCM to stabilize centrosome structure and enable it to anchor microtubules effectively. During mitosis, PCM undergoes significant reorganization, expanding to accommodate the formation of the mitotic spindle. Proper organization and function of PCM are essential not only for spindle formation but also for cilia formation,

as PCM defects can lead to centrosomal dysfunction and associated pathologies (Mennella et al., 2012; Hatch et al., 2010). Given its importance, PCM's structural and functional stability is crucial for maintaining cellular homeostasis and preventing errors in cell division.

PCNT, a critical scaffolding protein within PCM, plays a central role in stabilizing the PCM. As a molecular anchor, PCNT attaches γ-tubulin and CEP215 to the centrosome, facilitating the organization of microtubules and supporting PCM structure (Delaval & Doxsey, 2010). PCNT deficiency impairs these anchoring functions, resulting in chromosomal missegregation during cell division, developmental abnormalities, and severe conditions like MOPDII (Zimmerman et al., 2004; Rauch et al., 2008). Such associations underscore the critical role of PCNT in preserving centrosome integrity, genomic stability, and proper cellular function.

This study aims to investigate the effects of PCNT deficiency on the structural integrity of the centrosome, the stability of PCM, and chromosomal dynamics during cell division. Using *Pcnt* KO and KI mouse models, I explore how the absence of PCNT affects PCM localization, centriole cohesion, and chromosome stability. my findings reveal that PCNT is indispensable for centrosomal cohesion, chromosome integrity, and normal cell division. By highlighting the mechanistic role of PCNT in centrosome integrity, this study contributes to my understanding of how PCM integrity impacts cellular health and the development of disorders like MOPDII.

MATERIALS AND METHODS

Animals

The animal experiments in this study were permitted by Institutional Animal Care and Use Committee at Seoul National University (SNU-211112-3-3). PCNT KO mouse were made by Cre-LoxP system. sgRNA sequences using Pcnt KI mouse were 5'-ACCATTGTGACAGCGAGAGT-3'. Genotypes of Cep215 mutant mouse (Pcnt +/+, Pcnt +/-. Pcnt -/-) were determined with genomic PCR analyses using mouse tail. The PCR primers were PCNT-LRG-F1 (5'-CTTCTCTCAGCTTTGCGGTG-3'), PCNT-LRG-R1 (5'-TGTTCCCAGGGTAGAGTCTCA-3'), PCNT-RRG-R1 (5'-GAGCAGAACTCTTGCTGCGA-3') in Pcnt KO mouse and PCNT-KI-F2 (5'-TTCCGGGGTTGGCCTTAG-3'), PCNT-KI-R2 (5'-CTGTCTACCGTGTGGTTGG-3'). Tissue preparation was carried out after euthanasia using CO2 and perfusion with 1× PBS.

Immunoblot analyses

The cells were lysed on ice for 10min with RIPA buffer (150mM NaCl, 1% Triton X-100, 0.5% sodium deoxycolate, 0.1% SDS, 50 mM Tris-HCl at pH 8.0, 10 mM NaF, 1 mM Na3VO4, 1 mM EDTA, and 1 mM EGTA) containing a protease inhibitor cocktail (P8340; Sigma-Aldrich) and centrifuged with 12,000 rpm for 10 min at 4°C. The supernatants were mixed with 4×SDS sample buffer (250 mM Tris-HCl at pH 6.8, 8% SDS, 40% glycerol, and 0.04% bromophenol blue) and 10mMDTT (0281-25G; Amresco). Mixtures were boiled for 5 min. The protein samples were loaded in SDS polyacrylamide gels (3% stacking gel and 4–10% separating gel), electrophoresed, and transferred to Protran BA85 nitrocellulose membranes (10401196; GE Healthcare Life Sciences). The membranes were blocked with blocking solution (5% nonfat milk in 0.1% Tween 20 in TBS or 5% bovine serum albumin in 0.1% Tween 20 in TBS) for 2 h, incubated with

primary antibodies diluted in blocking solution for 16 h at 4°C, washed four times with TBST (0.1% Tween 20 in TBS), incubated with secondary antibodies in blocking solution for 30 min, and washed again. To detect the signals of secondary antibodies, the ECL reagent (ABfrontier, LF-QC0101) and x-ray films (Agfa, CPBU NEW) were used.

Antibodies

Rabbit anti-Cep215 (06-1398; IS, 1:200; Millipore), rabbit anti-centrin-2 (04-1624; IS, 1:500; Millipore), and mouse anti-GAPDH (AM4300; IB, 1:10,000; Invitrogen) antibodies were purchased from commercial suppliers. Rabbit anti-pericentrin (Kim and Rhee, 2011), rabbit anti-CEP135 (Kim et al., 2012), rabbit anti-CP110 (Chang et al., 2010) polyclonal antibodies were prepared as described previously. Alexa Fluor 488- and 594-conjugated secondary antibodies (Z25302; Invitrogen, Z25307; IS, 1:1,000; Invitrogen) were used for immunostaining. Anti-mouse IgG-HRP (A9044; IB, 1:1,000; Sigma-Aldrich), anti-rabbit IgG-HRP (AP132P; IB, 1:1,000; Millipore), and anti-goat IgG-HRP (SC-2056; IB, 1:500; Santa Cruz) were used as secondary antibodies for the immunoblot analyses.

Cell culture, transfection, and stable cell lines

MEFs were derived from wild-type, pericentrin knockout (PCNT KO), and MOPD II-mimicking knock-in (KI) mouse models. MEF cells were cultured in Dulbecco's Modified Eagle Medium (DMEM) supplemented with 10% fetal bovine serum (FBS) at 37°C in a 5% CO_2 environment. IMCD3 cells were cultured in Dulbecco's modified eagle medium/Nutrient mixture F-12 (F12/DMEM) supplemented with 10% FBS at 37°C under 5% CO2. To establish stable cell lines, PCNT and PCNT R2918X mutant were subcloned into a pcDNA5 FRT/TO vector from Dr. Hyun S. Lee (Seoul National university, Seoul, Korea).

Fluorescence in situ hybridization

Fluorescence in situ hybridization (FISH) was conducted to visualize specific DNA sequences within cells, using Chromosome 16 probes (FMPC-16; Creative Bioarray). Cells were fixed in 4% paraformaldehyde for 10 minutes at room temperature. Permeabilization was carried out with 0.1% Triton X-100 for 5 minutes to allow probe access to intracellular DNA. Following this, cells were treated with RNase A to degrade RNA, preventing nonspecific binding and ensuring DNA-only hybridization targets. For probe hybridization, preparing pre-denatured probe at 80°C for 5 minutes, DNA was denatured at 85°C for 5 minutes, followed by immediate cooling on ice to prevent reannealing. Fluorescently labeled DNA probes were applied to cells, which were incubated at 37°C for at least 18 hours to allow specific binding to target sequences. After hybridization, cells were washed sequentially in 2x SSC, 1x SSC, and 0.1x SSC buffers at 42°C. Nuclear DNA was counterstained with DAPI for 5 minutes. Images were acquired using a fluorescence microscope.

Immunocytochemistry and image processing

The cells were cultured on 12-mm coverslips and fixed with cold methanol for 10 min or the PEM buffer (80 mM PIPES pH 6.9, 1 mM MgCl2, 5 mM EGTA, and 0.5% Triton X-100). To detect primary cilia, microtubules were depolymerized via cold treatment for 60 min before fixation. The samples were blocked in PBST (PBS with 0.3% Triton X-100) with 3% BSA for 20 min, incubated with the primary antibodies for 1 h, and incubated with Alexa Fluor 488- and Alexa Fluor 594-conjugated secondary antibodies for 30 min (Life Technologies). 49,6-Diamidino-2-phenylindole (DAPI) solution was used for DNA staining. The samples were mounted in ProLong Gold antifade reagent (P36930; Invitrogen) and observed using a fluorescence microscope (IX51; Olympus) equipped with a CCD (Qicam Fast 1394; Qimaging) camera using PVCAM (version 3.9.0; Teledyne Photometrics). The images were analyzed using ImagePro 5.0 software (Media

Cybernetics, Inc.). Images were saved as Adobe Photoshop 2021 (version 22.4.2). For super-resolution images, the samples were observed using a super-resolution microscope (ELYRA PS.1; Carl Zeiss). SIM processing was performed with ZEN software 2012, black edition (Carl Zeiss), and the images were analyzed using ZEN lite software (Carl Zeiss).

Measurements and statistical analysis

Imaging was performed with an Olympus IX51 microscope equipped with a CCD (Qicam Fast 1394; Qimaging) camera using PVCAM (version 3.9.0; Teledyne Photometrics). The fluorescence intensity and ciliary length were measured using ImageJ 1.53e software (National Institutes of Health). The fluorescence intensity was quantified by assessing the cumulative intensity within a circular region (20 μm^2) centered between the centrioles. Statistical significance was determined using an unpaired two-tailed t-test and one-way analysis of variance (ANOVA) on Prism 6 (GraphPad software). Box and whisker plots display the median as a black center line, the interquartile range within the black box, and whiskers extending to the 10th and 90th percentiles. Bar graphs represent values as mean and SEM. In one-way ANOVA, groups sharing the same letter were not significantly different according to Tukey's post hoc test. *$P < 0.05$; P value of unpaired two-tailed t test.

RESULTS

Development abnormalities in *Pcnt* KO and KI mice

PCNT mutations are known to cause various developmental disorders, including MOPDII, though the precise mechanisms remain unclear (Rauch et al., 2008). In this study, I aimed to analyze the effects of PCNT deficiency in developmental disorders such as MOPDII. With the assistance of Professor Young-Hoon Sung at Asan Medical Center, he generated *Pcnt* KO mice to model PCNT deficiency and KI mice to reflect the MOPDII mutation (Fig. 23 A; Fig. 24 A). To assess the physiological impact of PCNT deficiency, I evaluated body weight and developmental abnormalities in *Pcnt* KO and KI mouse models. *Pcnt* KO and KI mice exhibited significantly lower body weight and smaller body size compared to control mice (Fig. 23, D and E; Fig. 24 D), indicating that PCNT deficiency may adversely affect growth and development. Additionally, developmental abnormalities, including polydactyly, were observed in *Pcnt* KO mice (Fig. 23, F and G). In addition, reduced brain and palate cleft were observed in *Pcnt* KI mice (Fig. 24, E and F). These findings suggest that PCNT deficiency affects broader developmental processes, such as body growth and morphogenesis. This emphasizes the essential role of PCNT in physiological development.

Confirmation of *Pcnt* KO and KI MEF cells

Using MEF cells derived from *Pcnt* KO and KI mouse models, I evaluated PCNT expression through immunoblotting and immunostaining. Results confirmed a complete absence of PCNT protein in *Pcnt* KO MEF cells (Fig. 25, A and B). Interestingly, expected PCNT protein expression was also not observed in *Pcnt* KI cells. To confirm this, I generated R2918X-rescued HeLa cells, revealing that the PCNT R2918X mutant protein was not stably expressed (Fig. 25, C and D). According to mRNA analysis conducted at

Asan Medical Center, *Pcnt* mRNA was transcribed normally, suggesting that the mutated protein was unstable and subsequently degraded. Therefore, it is likely that the phenotype of *Pcnt* KI cells resembles that of *Pcnt* KO cells, implying that PCNT deficiency or instability plays a critical role in the pathogenesis of MOPDII.

Effect of PCNT depletion on PCM localization at the centrosome

Previous studies have shown that in *PCNT* KO RPE1 and HeLa cells, PCM proteins, such as CEP215 and γ-Tubulin, fail to localize properly to the centrosome (Watanabe et al., 2020). PCNT is hypothesized to play a crucial role in positioning PCM proteins within the centrosome. To experimentally validate this, I analyzed the localization of PCM proteins, CEP215 and γ-Tubulin, at the centrosome in *Pcnt* KO and KI MEF cells using immunostaining. In *Pcnt* KO and KI MEF cells, I observed a significant reduction in CEP215 expression at the centrosome during interphase (Fig. 26, A and B), suggesting that PCNT is essential for CEP215 recruitment to the centrosome. In contrast, localization of γ-Tubulin at the centrosome was unaffected during interphase (Fig. 26, A and D). In further mitotic analysis, CEP215 remained improperly positioned at the centrosome (Fig. 27, A and B), while γ-Tubulin exhibited some abnormal localization (Fig. 27, A and D). These results indicate that specific PCM proteins, such as CEP215, require PCNT to be accurately positioned and maintained at the centrosome and suggest that PCNT is also crucial for γ-Tubulin proper localization during mitosis. This highlights PCNT is essential role in maintaining the centrosome structure and function, potentially disrupted in PCNT-deficient cells.

Abnormal centriole separation and overduplication in *Pcnt* KO and KI MEF cells

When PCM proteins are not appropriately loaded into the centrosome, the normal separation and duplication of centrioles may be disrupted (Shin et al., 2021). To test this, I assessed the separation and duplication status of centrioles in *Pcnt* KO and KI MEF

cells by immunostaining for CEP135 and centrin-2. In *Pcnt* KO and KI MEF cells, I observed a marked increase in centriole separation compared to the control group (Fig. 28, A and B), indicating that PCNT plays an essential role in maintaining centriole cohesion. Additionally, I observed an overduplication of centrioles in *Pcnt* KO and KI cells (Fig. 28, C and D), suggesting that PCNT deficiency disrupts the centriole duplication mechanisms. Normal centrosome structure relies on the proper replication and cohesion of centrioles, but the overduplication and abnormal separation of centrioles in both *Pcnt* KO and KI cells indicate a loss of centrosomal stability. Consequently, these defects may impair spindle pole formation during mitosis, potentially leading to chromosomal segregation errors. These abnormalities were supporting the conclusion that PCNT is essential for maintaining the cohesion and stability of the centrosome.

Chromosomal instability in *Pcnt* KO and KI MEF Cells

Abnormal centriole separation and duplication are expected to impact chromosomal stability. To confirm this, I evaluated chromosomal stability in *Pcnt* KO and KI MEF cells using fluorescence in situ hybridization (FISH) targeting chromosome 16. Results indicated a significant increase in aneuploidy in *Pcnt* KO and KI MEF cells compared to control cells (Fig. 29, A and B). This suggests that defects in centrosome cohesion and spindle apparatus resulting from PCNT deficiency may compromise chromosomal stability. The increased aneuploidy observed in *Pcnt* KO and KI cells highlights the critical role of PCNT in maintaining genomic stability and suggests that PCNT deficiency may contribute to chromosomal imbalance, as seen in developmental disorders such as MOPDII. This emphasizes the essential role of PCNT in centrosome cohesion, chromosomal stability, and physiological development.

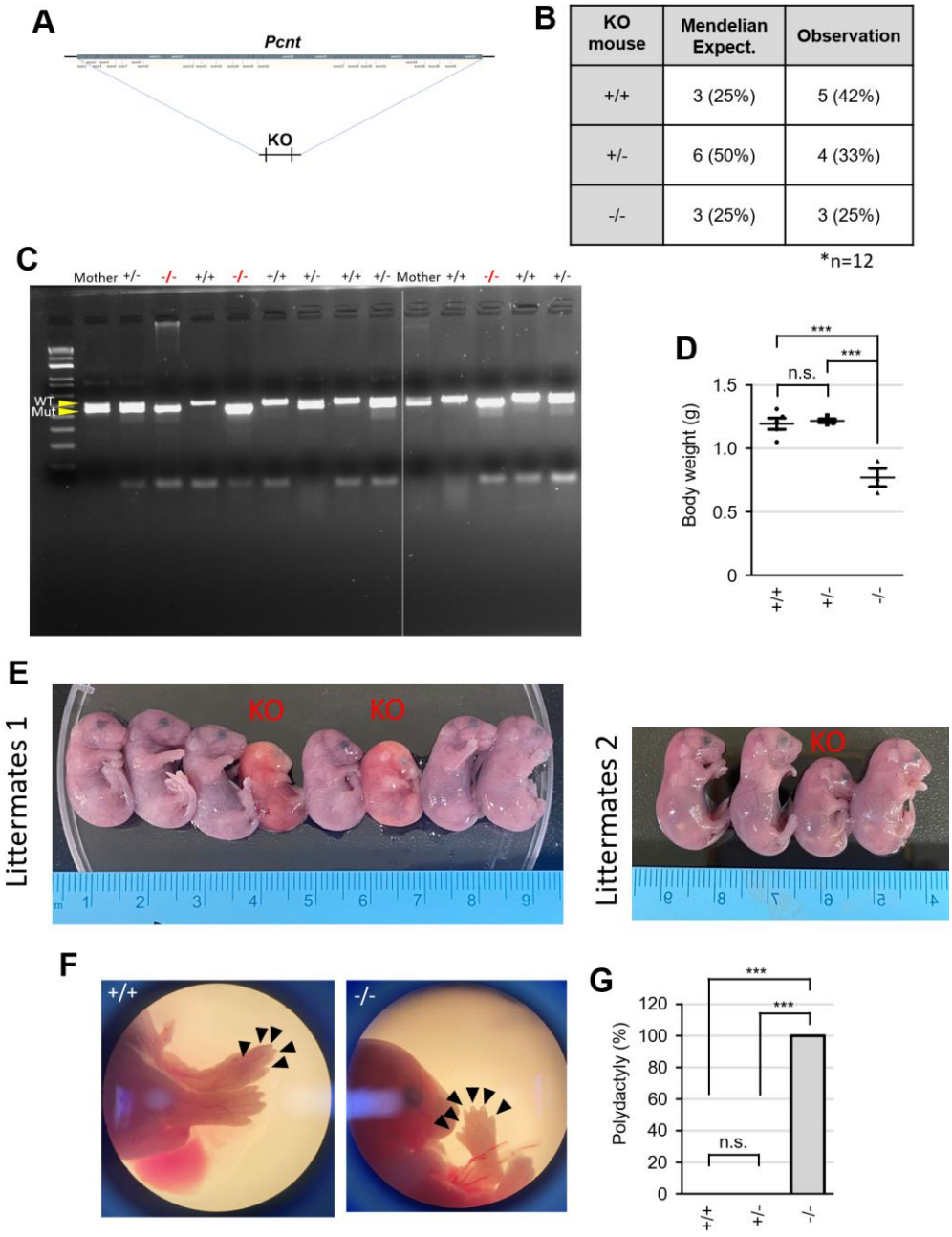

KO mouse	Mendelian Expect.	Observation
+/+	3 (25%)	5 (42%)
+/-	6 (50%)	4 (33%)
-/-	3 (25%)	3 (25%)

*n=12

Figure 23. Phenotypic analysis in *Pcnt* KO Mice.

(A) Generation of *Pcnt* KO mice using Cre-loxP system. (B) Popluation of *Pcnt* KO mouse embryo (C) Genotyping analysis of *Pcnt* KO mice. The lanes display genotypes for different individuals, indicating wild-type (+/+), heterozygous (+/-), and knockout (-/-) mice. (D) Body weight analysis of *Pcnt* KO mice. (E) Gross morphology of *Pcnt* KO mice. (F) Analysis of polydactyly in *Pcnt* KO embryos. The presence of arrowheads to the limb structure. (G) Quantification of polydactyly occurrence. Graph values are expressed as mean and SEM. Statistical significance was determined using one-way ANOVA with Tukey's post hoc test (*, $P < 0.05$; **, $P < 0.01$; ***, $P < 0.001$; n.s., not significant.

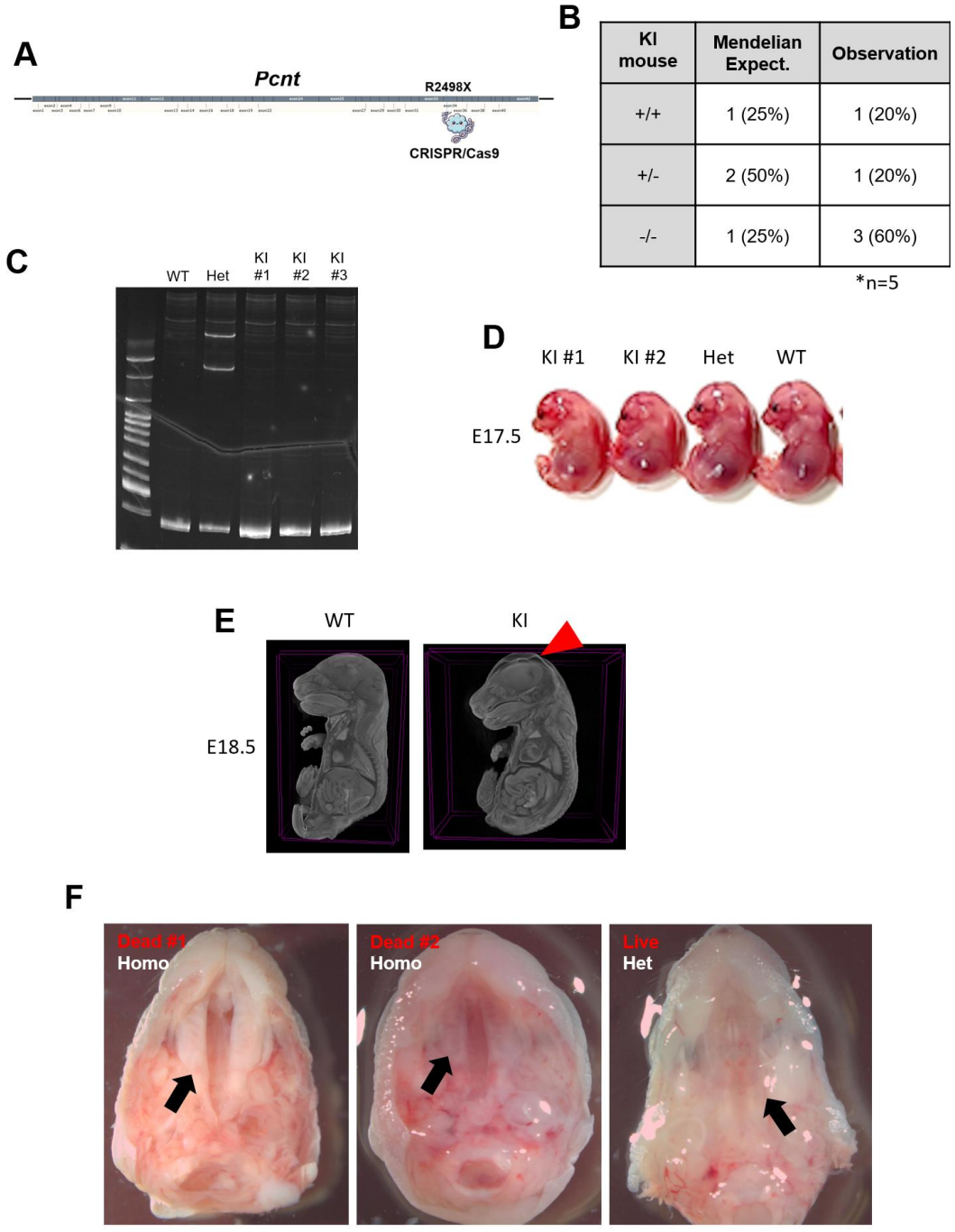

Figure 24. Phenotypic analysis in *Pcnt* KI Mice.
(A) Generation of *Pcnt* KI mice using CRISPR/Cas9 system. (B) Population of *Pcnt* KI mouse embryo (C) Genotyping analysis of *Pcnt* KI mice. The lanes display genotypes for different individuals, indicating wild-type, heterozygous, and knock-in mice. (D) Gross morphology of *Pcnt* KI mice. The presence of arrow head to reduced brain. (E) Computed tomography (CT) of *Pcnt* KI mice. (F) Analysis of cleft palate in *Pcnt* KI embryos. The presence of arrows to the cleft palate.

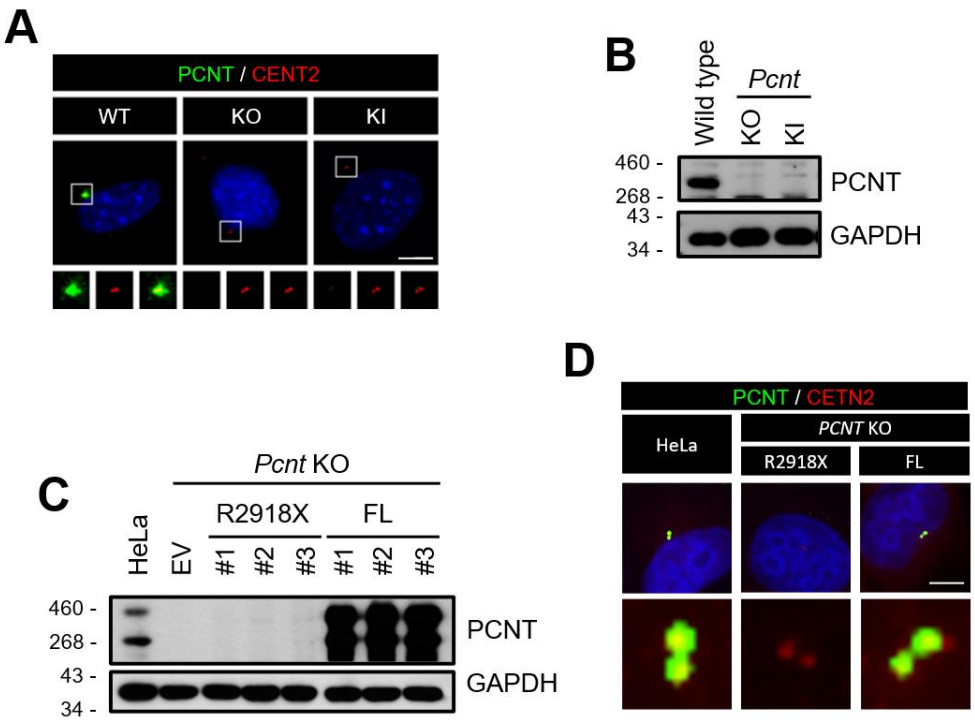

Figure 25. Confirmation of the *Pcnt* KO and KI MEF cells
(A) The *Pcnt* KO and KI MEF cells were coimmunostained with antibodies specific to PCNT (green) and centrin-2 (red). (B) The *Pcnt* KO and KI MEF cells were subjected to immunoblot analyses with antibodies specific to PCNT and GAPDH. (C) The *Pcnt* KO and R2918X mutant HeLa cells were subjected to immunoblot analyses with antibodies specific to PCNT and GAPDH. (D) The *Pcnt* KO and R2918X mutant HeLa cells were coimmunostained with antibodies specific to PCNT (green) and centrin-2 (red). (A and D) Scale bars, 10 μm.

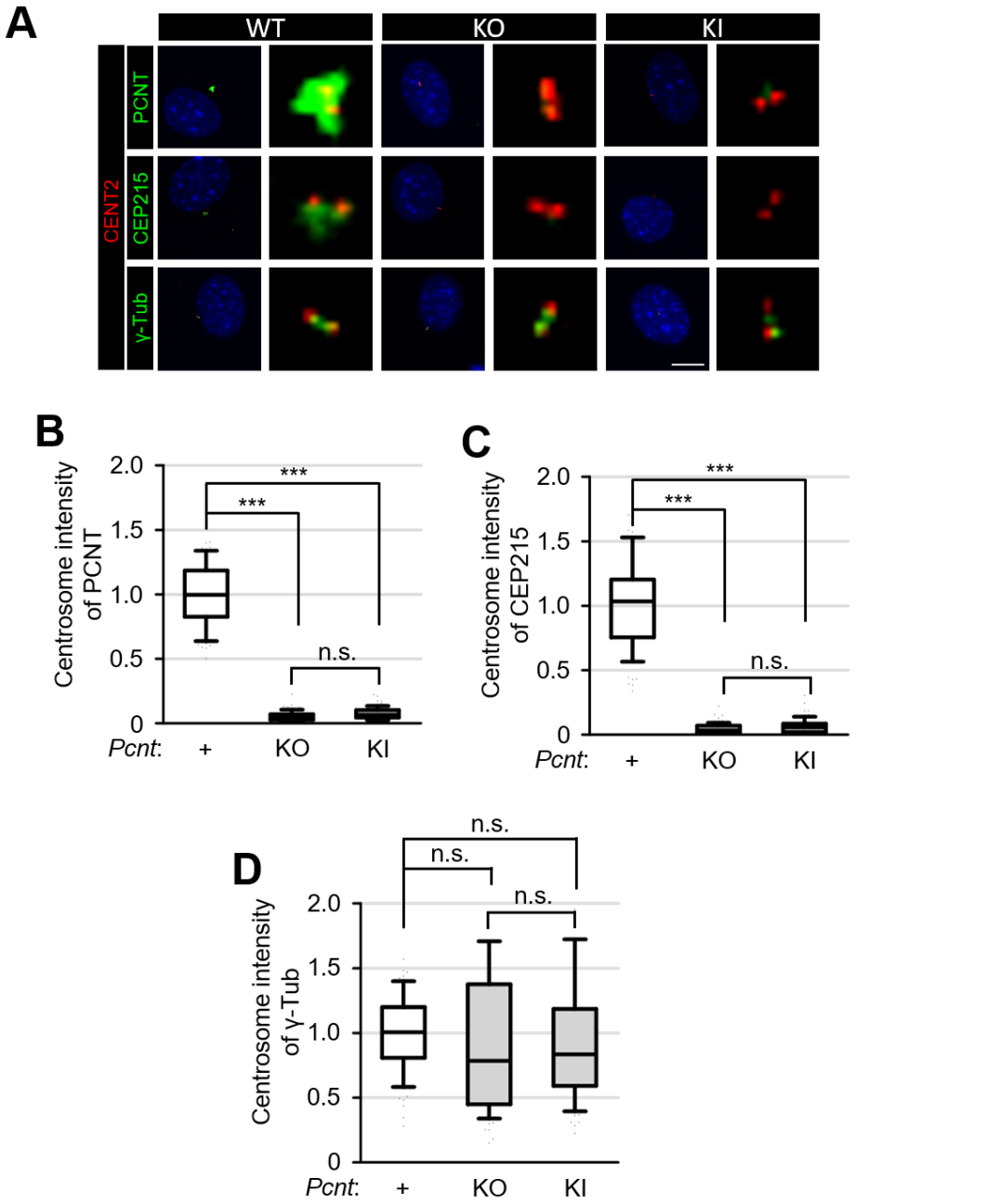

Figure 26. PCNT is important for CEP215 localization, but not γ-Tub at interphase
(A) The *Pcnt* KO and KI MEF cells were coimmunostained with antibodies specific to PCNT, CEP215 and γ-Tub (green) and centrin-2 (red) at interphase. Scale bars, 10 μm. (B-D) Centrosome intensities of PCNT, CEP215 and γ-Tub were determined at interphase. More than 30 cells per group were counted in three independent experiments. Within each box, the black center line represents the median value, the black box contains the interquartile range, and the black whiskers extend to the 10th and 90th percentiles. Statistical significance was determined using one-way ANOVA with Tukey's post hoc test (***, $P < 0.001$; n.s., not significant).

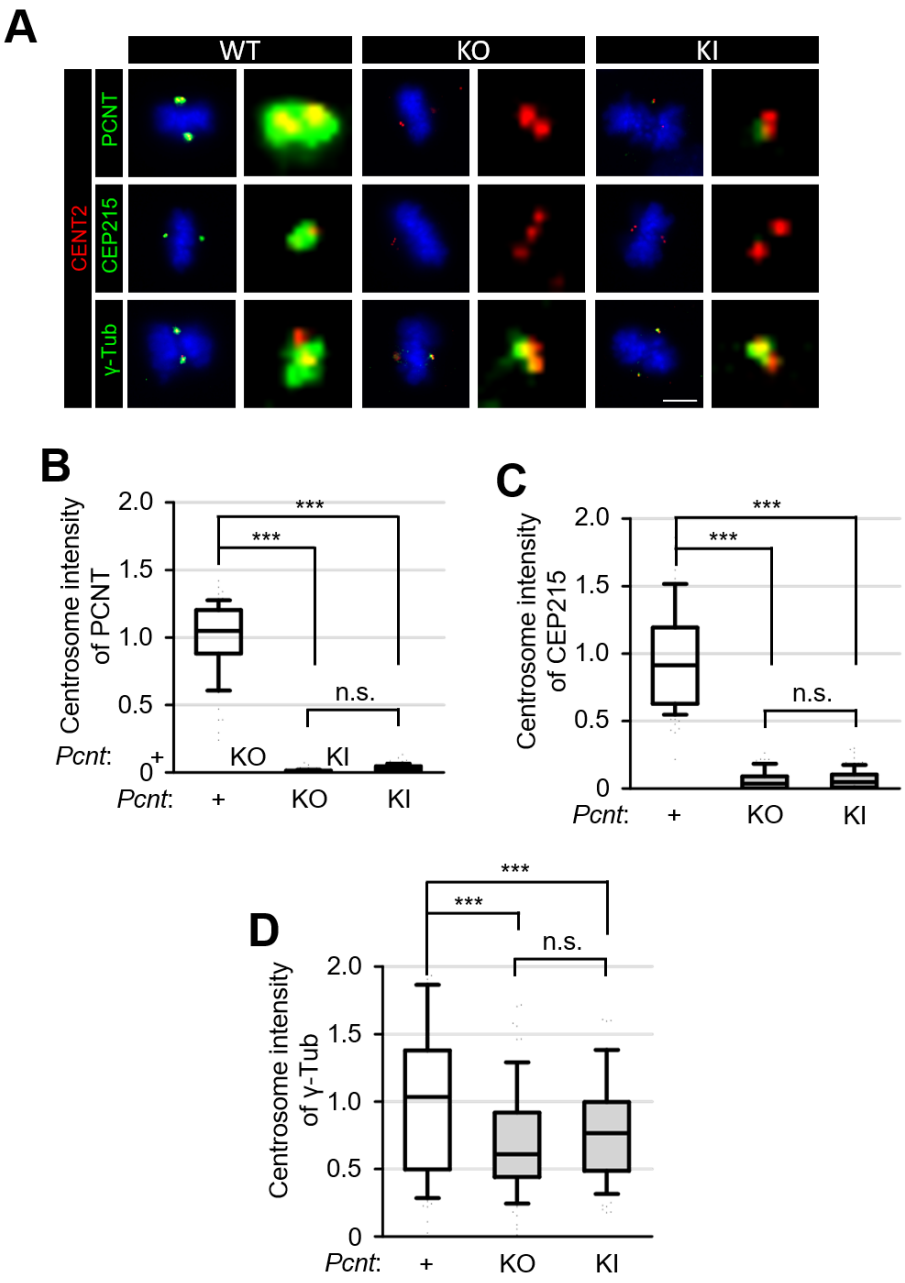

Figure 27. PCNT is important for CEP215 and γ-Tub localization at mitosis
(A) The *Pcnt* KO and KI MEF cells were coimmunostained with antibodies specific to PCNT, CEP215 and γ-Tub (green) and centrin-2 (red) at mitosis. Scale bars, 10 μm. (B-D) Centrosome intensities of PCNT, CEP215 and γ-Tub were determined at mitosis. More than 30 cells per group were counted in three independent experiments. Within each box, the black center line represents the median value, the black box contains the interquartile range, and the black whiskers extend to the 10th and 90th percentiles. Statistical significance was determined using one-way ANOVA with Tukey's post hoc test (***, $P < 0.001$; n.s., not significant).

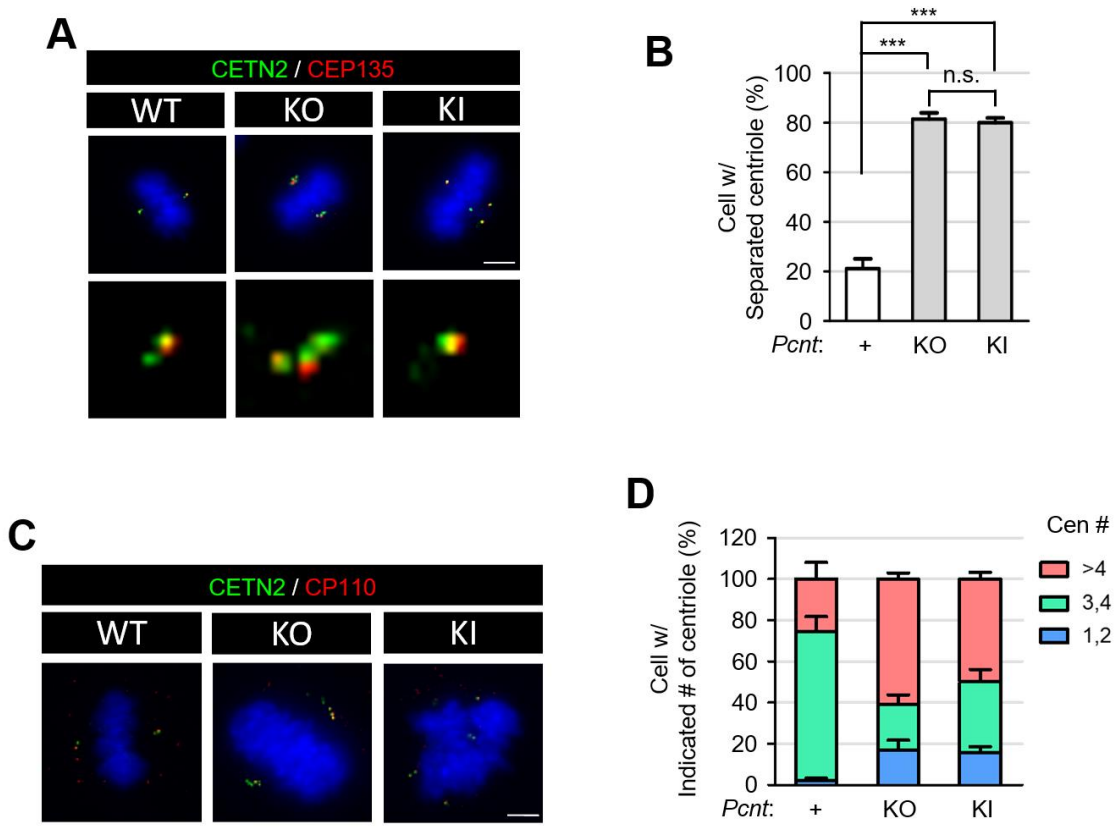

Figure 28. Abnormal centriole separation, and centriole number in *Pcnt* KO and KI MEF cells

(A) The *Pcnt* KO and KI MEF cells were coimmunostained with antibodies specific to centrin-2 (green) and CEP135 (red) at mitosis. (B) The number of cells with separated centriole was counted in *Pcnt* KO and KI MEF cells at mitosis. (C) The *Pcnt* KO and KI MEF cells were coimmunostained with antibodies specific to centrin-2 (green) and CP110 (red) at mitosis. (D) The number of centrioles was counted in *Pcnt* KO and KI MEF cells at mitosis. More than 30 cells per group were counted in three independent experiments. Graph values are expressed as mean and SEM. Statistical significance was determined using one-way ANOVA with Tukey's post hoc test (*, $P < 0.05$; **, $P < 0.01$; ***, $P < 0.001$; n.s., not significant). (A and C) Scale bars, 10 μm.

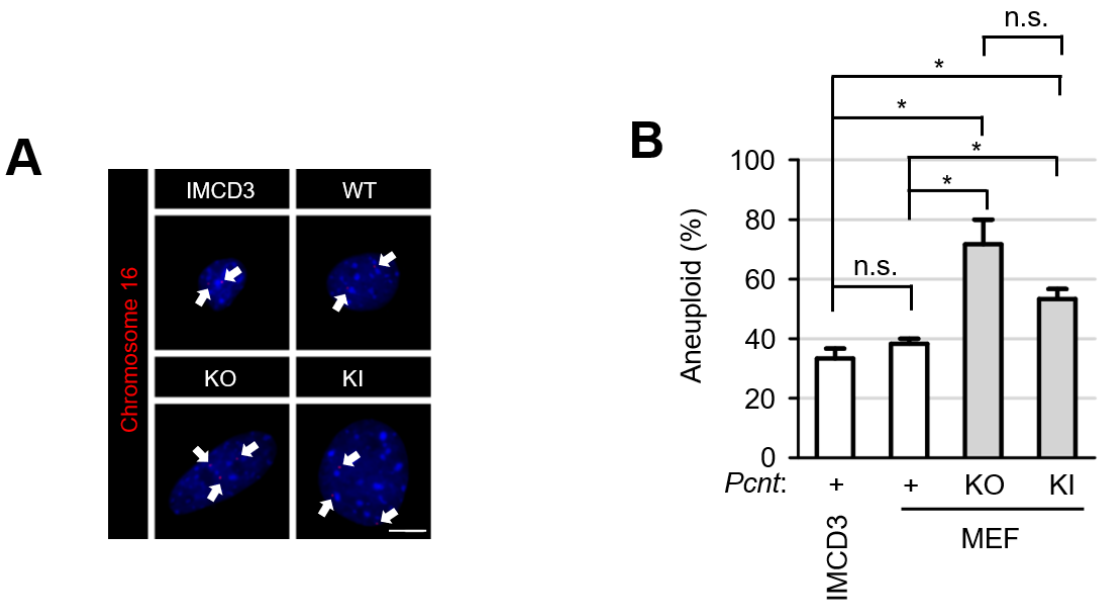

Figure 29. Occurrence of aneuploidy in *Pcnt* KO and KI MEF cells
(A) The *Pcnt* KO and KI MEF cells were immunostained by FISH performed using probe against chromosome 16. The presence of arrows to chromosome 16. Scale bars, 10 μm. (B) The number of cells with aneuploidy was counted in *Pcnt* KO and KI MEF cells. More than 30 cells per group were counted in two independent experiments. Graph values are expressed as mean and SEM. Statistical significance was determined using one-way ANOVA with Tukey's post hoc test (*, $P < 0.05$; **, $P < 0.01$; ***, $P < 0.001$; n.s., not significant).

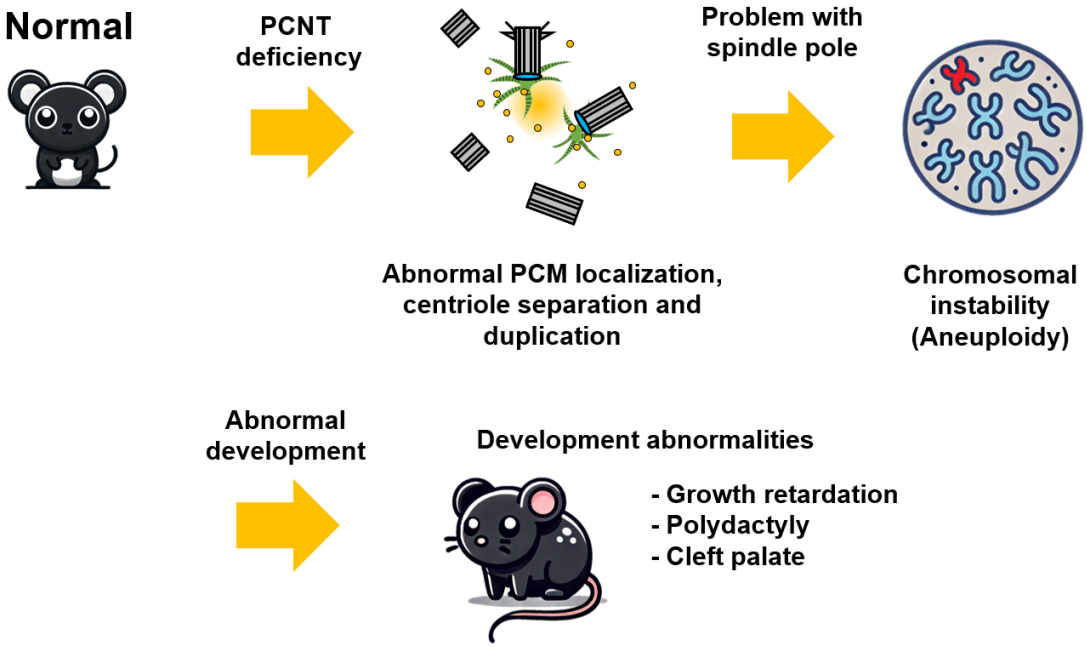

Figure 30. Model
The PCM is essential for normal cell division. In particular, PCNT, a critical scaffolding protein within the PCM, plays a central role in stabilizing the PCM. PCNT deficiency leads to the improper localization of PCM components like CEP215 and γ-tubulin at the centrosome. This improper localization disrupts normal chromosome segregation, resulting in chromosomal instability such as aneuploidy. Such instability affects the developmental process. As a result, PCNT is crucial for ensuring normal development.

DISCUSSION

This study demonstrates the essential role of PCNT in maintaining centrosome and genomic stability as well as normal development. By using *Pcnt* KO and KI models, I observed that the absence of PCNT compromises the integrity of the PCM, leading to defects in centriole cohesion and duplication. These deficiencies induce chromosomal instability and can result in developmental abnormalities such as MOPDII. The fact that both KO and KI models exhibited similar phenotypes emphasizes the critical role of PCNT in organizing the centrosome and supports the conclusion that PCNT deficiency influences developmental processes through these mechanisms (Fig. 30).

Interestingly, the phenotype of the MOPDII-mimicking KI mouse model was found to be similar to that of the *Pcnt* KO mouse. In the investigation of MEF cells, PCNT R2498X protein was undetectable, and further validation in HeLa cells with a PCNT R2918X mutation that shares homology with the mouse R2498X mutation confirmed that a single point mutation in PCNT is critical for protein stability (Fig. 25, C and D). This suggests that a point mutation in PCNT could be a decisive factor in the pathogenesis of diseases such as MOPDII (Rauch et al., 2008). It has also been shown that the Cep57-pericentrin module plays an important role in organizing PCM expansion and centriole cohesion, with PCM collapse potentially contributing to the onset of aneuploidy (Watanabe et al., 2019). Studies like these imply that PCM-related proteins like PCNT may drive developmental abnormalities linked to chromosomal instability, consistent with our findings.

PCNT serves as a scaffold protein within the PCM, organizing key microtubule-nucleating complexes, such as γ-tubulin and CEP215. By stabilizing the PCM, PCNT ensures the connection of mother and daughter centrioles during mitosis, thereby

facilitating proper spindle pole formation (Lee and Rhee, 2012; Nigg and Raff, 2009). PCNT deficiency disrupts the PCM, resulting in incomplete centrioles that cannot function as intact centrosomes. Unlike complete centrosomes seen in centrosome amplification, these incomplete centrioles fail to support proper spindle pole formation, leading to chromosomal segregation errors (Shin et al., 2021; Banterle and Gonczy, 2017). Studies emphasizing integrity of PCM as a precursor to chromosomal instability align with my observation of PCM disruption and subsequent centrosome dysfunction in PCNT-deficient cells, emphasizing the connection between genomic instability and developmental defects (Watanabe et al., 2019).

PCM collapse induced by PCNT deficiency may cause spindle misalignment, hindering cell division and impairing tissue and organ development (Cabral et al., 2013). Although my study did not directly examine spindle formation during mitosis, previous studies have reported that PCM instability can disrupt spindle pole alignment (Chen et al., 2014; Nigg and Raff, 2009). These studies suggest that PCNT deficiency could influence spindle assembly and chromosomal alignment. Additionally, the instability of centrioles resulting from PCM disruption may interfere with the activation of the spindle assembly checkpoint (SAC), potentially leading to chromosomal instability and aneuploidy. Future research should explore the effects of PCNT deficiency on spindle assembly and SAC regulation in greater depth.

PCNT deficiency weakens the PCM structure, promoting excessive centriole replication and premature centriole disengagement. Under normal circumstances, PCNT stabilizes the PCM, harmonizing centriole cohesion and separation throughout the cell cycle. However, without PCNT, the weakened PCM fails to maintain centriole cohesion, resulting in premature centriole separation and abnormal centrosome assembly during mitosis (Nigg and Raff, 2009). PCM collapse sustains PLK4 activity, promoting excessive centriole duplication even during mitosis (Jung and Rhee, 2021). The extra

centrioles contribute to multipolar spindle formation, increasing the risk of chromosomal missegregation and aneuploidy. However, the centrosomal clustering mechanism can inhibit multipolar spindle formation. Through the regulation of microtubule stability, motor proteins, and the SAC, the extra centrosomes are clustered into two poles to prevent multipolarity (Basto et al., 2008; Kwon et al., 2008; Quintyne et al., 2005; Yang et al., 2008). Failed centriole reduplication and cell fusion are mechanisms thought to generate excess centrosomes. Such supernumerary centrosomes may play a dual role in tumorigenesis, on one hand, they promote aneuploidy, while on the other, multipolar spindles induced by excess centrosomes could hinder cell proliferation, causing mitotic arrest and cytokinesis failure (Wang et al., 2014).

Spindle pole misalignment and abnormal spindle formation often lead to asymmetric chromosome segregation, ultimately causing aneuploidy (Jefford and Irminger-Finger, 2006; Breslow and Holland, 2019). When aneuploidy arises, it can delay cell cycle progression, increase DNA fragmentation, and reduce cell viability, causing developmental defects (Pauerova et al., 2020; Holubcova et al., 2015; Chen et al., 2011). Additionally, aneuploidy has been shown to impair cell proliferation in MEF cells, induce metabolic disruptions, and lead to abnormal characteristics such as increased cell size, adversely affecting development (Williams et al., 2008). The aneuploid state induced by PCNT deficiency increases cellular stress and fosters an unstable genomic environment that can promote specific developmental abnormalities. Notably, mosaic variegated aneuploidy syndrome (MVA), a disorder caused by genetic defects in chromosome segregation, results in abnormal chromosome numbers in many somatic cells and is associated with developmental delay and increased childhood cancer risk (Guo et al., 2024). The characteristics of MVA suggest a mechanism similar to that of aneuploidy induced by PCNT deficiency, indicating that chromosomal instability during development can disrupt normal development. In both the *Pcnt* KO and KI models, PCNT

deficiency caused excessive centriole duplication and chromosomal instability. FISH analysis revealed aneuploidy in *Pcnt* KO and KI MEF cells, suggesting that this chromosomal instability could negatively impact development.

PCNT deficiency disrupts spindle pole alignment and causes asymmetric cell division (Chen et al., 2014). This study suggests that PCNT is critical for proper spindle alignment and accurate cell division, emphasizing the important role of PCM proteins in spindle alignment and chromosomal stability (Rauch et al., 2008). Additionally, an increase in centrosome number generates multipolar spindles or abnormal spindle structures, compromising spindle stability (Mittasch et al., 2020). These defects result in chromosomal segregation errors, causing aneuploidy. This study emphasizes the necessity of PCM-related proteins in maintaining proper centrosome function, spindle assembly, and chromosomal stability, providing valuable insights into the consequences of PCNT deficiency.

Importantly, it cannot be excluded that PCNT deficiency could induce developmental abnormalities through alternative mechanisms. For example, the potential impact of PCNT deficiency on centrosome-independent spindle assembly warrants consideration (Heald et al., 1996; Walczak and Heald, 2008). Disruptions in this process may lead to chromosome misalignment and cell division failure, ultimately decreasing cell viability and impairing development. Additionally, if PCM instability interferes with cytokinesis, this could adversely affect cell proliferation, leading to multinucleated cell formation and cell cycle arrest (Doxsey et al., 2005; Steigemann and Gerlich, 2009). Further studies are needed to elucidate these alternative mechanisms and provide a more comprehensive understanding of how PCNT deficiency affects development (Meraldi and Nigg, 2001; Fukasawa, 2007).

In summary, this study emphasizes the essential role of PCNT in maintaining PCM stability, which is critical for proper centriole cohesion, duplication, and spindle assembly, all necessary to prevent chromosomal instability. Without PCNT, centrosome organization becomes unstable, leading to premature centriole disengagement, excessive duplication, and, ultimately, aneuploidy. Aneuploidy slows cell cycle progression, increases indicators of cellular damage such as DNA fragmentation, and decreases cell viability, causing developmental abnormalities (Pauerova et al., 2020). The cumulative effects of aneuploidy confirm the necessity of PCNT for maintaining normal development. This study emphasizes the significance of PCNT as a key component of PCM, providing crucial insights into developmental biology and establishing a foundation for future studies aimed at exploring specific interactions between PCNT and other PCM proteins and their potential therapeutic implications in developmental disorders associated with centrosomal dysfunction and chromosomal instability.

Conclusion and perspective

In Chapter 1, this study investigated the role of inter-centriolar fibers, specifically focusing on CROCC/rootletin in cilia formation. The findings revealed that CROCC is essential for the accurate localization of centriolar satellites, which are critical for proper ciliogenesis. Through KO experiments, the absence of CROCC/rootletin was shown to disrupt the organization of ciliary components, compromising centriolar satellite stability and cilia formation. This work provides foundational insights into how CROCC/rootletin contributes to cilia assembly and stability.

Chapter 2 explored the role of PCNT in maintaining centrosome integrity and its influence on development. Using *Pcnt* KO and MOPDII-mimicking KI mouse models, the study examined how PCNT deficiency affects PCM localization, centriole connection, and chromosomal segregation. The results showed that PCNT is indispensable for centrosome function. KO cells exhibited abnormalities in centriole separation, overduplication, and increased aneuploidy. Developmentally, *Pcnt* KO and KI mice displayed growth retardation, polydactyly, reduced brain, and cleft palate, underlining the critical role of PCNT in development. These findings indicate the significance of PCNT in centrosome duplication fidelity and chromosomal stability.

Together, this research provides insight into the key functions of CROCC/rootletin and PCNT in centrosome biology, establishing a framework for future studies into the roles of these proteins in centrosome and cilia function and their connections to disease. Future directions could involve investigating the molecular interactions between CROCC/rootletin, PCNT, and other PCM components. Advanced imaging and proteomic analyses could clarify how these interactions vary across cell types, developmental stages, and disease contexts, shedding light on tissue-specific vulnerabilities to centrosome dysfunction. Additionally, given the phenotypic similarities observed between KO and MOPDII-mimicking KI models, exploring mechanisms of centrosome-related diseases could enhance understanding of ciliopathies and other genetic disorders. Patient-derived induced pluripotent stem cells (iPSCs) with CROCC or

PCNT mutations could provide valuable models for examining disease phenotypes and testing potential therapies.

The findings of this study also suggest promising therapeutic avenues. Targeted interventions, such as small molecules or peptides designed to enhance PCM stability, support centriole connection, or promote cilia formation, could benefit treatments for disorders related to centrosome dysfunction. High-throughput drug screening in disease-specific iPSC models may accelerate the development of effective therapies for MOPDII and related conditions.

In conclusion, this research advances knowledge on the roles of CROCC/rootletin and PCNT in centrosome, genomic stability, and developmental processes. It points to the potential for targeted therapies aimed at restoring centrosome functionality, offering promising prospects for treating developmental disorders, cancer, and ciliopathies associated with centrosome dysfunction.

REFERENCES

Aydin, O.Z., Taflan, S.O., Gurkaslar, C., and Firat-Karalar, E.N. (2020). Acute inhibition of centriolar satellite function and positioning reveals their functions at the primary cilium. PLoS Biol 18, e3000679.

Azimzadeh, J., and Marshall, W.F. (2010). Building the centriole. Curr Biol 20, R816-825.

Bahe, S., Stierhof, Y.D., Wilkinson, C.J., Leiss, F., and Nigg, E.A. (2005). Rootletin forms centriole-associated filaments and functions in centrosome cohesion. J Cell Biol 171, 27-33.

Banterle, N., and Gonczy, P. (2017). Centriole biogenesis: from identifying the characters to understanding the plot. Annu Rev Cell Dev Biol 33, 23-49.

Basto, R., Brunk, K., Vinadogrova, T., Peel, N., Franz, A., Khodjakov, A., and Raff, J.W. (2008). Centrosome amplification can initiate tumorigenesis in flies. Cell 133, 1032-1042.

Bettencourt-Dias, M., and Glover, D.M. (2007). Centrosome biogenesis and function: centrosomics brings new understanding. Nat Rev Mol Cell Biol 8, 451-463.

Bornens, M. (2012). The centrosome in cells and organisms. Science 335, 422-426.

Bornens, M., and Azimzadeh, J. (2007). Origin and evolution of the centrosome. Adv Exp Med Biol 607, 119-129.

Breslow, D.K., and Holland, A.J. (2019). Mechanism and Regulation of Centriole and Cilium Biogenesis. Annu Rev Biochem 88, 691-724.

Cabral, G., Sans, S.S., Cowan, C.R., and Dammermann, A. (2013). Multiple mechanisms contribute to centriole separation in C. elegans. Curr Biol 23, 1380-1387.

Chen, C.T., Hehnly, H., Yu, Q., Farkas, D., Zheng, G., Redick, S.D., Hung, H.F., Samtani, R., Jurczyk, A., Akbarian, S., et al. (2014). A unique set of centrosome proteins requires pericentrin for spindle-pole localization and spindle orientation. Curr Biol 24, 2327-2334.

Chen, J.V., Kao, L.R., Jana, S.C., Sivan-Loukianova, E., Mendonca, S., Cabrera, O.A., Singh, P., Cabernard, C., Eberl, D.F., Bettencourt-Dias, M., et al. (2015). Rootletin organizes the ciliary rootlet to achieve neuron sensory function in Drosophila. J Cell Biol 211, 435-453.

Conduit, P.T., Wainman, A., Novak, Z.A., Weil, T.T., and Raff, J.W. (2015). Re-examining the role of Drosophila Sas-4 in centrosome assembly using two-colour-3D-SIM FRAP. Elife 4.

Conkar, D., Bayraktar, H., and Firat-Karalar, E.N. (2019). Centrosomal and ciliary targeting of CCDC66 requires cooperative action of centriolar satellites, microtubules and molecular motors. Sci Rep 9, 14250.

Dammermann, A., and Merdes, A. (2002). Assembly of centrosomal proteins and microtubule organization depends on PCM-1. J Cell Biol 159, 255-266.

Delaval, B., and Doxsey, S.J. (2010). Pericentrin in cellular function and disease. J Cell Biol 188, 181-190.

Fang, G., Zhang, D., Yin, H., Zheng, L., Bi, X., and Yuan, L. (2014). Centlein mediates an interaction between C-Nap1 and Cep68 to maintain centrosome cohesion. J Cell Sci 127, 1631-1639.

Doxsey, S., McCollum, D., and Theurkauf, W. (2005). Centrosomes in cellular regulation. Annu Rev Cell Dev Biol 21, 411-434.

Flanagan, A.M., Stavenschi, E., Basavaraju, S., Gaboriau, D., Hoey, D.A., and Morrison, C.G. (2017). Centriole splitting caused by loss of the centrosomal linker protein C-NAP1 reduces centriolar satellite density and impedes centrosome amplification. Mol Biol Cell 28, 736-745.

Fry, A.M., Mayor, T., Meraldi, P., Stierhof, Y.D., Tanaka, K., and Nigg, E.A. (1998). C-Nap1, a novel centrosomal coiled-coil protein and candidate substrate of the cell cycle-regulated protein kinase Nek2. J Cell Biol 141, 1563-1574.

Fukasawa, K. (2007). Oncogenes and tumour suppressors take on centrosomes. Nat Rev Cancer 7, 911-924.

Gheiratmand, L., Coyaud, E., Gupta, G.D., Laurent, E.M., Hasegan, M., Prosser, S.L., Goncalves, J., Raught, B., and Pelletier, L. (2019). Spatial and proteomic profiling reveals centrosome-independent features of centriolar satellites. EMBO J 38, e101109.

Graser, S., Stierhof, Y.D., and Nigg, E.A. (2007). Cep68 and Cep215 (Cdk5rap2) are required for centrosome cohesion. J Cell Sci 120, 4321-4331.

Guo, J., He, W.B., Dai, L., Tian, F., Luo, Z., Shen, F., Tu, M., Zheng, Y., Zhao, L., Tan, C., et al. (2024). Mosaic variegated aneuploidy syndrome with tetraploid, and predisposition to male infertility triggered by mutant CEP192. HGG Adv 5, 100256.

Hatch, E.M., Kulukian, A., Holland, A.J., Cleveland, D.W., and Stearns, T. (2010). Cep152 interacts with Plk4 and is required for centriole duplication. J Cell Biol 191, 721-729.

He, R., Huang, N., Bao, Y., Zhou, H., Teng, J., and Chen, J. (2013). LRRC45 is a centrosome linker component required for centrosome cohesion. Cell Rep 4, 1100-1107.

Heald, R., Tournebize, R., Blank, T., Sandaltzopoulos, R., Becker, P., Hyman, A., and Karsenti, E. (1996). Self-organization of microtubules into bipolar spindles around artificial chromosomes in Xenopus egg extracts. Nature 382, 420-425.

Holubcova, Z., Blayney, M., Elder, K., and Schuh, M. (2015). Human oocytes. Error-prone chromosome-mediated spindle assembly favors chromosome segregation defects in human oocytes. Science 348, 1143-1147.

Hori, A., and Toda, T. (2017). Regulation of centriolar satellite integrity and its physiology. Cell Mol Life Sci 74, 213-229.

Hossain, D., Shih, S.Y., Xiao, X., White, J., and Tsang, W.Y. (2020). Cep44 functions in centrosome cohesion by stabilizing rootletin. J Cell Sci 133.

Jefford, C.E., and Irminger-Finger, I. (2006). Mechanisms of chromosome instability in cancers. Crit Rev Oncol Hematol 59, 1-14.

Jurczyk, A., Gromley, A., Redick, S., San Agustin, J., Witman, G., Pazour, G.J., Peters, D.J., and Doxsey, S. (2004). Pericentrin forms a complex with intraflagellar transport proteins and polycystin-2 and is required for primary cilia assembly. J Cell Biol 166, 637-643.

Kim, K., Lee, S., Chang, J., and Rhee, K. (2008). A novel function of CEP135 as a platform protein of C-NAP1 for its centriolar localization. Exp Cell Res 314, 3692-3700.

Kim, K., and Rhee, K. (2011). The pericentriolar satellite protein CEP90 is crucial for integrity of the mitotic spindle pole. J Cell Sci 124, 338-347.

Kim, S., and Rhee, K. (2014). Importance of the CEP215-pericentrin interaction for centrosome maturation during mitosis. PLoS One 9, e87016.

Ko, D., Kim, J., Rhee, K., and Choi, H.J. (2020). Identification of a Structurally Dynamic Domain for Oligomer Formation in Rootletin. J Mol Biol 432, 3915-3932.

Kubo, A., and Tsukita, S. (2003). Non-membranous granular organelle consisting of PCM-1: subcellular distribution and cell-cycle-dependent assembly/disassembly. J Cell Sci 116, 919-928.

Kumar, D., Rains, A., Herranz-Perez, V., Lu, Q., Shi, X., Swaney, D.L., Stevenson, E., Krogan, N.J., Huang, B., Westlake, C., et al. (2021). A ciliopathy complex builds distal appendages to initiate ciliogenesis. J Cell Biol 220.

Kumar, D., and Reiter, J. (2021). How the centriole builds its cilium: of mothers, daughters, and the acquisition of appendages. Curr Opin Struct Biol 66, 41-48.

Kurtulmus, B., Wang, W., Ruppert, T., Neuner, A., Cerikan, B., Viol, L., Duenas-Sanchez, R., Gruss, O.J., and Pereira, G. (2016). WDR8 is a centriolar satellite and centriole-associated protein that promotes ciliary vesicle docking during ciliogenesis. J Cell Sci 129, 621-636.

Kwon, M., Godinho, S.A., Chandhok, N.S., Ganem, N.J., Azioune, A., Thery, M., and Pellman, D. (2008). Mechanisms to suppress multipolar divisions in cancer cells with extra centrosomes. Genes Dev 22, 2189-2203.

Lawo, S., Hasegan, M., Gupta, G.D., and Pelletier, L. (2012). Subdiffraction imaging of centrosomes reveals higher-order organizational features of pericentriolar material. Nat Cell Biol 14, 1148-1158.

Lee, K., and Rhee, K. (2012). Separase-dependent cleavage of pericentrin B is necessary and sufficient for centriole disengagement during mitosis. Cell Cycle 11, 2476-2485.

Luders, J., and Stearns, T. (2007). Microtubule-organizing centres: a re-evaluation. Nat Rev Mol Cell Biol 8, 161-167.

Mahen, R. (2018). Stable centrosomal roots disentangle to allow interphase centriole independence. PLoS Biol 16, e2003998.

Marthiens, V., Rujano, M.A., Pennetier, C., Tessier, S., Paul-Gilloteaux, P., and Basto, R. (2013). Centrosome amplification causes microcephaly. Nat Cell Biol 15, 731-740.

Mazo, G., Soplop, N., Wang, W.J., Uryu, K., and Tsou, M.F. (2016). Spatial Control of Primary Ciliogenesis by Subdistal Appendages Alters Sensation-Associated Properties of Cilia. Dev Cell 39, 424-437.

McConnachie, D.J., Stow, J.L., and Mallett, A.J. (2021). Ciliopathies and the Kidney: A Review. Am J Kidney Dis 77, 410-419.

Mennella, V., Keszthelyi, B., McDonald, K.L., Chhun, B., Kan, F., Rogers, G.C., Huang, B., and Agard, D.A. (2012). Subdiffraction-resolution fluorescence microscopy reveals a domain of the centrosome critical for pericentriolar material organization. Nat Cell Biol 14, 1159-1168.

Meraldi, P., and Nigg, E.A. (2001). Centrosome cohesion is regulated by a balance of kinase and phosphatase activities. J Cell Sci 114, 3749-3757.

Mittasch, M., Tran, V.M., Rios, M.U., Fritsch, A.W., Enos, S.J., Ferreira Gomes, B., Bond, A., Kreysing, M., and Woodruff, J.B. (2020). Regulated changes in material properties underlie centrosome disassembly during mitotic exit. J Cell Biol 219.

Nachury, M.V., Loktev, A.V., Zhang, Q., Westlake, C.J., Peranen, J., Merdes, A., Slusarski, D.C., Scheller, R.H., Bazan, J.F., Sheffield, V.C., et al. (2007). A core complex of BBS proteins cooperates with the GTPase Rab8 to promote ciliary membrane biogenesis. Cell 129, 1201-1213.

Nachury, M.V., Seeley, E.S., and Jin, H. (2010). Trafficking to the ciliary membrane: how to get across the periciliary diffusion barrier? Annu Rev Cell Dev Biol 26, 59-87.

Nigg, E.A., and Raff, J.W. (2009). Centrioles, centrosomes, and cilia in health and disease. Cell 139, 663-678.

Odabasi, E., Gul, S., Kavakli, I.H., and Firat-Karalar, E.N. (2019). Centriolar satellites are required for efficient ciliogenesis and ciliary content regulation. EMBO Rep 20.

Panic, M., Hata, S., Neuner, A., and Schiebel, E. (2015). The centrosomal linker and microtubules provide dual levels of spatial coordination of centrosomes. PLoS Genet 11, e1005243.

Prosser, S.L., and Pelletier, L. (2020). Centriolar satellite biogenesis and function in vertebrate cells. J Cell Sci 133.

Quarantotti, V., Chen, J.X., Tischer, J., Gonzalez Tejedo, C., Papachristou, E.K., D'Santos, C.S., Kilmartin, J.V., Miller, M.L., and Gergely, F. (2019). Centriolar satellites are acentriolar assemblies of centrosomal proteins. EMBO J 38, e101082.

Quintyne, N.J., Reing, J.E., Hoffelder, D.R., Gollin, S.M., and Saunders, W.S. (2005). Spindle multipolarity is prevented by centrosomal clustering. Science 307, 127-129.

Rauch, A., Thiel, C.T., Schindler, D., Wick, U., Crow, Y.J., Ekici, A.B., van Essen, A.J., Goecke, T.O., Al-Gazali, L., Chrzanowska, K.H., et al. (2008). Mutations in the pericentrin (PCNT) gene cause primordial dwarfism. Science 319, 816-819.

Reiter, J.F., Blacque, O.E., and Leroux, M.R. (2012). The base of the cilium: roles for transition fibres and the transition zone in ciliary formation, maintenance and compartmentalization. EMBO Rep 13, 608-618.
Remo, A., Li, X., Schiebel, E., and Pancione, M. (2020). The Centrosome Linker and Its Role in Cancer and Genetic Disorders. Trends Mol Med 26, 380-393.

Sanchez, I., and Dynlacht, B.D. (2016). Cilium assembly and disassembly. Nat Cell Biol 18, 711-717.

Sathananthan, A.H., Selvaraj, K., Girijashankar, M.L., Ganesh, V., Selvaraj, P., and Trounson, A.O. (2006). From oogonia to mature oocytes: inactivation of the maternal centrosome in humans. Microsc Res Tech 69, 396-407.

Seo, M.Y., Jang, W., and Rhee, K. (2015). Integrity of the Pericentriolar Material Is Essential for Maintaining Centriole Association during M Phase. PLoS One 10, e0138905.

Shin, B., Kim, M.S., Lee, Y., Jung, G.I., and Rhee, K. (2021). Generation and Fates of Supernumerary Centrioles in Dividing Cells. Mol Cells 44, 699-705.

Singla, V., and Reiter, J.F. (2006). The primary cilium as the cell's antenna: signaling at a sensory organelle. Science 313, 629-633.

Soung, N.K., Park, J.E., Yu, L.R., Lee, K.H., Lee, J.M., Bang, J.K., Veenstra, T.D., Rhee, K., and Lee, K.S. (2009). Plk1-dependent and -independent roles of an ODF2 splice variant, hCenexin1, at the centrosome of somatic cells. Dev Cell 16, 539-550.

Steigemann, P., and Gerlich, D.W. (2009). Cytokinetic abscission: cellular dynamics at the midbody. Trends Cell Biol 19, 606-616.

Stowe, T.R., Wilkinson, C.J., Iqbal, A., and Stearns, T. (2012). The centriolar satellite proteins Cep72 and Cep290 interact and are required for recruitment of BBS proteins to the cilium. Mol Biol Cell 23, 3322-3335.

Styczynska-Soczka, K., and Jarman, A.P. (2015). The Drosophila homologue of Rootletin is required for mechanosensory function and ciliary rootlet formation in chordotonal sensory neurons. Cilia 4, 9.

Sun, S.C., and Kim, N.H. (2012). Spindle assembly checkpoint and its regulators in meiosis. Hum Reprod Update 18, 60-72.

Vlijm, R., Li, X., Panic, M., Ruthnick, D., Hata, S., Herrmannsdorfer, F., Kuner, T., Heilemann, M., Engelhardt, J., Hell, S.W., et al. (2018). STED nanoscopy of the centrosome linker reveals a CEP68-organized, periodic rootletin network anchored to a C-Nap1 ring at centrioles. Proc Natl Acad Sci U S A 115, E2246-E2253.

Walczak, C.E., and Heald, R. (2008). Mechanisms of mitotic spindle assembly and function. Int Rev Cytol 265, 111-158.

Wang, G., Jiang, Q., and Zhang, C. (2014). The role of mitotic kinases in coupling the centrosome cycle with the assembly of the mitotic spindle. J Cell Sci 127, 4111-4122.

Wang, L., Lee, K., Malonis, R., Sanchez, I., and Dynlacht, B.D. (2016). Tethering of an E3 ligase by PCM1 regulates the abundance of centrosomal KIAA0586/Talpid3 and promotes ciliogenesis. Elife 5.

Wang, W.J., Soni, R.K., Uryu, K., and Tsou, M.F. (2011). The conversion of centrioles to centrosomes: essential coupling of duplication with segregation. J Cell Biol 193, 727-739.

Watanabe, S., Meitinger, F., Shiau, A.K., Oegema, K., and Desai, A. (2020). Centriole-independent mitotic spindle assembly relies on the PCNT-CDK5RAP2 pericentriolar matrix. J Cell Biol 219.

Watanabe, K., Takao, D., Ito, K.K., Takahashi, M., and Kitagawa, D. (2019). The Cep57-pericentrin module organizes PCM expansion and centriole engagement. Nat Commun 10, 931.

Werner, S., Pimenta-Marques, A., and Bettencourt-Dias, M. (2017). Maintaining centrosomes and cilia. J Cell Sci 130, 3789-3800.

Xia, Y., Huang, N., Chen, Z., Li, F., Fan, G., Ma, D., Chen, J., and Teng, J. (2018). CCDC102B functions in centrosome linker assembly and centrosome cohesion. J Cell Sci 131.

Yang, J., Liu, X., Yue, G., Adamian, M., Bulgakov, O., and Li, T. (2002). Rootletin, a novel coiled-coil protein, is a structural component of the ciliary rootlet. J Cell Biol 159, 431-440.

Yang, Z., Loncarek, J., Khodjakov, A., and Rieder, C.L. (2008). Extra centrosomes and/or chromosomes prolong mitosis in human cells. Nat Cell Biol 10, 748-751.

Zimmerman, W.C., Sillibourne, J., Rosa, J., and Doxsey, S.J. (2004). Mitosis-specific anchoring of gamma tubulin complexes by pericentrin controls spindle organization and mitotic entry. Mol Biol Cell 15, 3642-3657.

국문초록

중심체는 미세소관의 조직화, 세포 분열, 섬모 형성에 중요한 역할을 한다. 중심체 관련 단백질의 기능 이상은 발달 장애, 섬모병증, 암과 연관되어 있다. 중심체는 중심립 쌍과 이를 연결하는 중심립간 섬유(inter-centriolar fibers), 그리고 단백질 매트릭스인 중심립 주위 물질(pericentriolar material, PCM)로 구성된다. CROCC 는 중심립간 섬유의 주요 구성 요소로 중심립 결합에 기여하며, PCNT 는 유사분열 동안 PCM 의 안정성을 유지하는 것으로 알려져 있다. 그러나 이 단백질들이 세포 및 조직 발달 수준에서 수행하는 구체적인 역할은 명확히 밝혀지지 않았다. 따라서 본 연구는 중심체 기능에서 CROCC 와 PCNT 의 역할 및 이들이 세포 안정성과 조직 발달에 미치는 영향을 조사하는 것을 목표로 한다.

1 장에서 중심립간 섬유가 섬모 형성에 미치는 역할을 이해하는 데 중점을 뒀다. CROCC 는 중심립간 섬유의 주요 구성 요소로 중심체 결합을 유지하며, 병렬적 호모다이머(homodimer)를 기본 단위로 형성한다. 중심립간 섬유는 섬모 안정성을 유지하는 역할로 잘 알려져 있지만, 섬모 형성 과정에서의 구체적인 역할은 명확히 밝혀지지 않았다. 이에 따라 본 연구에서는 중심립간 섬유가 섬모 형성(ciliogenesis)에 미치는 영향을 조사했다. CROCC 와 CEP250 유전자 결손(KO) 세포주를 생성하여 섬모 형성과 섬모 형성에 필요한 단백질을 중심체로 운반하는 대표적인 중심립 위성 단백질 PCM1 의 위치 변화를 분석했다. 연구 결과, CROCC 와 CEP250 의

결손은 PCM1 의 중심체 위치를 교란시켰으나, PCM1 의 발현 수준에는 영향을 미치지 않았다. 또한 PCM1 이 CROCC 와 직접적으로 결합하며, 이 상호작용이 중심립 위성체가 중심체 근처에 축적되어 섬모 형성을 효과적으로 진행하는 데 필수적이라는 것을 발견했다. 이 연구는 중심립간 섬유가 중심립 위성과의 상호작용을 통해 섬모 형성을 조직화하는 데 중요한 역할을 한다는 것을 밝혔다.

2 장에서는 Pericentrin(PCNT)이 발달에 미치는 역할을 이해하는 데 중점을 뒀다. PCNT 는 PCM 내의 주요 스캐폴딩 단백질로 PCM 을 안정화하는 데 중심적인 역할을 한다. PCNT 는 γ-tubulin 과 CEP215 를 중심체로 유도하여 미세소관을 조직화하고 PCM 구조를 지지한다. PCNT 결핍은 PCM 구조와 유사분열 방추극을 손상시킨다. 그러나 PCNT 의 발달 과정에서의 구체적인 역할은 명확히 규명되지 않았다. 따라서 본 연구에서는 PCNT 의 기전적 역할을 조사하였으며, Pcnt 유전자 결손(KO) 및 Microcephalic osteodysplastic primordial dwarfism II(MOPDII)를 모방한 KI(knock-in) 생쥐 모델과 생쥐 배아 섬유아세포(MEF) 세포를 사용하여 PCNT 의 결핍이 미치는 영향을 분석했다. 연구 결과, KO 및 KI 생쥐는 신생아기 치사를 보였으며, 배아는 성장 지연, 다지증, 뇌 크기 감소, 구개열 등의 유사한 표현형을 보였다. 또한 KO 및 KI MEF 세포에서는 비정상적인 중심립 분리, 중심립 과다복제, 염색체 비분리(aneuploidy)가 증가한 것으로 나타났다. 이러한 결과는 PCNT 가 발달 과정에서 중심체 안정성을 유지하는 데 중요한 역할을 하며, MOPDII 의 병리학적 발달 과정과 연관이 있음을 보여준다. 또한 이는 잠재적인 치료 타겟을 제공할 가능성을 시사한다.

본 연구는 CRISPR/Cas9 기반 KO 세포주와 질환 모방 생쥐 모델을 사용하여 중심체 단백질 CROCC 와 PCNT 가 세포 조직화와 정상적인 발달 과정에서 중요한 역할을 수행한다는 점을 강조한다. CROCC 는 중심립 위성체를 조직화하여 섬모를 정밀하게 형성하는 데 기여하며, PCNT 는 PCM 을 안정화하여 염색체 분리를 정확히 수행하고 발달 결함을 방지한다. 본 연구는 이러한 단백질의 결핍이 세포 및 발달 과정에 미치는 영향을 설명하며, 중심체 관련 질환의 분자적 기전을 이해하고 새로운 치료 전략을 위한 중요한 통찰을 제공한다.

키워드: 중심체, 섬모 형성, Inter-centriolar fiber, Pericentrin, 염색체 불안정성
학번: 2020-20188

감사의 글

많은 분들의 도움 덕분에 이 논문을 마무리하고 무사히 학위 과정을 끝마칠 수 있었습니다.

먼저, 학위 과정 동안 저에게 과학뿐만 아니라 인생 자체를 가르쳐 주신 이건수 교수님께 진심으로 감사드립니다. 언제나 아버지처럼 따뜻한 보살핌과 가르침을 베풀어 주셔서 깊이 존경하고 감사드립니다. 또한, 학위 논문을 심사해 주신 공영윤, 김진홍, 장원열, 성영훈 교수님께도 감사의 인사를 전합니다.

이 여정을 함께해 준 연구실 동료들에게도 진심으로 감사드립니다. 여러분 덕분에 배울 점이 많았고, 저 역시 여러분께 작은 도움이 되었기를 바랍니다. 그리고 무엇보다도, 저를 믿고 묵묵히 응원해 주신 부모님과 가족들, 친구들 그리고 제 곁에서 함께 힘든 시간을 견뎌 준 아내에게 깊은 감사의 마음을 전합니다.

마지막으로, 저에게 가장 큰 축복과 같은 사랑스러운 우리 딸, 류서령. 함께 행복한 미래를 만들어 가자고 전하고 싶습니다.

이 학위 과정은 저에게 잊지 못할 많은 추억을 남겼고, 인생의 중요한 전환점이 되었습니다. 앞으로도 이 경험을 바탕으로 원래의 꿈을 포기하지 않고 끊임없이 나아가며, 주변에 행복을 전하는 사람이 되도록 노력하겠습니다. 감사합니다.

2025 년 1 월 류성진